„Impact of gonadal steroid hormones on neuroinflammation and inflammasome activation in a rodent stroke model"

Von der Fakultät für Mathematik, Informatik und Naturwissenschaften der RWTH Aachen University zur Erlangung des akademischen Grades eines Doktors der Naturwissenschaften genehmigte Dissertation

vorgelegt von

Master of Science

Alexander Slowik

aus Tiegenhof (Polen)

Berichter: Univ.-Prof. Dr. rer. nat. Hermann Wagner
Univ.-Prof. Dr. rer. nat. Cordian Beyer

Tag der mündlichen Prüfung: 21.12.2016

Diese Dissertation ist auf den Internetseiten der Universitätsbibliothek online verfügbar.

Summary

Stroke is the third most common cause of death in the developed countries. Understanding of the underlying pathophysiological processes of stroke is essential to develop novel and effective treatments. Until now, only the intravenous thrombolysis therapy has proven as an effective pharmacologic treatment strategy after acute stroke. Early inflammatory responses occur after an ischemic insult leading to neuroinflammatory processes in the affected brain area. Intracellular receptors sensing pathogen or danger-associated molecules termed inflammasomes, such as NLRP3, NLRP1b, NLRC4 or AIM2, are part of the innate immunity. 17β-estradiol (E2) and progesterone (P) were neuroprotective and anti-inflammatory agents in several neuropathological animal studies. MicroRNAs (miRNA) are small nucleotide sequences regulating mRNA expression and translation on the post-transcriptional level. MiR-223 is a natural regulator of the inflammasome NLRP3.

I used a rat transient medial cerebral artery occlusion model (tMCAO) to address the role of inflammasomes and miR-223 in stroke pathology. Additionally, I used an *in vitro* hypoxia approach to investigate the impact of hypoxic conditions of inflammasome activation in the microglia-like cell line BV-2 and primary astrocytes. Finally, I studied the impact of E2 and P on inflammasome expression and activation as well as miRNA-223 regulation. Ischemia lead to increased expression profiles of several cytokines (IL1β, IL18, and TNFα) and inflammasome components. I found that hypoxia selectively and time-dependently induced inflammasome components such as NLRP3 and ASC on the gene and protein level. Further, I could allocate NLRP3 to neuronal cells and ASC to microglia. E2 and P selectively attenuated NLRP3, ASC and active Casp1 protein expression. In agreement, hypoxia regulated miR-223 expression, and gonadal steroids antagonized this effect. Hypoxia *in vitro* induced the expression of IL1β, NLRP3, ASC and AIM2 in BV-2 cells and astrocytes. E2 and P selectively dampened NLRP3 and ASC expression but showed no effect on Casp1 activity.

In conclusion, my data highlight the importance of early inflammasome activation for stroke pathophysiology. Since gonadal steroids are able to alleviate inflammasome activation, I assume that the neuroprotective mechanisms triggered by E2 and P are based upon their anti-inflammatory potential.

Zusammenfassung

Der Schlaganfall betrifft meist ältere Menschen und stellt die dritthäufigste Todesursache in technisch hochentwickelten Ländern dar. Leider sind trotz intensiver Forschungsarbeiten die pathophysiologischen Prozesse beim Schlaganfall kaum verstanden und neue therapeutische Ansätze fehlen. Die einzige bisher zugelassene Substanz ist der rekombinante gewebespezifische Plasminogenaktivator (rtPA). Nach einem Schlaganfall kommt es zu lokalen inflammatorischen Prozessen, bei denen Interleukin-1β (IL1β) eine wichtige Rolle spielt. An der Prozessierung von IL1β sind die Inflammasome (NLRP3, NLRP1b, NLRC4, AIM2) beteiligt. Dies sind intrazelluläre Rezeptoren, die sich nach Aktivierung zu Multiproteinkomplexen zusammenlagern und die IL1β Reifung ermöglichen. Das am besten untersuchte Inflammasom NLRP3 wird u.a. von kurzen RNA-Sequenzen (microRNAs, miRNA) reguliert. MiR-223 ist der bis heute bekannteste NLRP3 Suppressor. Weibliche Steroide, 17β-Östradiol (E2) und Progesteron (P), zeigen in Tierversuchen neuroprotektive Wirkungen, die auf einer Verringerung der Entzündungsreaktion beruhen. Es war Gegenstand dieser Studie, inwieweit E2 und P die Aktivierung von Inflammasomen regulieren. In Ratten wurde ein temporärer Schlaganfall durch Okklusion der *Arteria cerebri media* induziert. Zelltyp-spezifische Effekte wurden *in vitro* an BV-2 Zellen (Mikroglia ähnlich) und Astrozyten analysiert. Nach Hypoxie *in vitro* wurde die Regulation der Inflammasome, deren zelluläre Zuordnung und der Effekt der Hormone bestimmt. Meine *in vivo* Untersuchungen zeigten einen selektiven und zeitabhängigen Anstieg der Inflammasome NLRP3 und ASC und der Zytokine IL1β, IL18 und TNFα. E2 und P verminderten die Induktion von NLRP3, ASC und Casp1. Gleichzeitig konnte ich nachweisen, dass NLRP3 vornehmlich in Nervenzellen und ASC in Mikrogliazellen vorkommt. NLRP3, ASC und AIM2 wurden ebenso *in vitro* nach Hypoxie in BV-2 Zellen und Astrozyten induziert. Die Expression dieser Inflammasome wurde selektiv durch E2 und P abgeschwächt, wohingegen die Casp1 Aktivität durch E2 und P nicht beeinflusst wurde.

Diese Ergebnisse zeigen sehr deutlich die Bedeutung der Inflammasom Aktivierung für frühe pathologische Prozesse nach Schlaganfall. Beide Hormone hemmen die Aktivierung der Inflammasome. Daher ist anzunehmen, dass die neuroprotektive Wirkung beider Steroide vornehmlich auf der Kontrolle dieser inflammatorischen Komponenten beruht.

Table of content

List of figures

List of tables

List of abbreviations

Ago2	argonaute-2
AIM2	absent in melanoma 2
as	antisense
ASC	adaptor apoptosis-associated speck-like protein containing a CARD
AT	annealing temperature
BBB	blood-brain barrier
BCA	bicinchonic acid
BDNF	brain-derived neurotrophic factor
Bg	basal ganglia
BP	base pairs
BPU	blood perfusion units
CA	climbing ability
CARD	caspase activation and recruitment domain
Casp1	caspase-1
CCA	common carotid artery
cDNA	complementary deoxyribonucleic acid
CNS	central nervous system
$CoCl_2$	cobalt chloride
CSFCS	charcoal-stripped FCS
CT	computer tomography
Ct	cycle threshold
Cx	cortex
CycloA	cyclophilin
DAMPs	damage-associated molecular patterns
DMEM	Dulbecco's modified Eagle's medium
DTT	dithiothreitol
E2	17β-estradiol
EAIV	edema-adjusted infarct volume
EBBP	estrogen-responsive B box protein
ECA	external carotid artery
ERα	estrogen receptor α
ERβ	estrogen receptor beta

EREs	estrogen response elements
FCS	fetal calf serum
FIIND	function-to-find domain
FO	forepaw outstretching
GAPDH	glyceraldehyde-3-phosphate dehydrogenase
GFAP	glial fibrillary acidic protein
h	human
HEPES	4-(2-hydroxyethyl)-1-piperazineethanesulfonic acid
Hif1	hypoxia inducible factor 1
HPRT	hypoxanthine-guanine phosphoribosyltransferase
i.m.	intramuscular
Iba1	ionized calcium-binding adapter molecule 1
ICA	internal carotid artery
ICC	immunocytochemistry
IF	immunofluorescence
IFF	immunofluorescence buffer
IHC	Immunohistochemistry
IL1β	interleukin-1 beta
iNOS	inducible nitric oxide synthase
IVIg	intravenous immunoglobulin
KCl	potassium chloride
LDH	lactate dehydrogenase
LRR	leucine-rich repeat
m	mouse
MCA	middle cerebral artery
$MgCl_2$	magnesium dichloride
miRNA(s)	microRNA(s)
miRqrtPCR	miRNA-semi-quantitative real time PCR
MM	master mix
M-MLV	murine leukemia virus
mPR	membrane-bound PR
NaCl	sodium chloride
NBD	nucleotide-binding domain
NeuN	neuronal nuclear antigen

NF-κB	nuclear factor-kappa B
NLR	NOD-like receptor
NLRC4	NLR family CARD domain-containing protein 4
NLRPs	NACHT, LRR and PYD domain containing proteins
NMDAR	N-methyl-D-aspartate receptor
NOD	nucleotide-binding oligomerization domain
NR100	amino-terminal domain of rodent NLRP1 of about 100 amino acids
Nrf2	nuclear factor E2-related Factor-2
nt	nucleotides
OGD	oxygen glucose deprivation
P	progesterone
PAMPs	pathogen-associated molecular patterns
PBS	phosphate-buffered saline
PCR	poly chain reaction
PFA	paraformaldehyde
Pol II	RNA polymerase II
PR	progesterone receptor
pre-miRNA	precursor miRNA
pri-miRNA	primary transcript miRNA
PRRs	pattern recognition receptors
PS	penicillin/streptomycin
PVDF	polyvinylidene difluoride
PYD	pyrin domain
PYHIN	pyrin and HIN domain-containing
qrtPCR	semi-quantitative real time PCR
r	rat
RIPA	radioimmunoprecipitation assay buffer
RISC	RNA-induced silencing complex
RNA	ribonucleic acid
ROS	reactive oxygen species
rpm	rounds per minute
RPMI 1640	Roswell Park Memorial Institute 1640 medium
RT	reverse transcription
rtPA	recombinant tissue plasminogen activator

s	sense
S	species
SA	spontaneous activity
SDS	sodium dodecyl sulfate
SDS-PAGE	SDS polyacrylamide gel electrophoresis
SERM	selective estrogen receptor modulator
SF	sensory function
SREBP	sterol regulatory element binding protein
STAT3	signal transducer and activator of transcription 3
SW	spontaneous walking
TBI	traumatic brain injury
TBS	Tris-buffered saline
TBST	TBS–Tween 0.01 %
THP	tetrahydroprogesterone
TLR	Toll-like receptor
tMCAO	transient middle cerebral artery occlusion
TNFα	tumor necrosis factor α
TTC	2,3,5-triphenyltetrazolium chloride
UP	ultrapure water
UTR	untranslated region
V	volts
vs.	versus
WB	Western Blot
wt	wild type
XIAP	X-linked inhibitor of apoptosis protein

1. Introduction

1.1. Stroke

Stroke is the third most common cause of death in the developed countries after coronary heart disease and cancer. About 5.5 million people died 2013 worldwide after suffering of stroke [1]. Of those who suffer from stroke, around 60 % die or become dependent. Those who survive a stroke attack need afterwards ongoing care and rehabilitation that is associated with high costs for the health system and their families. The world health organization presents numbers which show that about 3 to 4 % of the National Health Service per country is spend for medical care and therapy after stroke [1]. There is a variety of risk factors leading to stroke such as high blood pressure, smoking, arteriosclerosis or diabetes. The highest predictors of death from stroke are the age, i.e. people aged 65 years and older, and those with a previously experienced stroke. Therefore, therapy and intensive medical care to reduce a second stroke attack is important. In the focus of many studies worldwide is the understanding of the underlying pathophysiological processes of stroke and the development of novel and effective treatments [2]. Until now, only the intravenous thrombolysis therapy has proven as an effective pharmacologic treatment strategy after acute stroke [3]. More than hundred controlled clinical trials have failed in the past [4] to show clear neuroprotective effects in stroke therapy, although preclinical testing in animal models was promising [5]. The understanding of the processes leading to cell death after an ischemic event is important to develop new strategies that will allow the transfer of information gained from animal experiments to the clinic.

1.1.1. General aspects of stroke

Stroke is an event where reduced blood flow in a brain region results in cell death and tissue damage. This is also known as cerebrovascular accident, cerebrovascular insult or ischemic brain attack. There are two major types of stroke. First, ischemic stroke results from a lack of blood flow and second, hemorrhagic stroke that is the result of an intracerebral bleeding caused by leaking or a burst of blood vessel in the brain. Both types finally lead to a dysfunction of those brain areas which were supplied by the affected blood vessel [6]. The incidence for both types differs depending on the sources and date of the statistical data. Nevertheless, the most

prominent type of stroke is the ischemic form (approximately 80 – 90 %), whereas hemorrhagic stroke is a more rare case (10 – 20 %) [7,8]. In addition, a small number of incidents cannot be attributed to one of the above forms [9].

Ischemic stroke results from a transient or permanent reduction in cerebral blood flow that is restricted to the territory of a major brain artery [10]. Occlusion of large intracranial arteries accounts for 79 % of ischemic stroke cases, where the *Arteria cerebri media* (middle cerebral artery, MCA) is the most frequently affected vessel followed by the *A. carotis interna* (internal carotid artery) [11]. In consequence, stroke has subdivided into a reversible ischemic vs. a progressive from. On the one hand, neurological symptoms that occur in a reversible stroke decline and demise within 24 h after onset. On the other hand and linked with the progressive form, neurological dysfunction can persist for hours and days without remission resulting in a long-lasting motoric- and sensory-functional disability including speech disorders [12]. By now, recombinant tissue plasminogen activator (rtPA) is the only successfully used therapeutic agent. But the timeframe of rtPA application is short and the medical guidelines only allow to use this compound within the first 4.5 h after the onset of ischemia [13]. Further, it is crucial within this timeframe to exclude a hemorrhagic event by the use of computer tomography (CT) or magnetic resonance scanning (MRT) because in such a case, rtPA would worsen the clinical scenario (bleeding). The immediate thrombolytic recanalization after diagnostic determination of an ischemic stroke results in considerable recovery, smaller infarcts and ameliorates the functional outcome [14,15]. Nevertheless, after failure of many translational clinical trials to replicate animal *in vivo* studies of neuroprotective drugs, rtPA treatment is still the only treatment after acute ischemic stroke [16].

1.1.2. Stroke pathophysiology

Brain function depends on the continuous delivery of oxygen and glucose through blood flow, and interruption of the cerebral blood supply leads to irretrievable brain damage [2]. In an occurring cerebral ischemia, damage is causing a cascade of cellular and molecular events triggered by the sudden lack of blood flow and subsequent reperfusion of the ischemic territory. Neurons are more prone to oxygen/glucose deprivation and therefore more vulnerable than glia or vascular cells. Nerve cells become quickly dysfunctional or die when exposed to hypoxic conditions [17]. In the most common type of stroke, the transient occlusion of the middle cerebral artery (tMCAO), the acute damage is more rapid and severe in the center of the

ischemic territory, the so-called ischemic core, due to the lowest blood flow in this area [2]. In the periphery of the ischemic region (so-called ischemic penumbra or peri-infarct zone), neuronal damage develops more slowly. In this particular area, blood supply also comes from adjacent vascular territories (collateral flow) and therefore, cerebral perfusion is kept above the threshold for immediate cell death [2]. Energy failure is the major mechanism of cell death in the ischemic core, where neurons cannot generate ATP without oxygen and glucose. Thereby, ATP is an energy source for ionic pumps, mainly Na^+- K^+ ATPase, to maintain the ionic gradient across the neuronal membrane [17]. Linked with the failure of the ionic pumps is a massive cytoplasmic accumulation of Na^+ and Ca^{2+} ions which results in tissue swelling (edema) and degeneration of the organelles, loss of the membrane integrity and necrotic termination of the cell [2]. In contrast, blood flow reduction in the penumbra is not sufficient to cause energy failure, so that neurons remain at a fine line between viability and vulnerability to pathogenic events after an ischemic insult [2]. Excessive extracellular accumulation of glutamate is an additional major factor contributing to the demise of the ischemic penumbra. In consequence, NMDA subtypes of glutamate receptors are over activated leading to cytoplasmic accumulation of Ca^{2+}. Finally, Ca^{2+}-dependent enzymes, including the proteases calpain and caspase, and enzymes producing nitric oxide, free radicals and arachidonic acid metabolites are activated [17]. These events lead to necrosis or programmed cell death depending on the intensity of the insult and the metabolic state of the neurons [2,17]. At the end of the ischemic cascade, injured or dying cells have a key role in post-ischemic inflammation because they release danger signals that activate the immune system.

1.1.3. Neuroinflammation

Neuroinflammation is a natural response and important defense mechanism in the brain to eliminate the initial cause of brain cell injury and necrotic cells. After an acute boost of local inflammatory responses and failure of restoring brain homeostasis, neuroinflammation becomes a chronic condition that erodes the surrounding tissues and causes late sequela. Under such conditions, tissue deterioration and healing proceed simultaneously. Otherwise, uncontrolled or extended neuroinflammation is harmful and can induce rapid neuronal death in the ischemic core which progressively expands toward the penumbral area [18,19]. In the penumbra, a subset of inflammatory mediators, reactive oxygen species (ROS) or proteases disrupt

the blood-brain barrier (BBB) and stimulate the formation of gliosis which elevates the vulnerability of neurons following ischemia [20]. Processes such as Ca^{2+}-induced activation of intracellular signaling pathways, the rise of ROS and the condition of hypoxia itself all trigger the expression of a number of pro-inflammatory genes such as nuclear factor-kappa B (NF-κB), hypoxia inducible factor 1 (Hif1), tumor necrosis factor alpha (TNFα) or interleukin-1beta (IL1β) [21,22]. Additionally, the local secretion of chemokines attracts and activates surrounding microglia as well as astrocytes [23]. Microglia can undergo morphological transformation into a phagocytic state which is capable of releasing a variety of cytotoxic and/or cell protective substances [24]. Microglia activation is evident already 30 min after ischemia with increasing numbers of activated microglial cells progressively over time [25]. It is not fully clear, whether microglial activation is solely destructive. Nevertheless, there is good evidence that activated microglia is worsening brain injury after ischemic stroke. Suppression of microglia activation leads to a smaller infarct size or positive neurological outcome [26,27]. *Vice versa*, phagocytic microglia can eliminate infiltrating neutrophils releasing inflammatory mediators and excitotoxic toxins from the extracellular space resulting in a positive outcome after stroke [28]. Additionally, microglia can synthesize and release several compounds that promote neuronal survival and brain tissue repair in the event of brain injury [29,30]. It is well known that astrocytes carry out a variety of critical functions, including scavenging free radicals, prevention of excitotoxicity and maintenance of ionic homeostasis which are all important to guarantee normal brain homeostasis and function [19,31]. Astrocytes are also activated following brain ischemia resulting in a functional switch leading to an increased production of intermediate filament proteins and a general phenomenon called reactive astrogliosis which is characterized by profound morphological and functional changes [32]. Additionally, astrocytes can act like microglia and participate in brain inflammation by releasing cytokines and nitric oxide synthase (iNOS) as well as factors that can induce additional microglial activation [33].

1.2. Inflammasomes

The CNS is as an “immune-privileged” organ due to the presence of a selective BBB that hampers the entry of foreign pathogens and immune mediators. Consequentially, all neural cells and not only local microglia participate in the control of neuroinflammatory processes. Multi-protein complexes termed inflammasomes play a decisive role for the initiation and perpetuation of inflammation in the central nervous

system (CNS) and therefore, inflammasome-mediated pathways are under intensive investigation [34,35]. The innate immunity is the first line of the host defense whether sterile or non-sterile (pathogenic) inflammation occurs. The activation of inflammasome components in innate brain immune cells typically reflects one of the primary and critical steps of neuroinflammation. In consequence, activation is triggered by harmful stimuli and traumatic challenges through pathogen-associated molecular pattern (PAMPs) and damage-associated molecular pattern (DAMPs) molecules followed by chemokine and cytokine production and release [36]. Different receptors on the membrane surface, like Toll-like receptors (TLR), or at the intracellular level, like different NOD-like receptors (NLRs), are able to sense PAMPs (infectious stimuli) or DAMPs (non-infectious stimuli). Both types belong to pattern recognition receptors (PRRs) discriminating the presence of PAMPs or DAMPs to trigger an inflammatory cascade. Intracellular NACHT, LRR and PYD domains-containing proteins (NLRPs) are the most studied and best characterized protein complexes during inflammation, and in particular NLRP3 [37,38]. NLRP inflammasomes such as NLRP1 and NLRP3 belong to cytosolic macromolecular complexes comprising the NLRP receptor, the adaptor apoptosis-associated speck-like protein containing a CARD (ASC) containing a caspase activation and recruitment domain (CARD), precursor caspase-1 (Casp1), precursor caspase-11 and/or X-linked inhibitor of apoptosis protein (XIAP) [39]. Most NLRPs contain a pyrin domain (PYD), a nucleotide-binding domain (NBD) needed for oligomerization and a carboxy-terminal leucine-rich repeat (LRR) representing the putative sensory component [40]. In the case of NLRP1, further domains occur in comparison with NLRP3, such a unique function-to-find domain (FIIND) and CARD, leading to caspase activation without ASC recruitment. Interestingly, in murine NLRP1, the PYD domain found in human NLRP1 is replaced by an NR100 domain (amino-terminal domain of rodent NLRP1 of about 100 amino acids) resulting in three homologs, NLRP1a, NLRP1b and NLRP1c [40]. Second, murine NLRP1 inflammasome components are preassembled before activation in the CNS, whereas human unassembled NLRP1 active complex is rapidly formed after stimulation [41,42]. NLR family CARD domain-containing protein 4 (NLRC4) has a CARD instead of a PYD domain in its structure compared to NLRP3, so that NLRC4 can activate caspases without ASC recruitment. Absent in melanoma 2 (AIM2) belongs to the pyrin and HIN domain-containing (PYHIN) inflammasomes and consists of two major domains. First, a C-terminal

DNA-binding HIN and, second, an N-terminal PYD domain which interacts with ASC after sensing and binding double stranded DNA [43]. Figure 1 summarizes the present knowledge about the composition of the different inflammasome complexes and structural-functional units.

After performing tissue expression profiles in pilot studies, we can assume that the CNS is fully equipped with the inflammasome components. In the mouse brain, NLRP1 and NLRP3 inflammasomes are localized in neurons and microglia, respectively [44–46]. Further, mouse microglia express parts of the NLRP3 and NLRC4 inflammasomes [47,48], whereas AIM2 and NLRP1 inflammasomes are mainly expressed in neurons [46,49]. A two-step model is widely accepted and described for NLRP3 inflammasome activation. In the first priming step, pro-IL1β mRNA is expressed and the corresponding protein produced. This is followed by the second activation step that involves the recruitment of Casp1. Then, pro-IL1β is cleaved by Casp1 in the inflammasome complex into mature IL1β, which finally is released from the cell [50,51]. The priming and activation steps for NLRP3 are shown in Figure 2. Recently, it became evident that a novel NLRP2 inflammasome is expressed in human astrocytes and might have an important role in the CNS [52]. NLPR2 participates in the inflammatory cascade similar to the other known NLRPs, since it interacts with the P2X7 receptor and the pannexin-1 channel [52]. Beside its actions in inflammatory actions, NLRP2 was recently discovered in mouse oocytes and granulosa cells during folliculogenesis and described as a regulator of early embryogenesis and disappearing over time [53]. Knockdown of NLRP2 leads to an early embryonic arrest and suggest NLRP2 as a mammalian maternal effect gene required for normal embryonic development.

1.2.1. Inflammasomes and stroke pathophysiology

Stroke represents an almost prototypical paradigm for sterile inflammation [54]. NLRP3 expression is induced after cerebral ischemia in microglia and endothelial cells [55]. Further evidence shows that necrosis is mediated via NLRP3 and leads to sterile (non-infectious agents) inflammation after an ischemic insult [56]. Linked with NLRP3 activation, the application of different pro-Casp1 inhibitors into cerebral

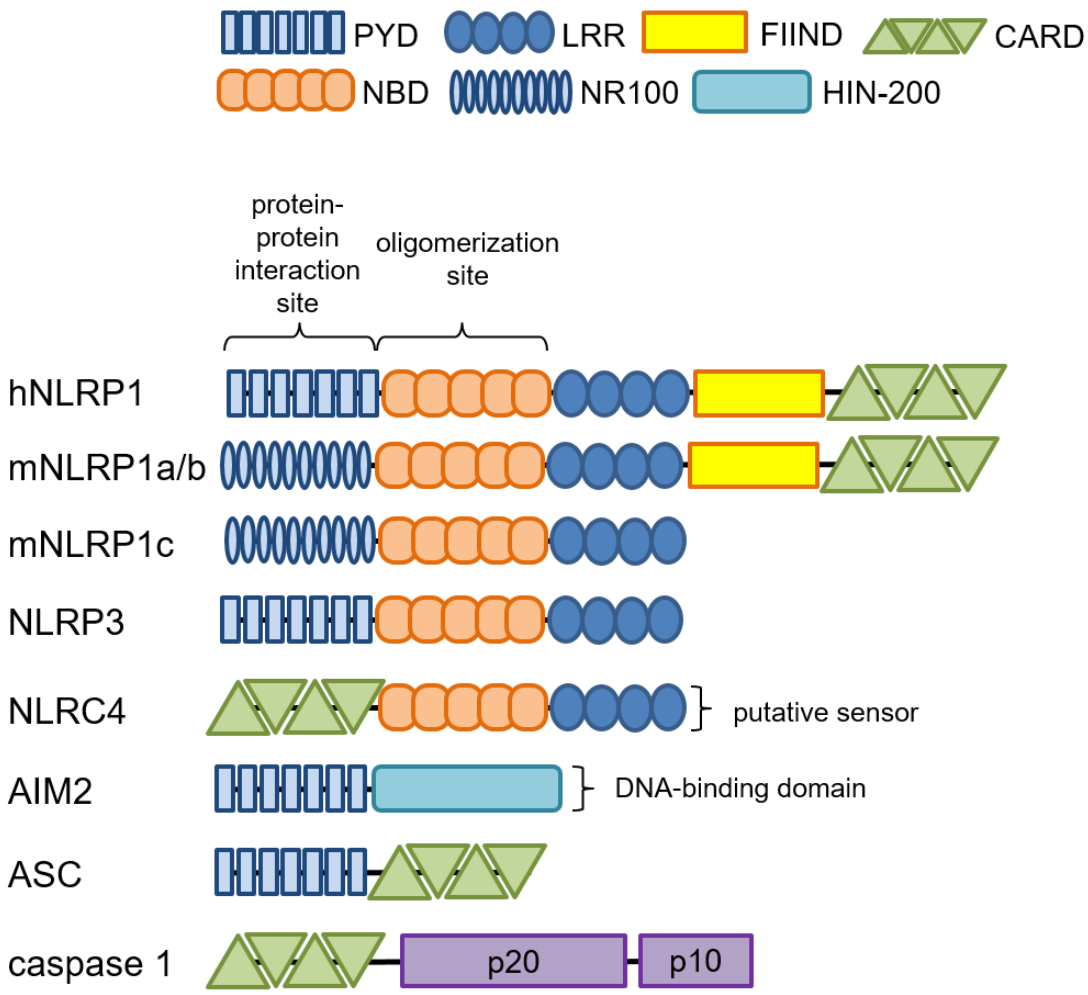

Figure 1: Schematic structure of inflammasome components

Basic structural composition of the different inflammasomes reveals protein-protein interaction- and oligomerization domains. Except AIM2, parts of the NLR inflammasomes are the NBD oligomerization and the LRR domain. Whereas NLRP3 and the human NLRP1 (hNLRP1) containing the protein-protein interaction side PYD, hNLRP1 is prolonged with the FIIND and CARD interaction domain. These domains are also present in the rodent subtypes NLRP1a/b but differ in the interaction domain carrying NR100 instead of PYD. Further, the subtype NLRP1c lacks the FIIND and CARD domains in rodents. NLRC4 contains CARD as protein interaction site. Therefore, except for rodent NLRP1c, all inflammasome components are able to interact with ASC through the PYD or CARD domains. ASC contains both, the PYD and CARD domains. Abbreviations are listed separately. The graph is adapted from Walsh et al. [40].

ventricles protects rodents against ischemic injury up to 7 days after the onset of cerebral ischemia [57–59]. This clearly demonstrates the participation of Casp1-

mediated pathways in stroke injury. Knocking out the NLRP3 gene or the administration of a blocking antibody IVIg against NLPR3 or NLRP1 in mouse results in a smaller infarct size and is supportive for the participation of inflammasomes in stroke [55,60,61]. These antibodies are also able to protect neurons in an experimentally-induced stroke model when neurons are either subjected directly to oxygen glucose deprivation (OGD) or co-incubated with OGD-treated microglia with reduced NLRP3 expression [55,60]. Thus, it is evident that both inflammasomes are active during an ischemic insult. Several mechanisms were discussed in the context of inflammasome activation. It is believed that ROS released from mitochondria in ischemia-affected brain areas take part in inflammasome activation and the induction of neuroinflammatory processes [55]. It is postulated after using ROS-inhibitors that ROS formation leads to NLRP3-priming, but it is not essential for NLRP3-activation itself [62]. Anti-oxidative cellular mechanisms are activated after stroke in rodent stroke models [63,64]. In this context, it is reported that nuclear factor E2-related factor-2 (Nrf2), a key player in the intracellular oxidative stress response, is required for NLRP3 and AIM2 but not NLRC4 activation [65]. ATP may also represent a major inflammasome-activating signal in cerebral ischemia. Extracellular ATP is able to direct systemic inflammation, tissue damage and mortality by regulating cytokine availability through inflammasome-dependent but also inflammasome-independent pathways [66]. NLRP1 and NLRP3 activation can also be achieved by intracellular low potassium levels or by K^+ efflux as shown in macrophages [67–69]. The latter changes in ion concentrations are the consequence of energy depletion after cerebral ischemia and are linked with P2X7 receptor opening which is conveyed by ATP [69]. To close the ATP loop, ATP is released by pannexin channels which take part in neuronal pyroptosis mediated via AIM2 after cortical neurons are stimulated with cerebrospinal fluid of patient with traumatic brain injury [49]. In addition, Denes et al. has shown a pivotal role for ASC during ischemic stroke in rodents and an independent activation of AIM2 and NLRC4 linked with ASC where NLRP3 was not required [70]. These findings together demonstrate the complexity of inflammasome regulation during stroke and are further complicated by more regulatory factors which seem to have an impact of inflammasome modulation in the brain, i.e. HMGB1, heat shock proteins or MRP14 [71–74].

1.3. MicroRNAs

MicroRNAs (miRNAs) are small, endogenous, non-coding RNA molecules that are generally 19-24 nucleotides (nt) long and cleaved from a 70-80 nt partially duplexed precursor (pre-miRNA). MiRNAs usually regulate gene expression at a post-transcriptional level and can therefore modulate diverse biological processes, including cell differentiation, cell cycle, proliferation, apoptosis and cellular responses to stress [75–77]. Transcription of miRNA genes occurs in different ways depending on the localization and origin of the miRNA gene. MiRNA transcripts were localized in intronic regions of non-coding transcripts. Smaller amounts were found in exonic non-coding transcripts. Additionally, miRNA-transcripts are also present in coding transcripts of the intronic region and in a minority of cases in the exonic region [78].

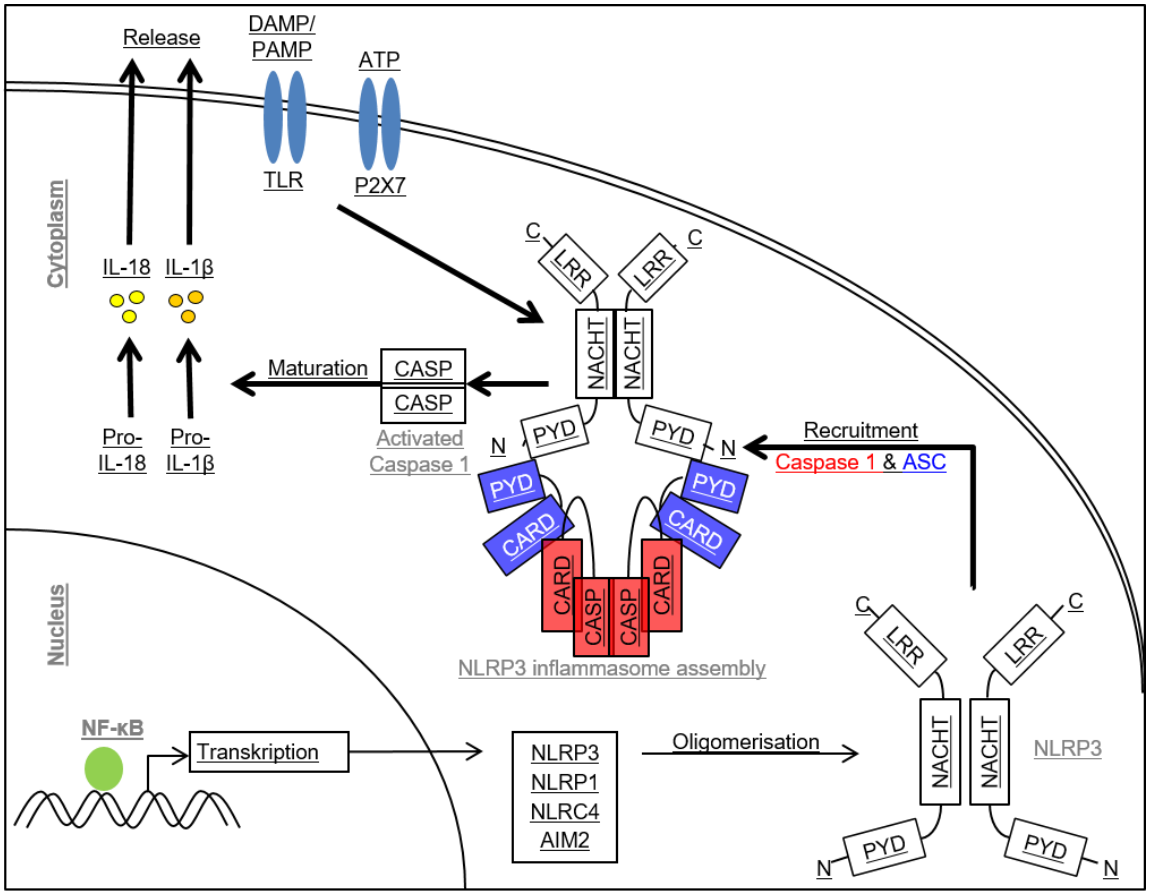

Figure 2: Schematic illustration of inflammasome activation

Depending on the different inflammasomes, DAMPs or PAMPs lead to oligomerization and recruitment of ASC and Casp1 that is followed by the maturing of the preforms of IL1β and IL18. These cytokines are released into the extracellular space. Besides oligomerization and activation, a priming step is part of the two-step model described for NLRP3 activation, leading to expression of distinct inflammasome component genes.

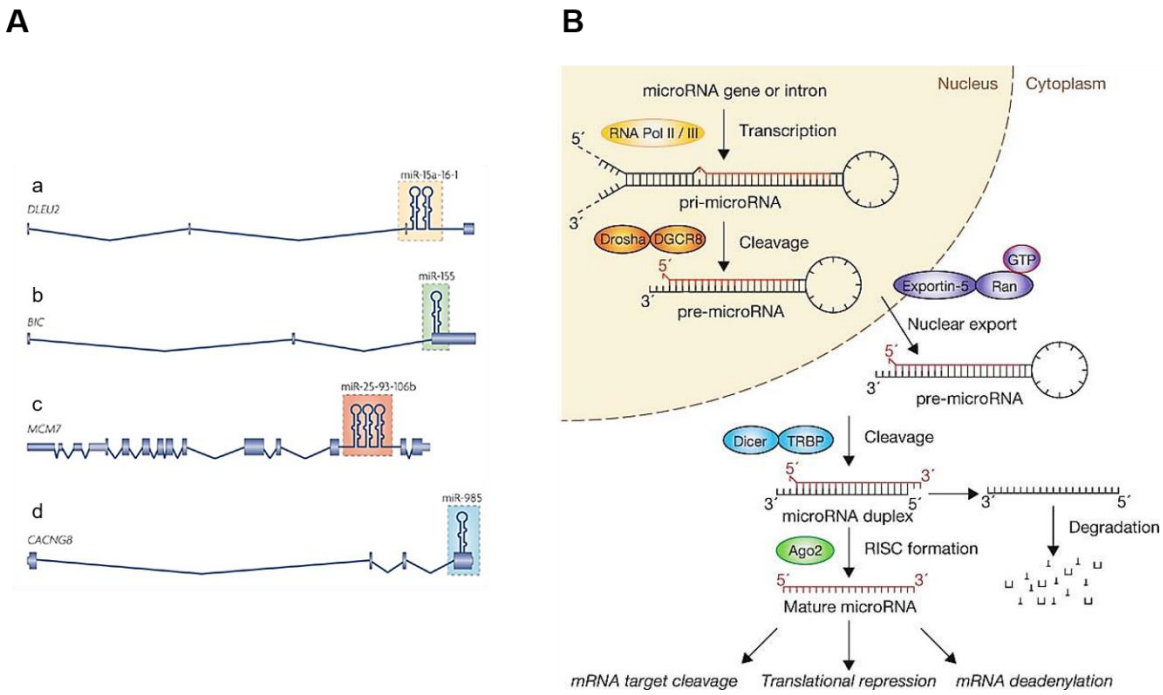

Figure 3: Schematic illustration of miRNA gene location and processing

(A) The cartoon shows the categorization of miRNAs according to their genomic locations relative to exon and intron position. (a) intronic and (b) exonic miRNA in non-coding transcripts; (c) intronic and (d) exonic miRNA in protein-coding transcripts. MicroRNA examples were highlighted above. (B) shows the linear canonical pathways of miRNA processing. First, miRNA gene is transcribed into pri-miRNA by RNA polymerase II or III followed by cleavage by the Drosha complex into pre-miRNA located in the nucleus. This pre-miRNA is translocated into the cytoplasm by the exportin-5 pathway where it is cleaved by the Dicer complex into mature miRNA duplex strands. One of these two is degraded, whereas the second one is loaded with Ago2 into the RISC complex, where it guides the RISC complex to silence target mRNA through mRNA cleavage, translation repression or deadenylation of target mRNA. The graph is adapted from Kim et al. (2009) [79] and Winter et al. (2009) [80].

Transcription of miRNAs can be initiated by an unique or a commonly shared promoter [79]. The function of RNA polymerase II (Pol II) leads to several kb long primary transcripts (pri-miRNAs) which are subsequently processed [81,82]. In the nucleus, pri-miRNAs are truncated by RNase III-type protein Drosha resulting in hairpin structures which are termed pre-miRNAs [78,83]. Next, pre-miRNAs are shuttled to the cytoplasm by the exportin-5 pathway where they are further processed by the Dicer endonuclease into mature approx. 22-nt long miRNA duplexes with a 3' overhang [84]. One of these two miRNA strands is loaded onto an Ago protein to gener-

ate the effector complex termed RNA-induced silencing complex (RISC), whereas the second miRNA strand is degraded [79]. Finally, the RISC complex containing the miRNA strand can bind to the 3′-UTR (untranslated region) of target mRNAs in a sequence-dependent manner. Supplementary, the RISC-miRNA complex can also bind to protein-coding regions as well as the 5′-UTR after forming heteroduplexes. This leads to post-transcriptional silencing by translational repression or/and mRNA degradation [85,86]. Figure 3 schematically summarizes miRNA gene localization and processing.

Due to the short binding sequence of miRNAs, each of them can have multiple binding targets and *vice versa* a given mRNA may have several miRNAs that can exhibit a regulatory function [87,88]. Therefore, several pathways can be regulated simultaneously by a concomitant focus on numerous target mRNAs [89,90]. The predicted targets of miRNAs are involved in inflammation, apoptosis and neuronal repair. Specific miRNAs play a critical role for the development of the brain, i.e. miR-9 or miR-153 in differentiating neurons. It is suggested that these miRNAs control distinct functions of the neuronal system [90,91]. Tissue-specific expression profiles are also demonstrated where i.e. miR-92b is higher expressed in rat hippocampus as compared to cortex tissue [92,93]. In the case of cerebral ischemia, it was shown that miRNAs, i.e. miR-34b or miR-498, revealed specific expression profiles in peripheral blood samples of young stroke patients when compared to healthy controls [94]. This group demonstrated additionally that miR-25 was upregulated in stroke-risk patients and was useable as a biomarker for stroke pathogenesis. During the course of cerebral ischemia, a participation of miRNAs for the regulation and tuning of distinct signaling pathways such as the toll-like receptors or NF-κB pathway is demonstrated [95].

1.3.1. miRNA-223

MiRNA-223 is a short RNA molecule and consists of 22 nt in mouse and humans (5´-UGUCAGUUUGUCAAAUACCCCA-3´) compared to rats, where the sequence is one nt shorter (5´-UGUCAGUUUGUCAAAUACCCC-3´). It is a hematopoietic-related miRNA with crucial functions in myeloid lineage development and granulocyte differentiation [96–98]. Nonetheless, association of miR-223 with other diseases like rheumatoid arthritis, sepsis or hepatic ischemia was shown [99–101]. Recently, Bauernfeind et al. presented data suggesting miR-223 as a strong suppressor of NLRP3 by negative regulation in myeloid cells [102]. In the nervous system,

miR-223 is normally expressed at low levels. Under conditions such as cerebral ischemia, miR-223 becomes more important and a neuroprotective function is attested, when miR-223 is overexpressed. In particular, the glutamate receptor subunits GluR2 and NR2B are targeted by miR-223 and their expression is inhibited which yields a positive outcome after induced ischemia [103].

1.4. Steroid hormones

The gonadal steroid hormones 17β-estradiol (E2) and progesterone (P) have many regulatory reproductive and other physiological functions in the brain and other organ systems. Besides, both hormones play a crucial role in the prevention and protection against cardiovascular diseases after menopause [104,105]. Linked with postmenopausal changes, neurodegenerative disorders also increase [106,107]. In general, both steroids can be attributed a neuroprotective role under acute brain challenging conditions (stroke, trauma etc.) but also for chronic degenerative brain diseases (Alzheimer´s disease, Parkinson´s disease etc.) [108–111]. Several of the mentioned disorders show clear-cut male-to-female ratios or are obviously associated with decreasing steroid plasma levels after menopause [112–114]. It has been proposed that the incidence rate and vulnerability for ischemic stroke shows a male-female prevalence [115,116]. In a number of experimental animal studies using different strategies (i.e. tMCAO) to analyze stroke characteristics and protective mechanisms, both steroids have been demonstrated to possess a solid neuroprotective potential [117–119].

1.4.1. 17β-estradiol

17β-estradiol, the primary female gonadal sex hormone, was used for decades to study the hormonal contribution for brain development and function. It was shown that E2 influences the development of a variety of neuronal systems and regulates physiological processes in the adult brain such as synaptic plasticity and neurotransmission [114,120]. Thereby, E2 modulates cognition, memory and fine motor skills, besides being a major regulator of neuroendocrine functions [121,122]. Furthermore, and as pointed out in section 1.4, E2 is a strong neuroprotective and antioxidative agent [123]. The two classical nuclear E2 receptors are found in astro- and microglia cells as well as in neurons [124–127]. Namely, estrogen receptor alpha and beta (ERα and ERβ) are expressed in various brain cell types. These receptors

typically interact with estrogen response elements (EREs) and modulate gene expression and cell function [125,128,129]. In addition, non-classical, non-nuclear E2 receptors such as GPER1 (earlier termed GPR30), ER-X and Gq-mER have been described in the brain similarly to other organs [130–133]. This clearly highlights the diversity and complexity of E2 signaling in the brain. Neuroprotection by E2 administration is mediated by different estrogen receptors depending on the disease model and brain regions. For instance, it was shown that neuroprotective effects of E2 were mediated by ERα and ERβ in a rat traumatic brain injury (TBI) model [134]. Interestingly, E2 neuroprotection depends on ERα signaling with ERβ as an antagonist and *vice versa* but neuroprotection is absent when both receptors synergistically operate. ERα is crucial for mediation of neuroprotection by E2 in neurons in a mice stroke model but deletion of ERα in microglia cells does not interfere with this neuroprotective effect of E2 [135]. On the other hand, attenuation of neuroinflammation in microglia cells is ERβ-driven by suppressing microglia activation [136]. Membrane associated ERs, like ER-X, interact with the MAPK pathway and activate signal-regulated kinases (ERK1 and ERK2) when E2 is bound [130]. ERα seems to be a negative regulator of this pathway. Recent studies highlight the importance of inhibition of the MAPK pathway, due to reduced infarct size and improved neurological score after stroke [137]. A mediation of neuroprotection by E2 was recently shown for the GPER1 receptor in the hippocampus after cerebral ischemia. Altogether, E2 has given an immensely variable role to play during neuroprotection.

1.4.2. Progesterone

Progesterone has multiple functions in the CNS similar to those described for E2 including stimulation of brain development, neuroendocrine control and modification of distinct neural functions related to non-endocrine brain regions [138]. As mentioned for E2, P also influences neuroprotective mechanisms, regulates neuroinflammation and interferes with neuroregenerative processes [138–140]. P effects are mediated through the classical intracellular progesterone receptor (PR) and non-classical membrane-bound PR (mPR) and GABA-A receptor [141–143]. The latter receptor mediates P action by the P metabolite 3α-THP [144]. These receptors are widely expressed in the CNS with no restriction to a specific cell type and are found in the cortex, hippocampus, hypothalamus and the cerebellum [145,146]. Activation and binding of P by PRs results in interactions of the PR complex with P response elements of distinct target genes [146] or activation of the MAPK pathway [147].

Even though E2 is more in the focus for its neuroprotective properties than P, there are some findings certifying the potential of P in neuroprotection [148]. The potential of P protection was shown in diverse brain injuries including stroke where P administration positively influences the short- and long-term outcome [117,118,149–151]. Moreover, it can dampen inflammation and oxidative stress as well as decrease edema after cerebral ischemia or TBI [152–156]. Further, P impact on reduction of neuroinflammation, oxidative stress and brain damage was recently shown in a repeated mild traumatic brain injury [157].

1.4.3. Steroid hormone interactions with inflammasome components and microRNAs

It is widely accepted that E2 and P, either individually or in concert, hamper the initiation and perpetuation of innate and adaptive inflammatory responses. These effects are due to their regulatory role for innate immune cells (T- and B-cells, microglia, macrophages) and immune-associated cells in the brain (astroglia) which carry the respective nuclear and non-nuclear steroid receptors at a variable extent and in relation to their activation status [158–163]. It remains unclear where and how these steroid hormones execute anti-inflammatory functions and how they influence inflammasomes and inflammasome-related components or actions.

The first observations concerning inflammasomes and tissue/brain destruction date back until 2002 [39]. Since that, only sparse information is available whether gonadal hormones act on inflammasomes in general or in CNS-related cells. For instance, P influences the inflammasome system of the uterus by targeting miR-199a and miR-214 inflammasome-related enzymes such as the cyclooxygenase-2 and others [164]. Further, P administration hampers TLR4 expression in a dose-dependent way at the mRNA level in peripheral blood mononuclear cells of pre-eclampsia patients and positively affects ROS formation, NF-κB signaling and recovery after TBI and in neurodegenerative disorders [165–168]. Both pathological stressors (ROS and NF-κB) of cell physiology and function are, in turn, identified as important stimulators and activators of the inflammasome multiprotein complexes [169,170]. More information is available regarding E2-mediated effects or E2-related pathways on inflammasome action. The estrogen-responsive B box protein (EBBP) builds a common platform with NLRP1 which leads to increased IL1β secretion in COS-1 kidney fibroblasts [171]. Again in the kidney, albumin-bound free fatty acids trigger

inflammasome expression and activation (NLRP3 and ASC) in human proximal tubule epithelial cells *in vitro* which is inhibited by the selective estrogen receptor modulator (SERM) raloxifene showing renoprotective effects [172]. An indirect upstream regulatory role for E2 in NLRP3 regulation is also most likely, since E2 up-regulates miR-223 levels in lymphocytes [173] and this miRNA subtype is one of the strongest transcriptional repressors of NLRP3 expression [102]. Both steroid hormones can affect miRNA expression by targeting miRNA biogenesis components [174]. It was also shown that E2 or P selectively increase mRNA and protein levels of exportin-5 and Dicer, key players in the miRNA biogenesis [175,176].

1.5. Author's contributions

Part of this work was published in a peer-reviewed manuscript. Name of articles and author's contributions are mentioned below:

Article:

Lammerding*, L., **Slowik*, A**., Johann, S., Beyer, C., Zendedel, A., 2015. Post-Stroke Inflammasome Expression and Regulation in the Peri-Infarct Area by Gonadal Steroids after Transient Focal Ischemia in the Rat Brain. Neuroendocrinology. 10.1159/000439435

* authors contribute equally to this work

Contributions:

Lammerding, L: performed in part hormone application, practical performance of gene expression study and NLRP3, NLRP1b and IL1β WB, IF stainings, part of manuscript preparation

Slowik, A: performed in part hormone application, sacrifice of the animals and TTC staining, sample preparation, gene selection, primer design, ASC WB, statistical analysis of gene expression study and densitometric determination of all WB data, microscopic images of IF stainings, manuscript preparation, references, discussion of review, grant holder

Johann, S: performed Casp1 WB

Beyer, C: conception of the project, manuscript preparation, discussion of review

Zendedel, A: performed tMCAO operation of all animals, manuscript preparation

I hereby declare that the above information is true.

Alexander Slowik

Place, date _____ Signature _____

1.6. Focus of the study

Experimental stroke research identified several potentially neuroprotective pharmaceutical agents which revealed promising results in the reduction of the infarct volume and behavioral deficits. Some of these compounds were targeting the ischemic cascade by suppressing inflammation. Others attempted to rescue neurons from apoptotic pathways and to ameliorate oxidative stress as well as ion- and neurotransmitter dysbalances. Unfortunately, none of these compounds achieved to receive a guideline-approved therapeutic agent for the treatment of stroke in humans [5]. This points at the existing pathophysiological differences between rodents and humans and highlights the special and complex ischemic scenario in man.

Irrespective of this failure to develop new therapeutic options, there is a clear demand to a better understanding of the stroke-related (early acute and late chronic) neuroinflammatory processes in the affected brain regions. A more profound knowledge of immune-related mechanisms in stroke is required [54,72].

The information about brain-intrinsic inflammasomes and neuroinflammation as well as miRNA-dependent mechanisms that regulates the inflammatory cascades is poor. Neuroprotective effects of E2 and P in stroke are well-documented. Not much is known whether inflammasome-driven inflammation is a target for both hormones. In this study, I have therefore analyzed (i) the chronological profile of inflammasome activation and miRNA regulation in rats during early and late periods after experimentally induced stroke in the penumbra, (ii) aimed at co-localizing inflammasome components to different brain cells, (iii) and tested the possibility that E2 and P might regulate inflammasome activation at the transcriptional and post-transcriptional level. For cellular studies, we established accurate *in vitro* hypoxic culture models including pure astroglia and BV-2 cells (microglia-like cell line).

2. Material and Methods

2.1. Animal care

The Review Board of the *Landesamt für Natur, Umwelt und Verbraucherschutz* (LANUV) formally approved animal care and experimental procedures for the care of animal subjects of the district government (North Rhine-Westphalia, Germany, file number: 84-02.04.2013.A212). All experiments involving animals are reported in accordance with the ARRIVE guidelines for reporting experiments involving animals [177,178]. 51 animals were used for the *in vivo* experiments. Wistar rats (Charles-River, Germany) were bred and maintained in a pathogen-free environment with a maximum of five animals per cage in a 12 h day and 12 h night cycle. Animals underwent routine cage maintenance according to the UKA Aachen guidelines once a week and microbiological monitoring according to the Federation of European Laboratory Animal Science Association recommendations. Food and water were available *ad libitum*.

Table 1: Animal numbers

MB: molecular biological methods, IF: immunofluorescence staining

time point	methods	E2 or P treatment	group size
sham	MB	-	4
sham	IF	-	2
6 h	MB	-	4
12 h	MB	-	4
24 h	MB	-	5
24 h	MB	+ / +	4 / 4
24 h	IF	-	2
24 h	IF	+ / +	2 / 2
72 h	MB	-	4
72 h	MB	+ / +	4 / 4
72 h	IF	-	2
72 h	IF	+ / +	2 / 2
		in total:	51

2.2. Stroke surgery

The method of tMCAO was adapted from the filament method described by Longa *et al.* 1989 [179] and modified as previously published [117,118,180] (see Figure 4). For our study, we used 12 weeks old male Wistar rats (300 – 350 g). During the whole operation procedure, animals were kept on a heating pad (Harvard Apparatus, USA) to maintain the body temperature at 37±0.5 °C. A thermometer was rectally introduced to measure the body core temperature. The animals were initially anesthetized with 4 % isoflurane (Abbott, Germany) for 2 min. Anesthesia was maintained with 2 % isoflurane during the whole operation process using a face mask (Harvard Apparatus, USA). After anesthesia, 100 µL (0.01 g) of metamizole (Novaminsulfon-ratiopharm, 1 g/2 mL injection solution, diluted 1:5, Germany) was applied intramuscular (i.m.) into the right hind limb. Then, the operation areas, ventral neck and dorsal head between both ears, were shaved and sterilized with 70 % (v/v) ethanol. After a skin incision, the skull was cleaned, dried with a cotton tip, and the bregma was exposed. For blood flow measurement, the skull was carefully thinned out with a drill 1 – 2 mm posterior and 4 – 5 mm lateral to the bregma on the left and right skull hemisphere were the sensors were placed. The skull was thinned out because of the limitation of the measuring depth of the sensors to assure that the reduction of the blood flow is not due to the reduction in external carotid artery (ECA) blood flow. The blood flow measurement was performed by placing the 2 mm Laser-Doppler measuring sensors (Moor Instruments VMS-LDF2, UK) into the drilled depression of the skull to measure the blood perfusion units (BPU). To ensure that the BPU digitized the cortical vascular territory of the MCA, the common carotid artery (CCA) was clipped temporary resulting in a decrease of BPU. Finally, the sensors were glued onto the skull with a tissue compatible medical adhesive and the skin incision was filled with this. Then, the rat was turned and following a small midline neck skin incision, the left CCA, internal carotid artery (ICA) and the ECA were exposed. First, the vagal nerve was carefully preserved and then the ECA transiently clipped with a small vessel clip (Aesculap AG, Germany). On the proximal site, the CCA was permanently ligated with a monofilament 5-0 (FST, Germany), and the ICA was transiently clipped with a vessel clip. Then, a vessel incision in the CCA was made 5 mm prior the bifurcation of the ICA and ECA. A commercial silicon-coated monofilament (diameter 0.41 mm, Doccol Corporation, USA) was

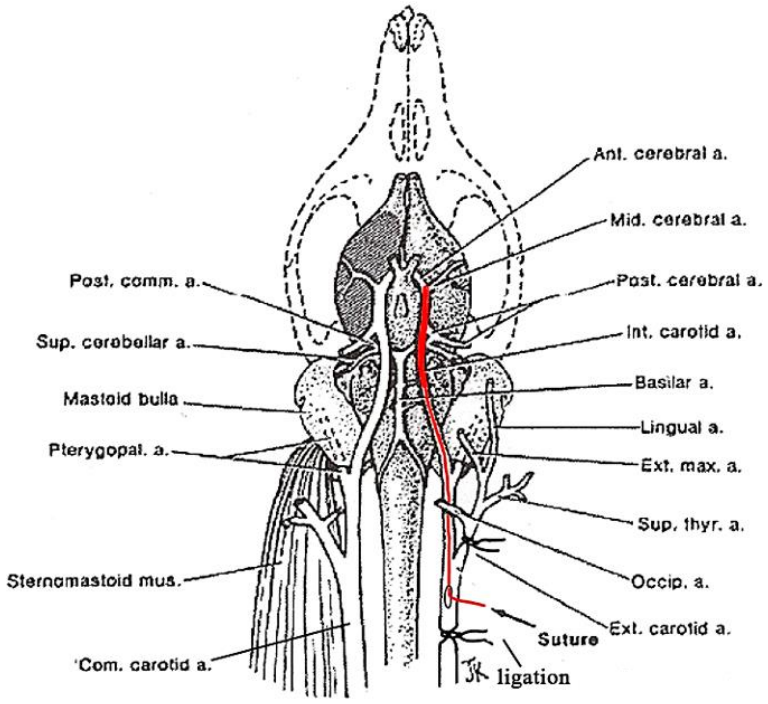

Figure 4: Schematic illustration of tMCAO

Schematic illustration of transient middle cerebral artery occlusion (tMCAO) by inserting a silicon-coated filament (red) into the common carotid artery and advancing it to the origin of the MCA through the internal carotid artery to reduce the blood flow in the MCA-supplied brain regions. Adapted and modified from Longa et al. (1989) [179].

subsequently introduced from the lumen of the distal CCA and pushed forward until mild resistance was perceived. To avoid a slip out of the filament or a slip down of the vessel clip resulting in bleeding off the CCA incision, a temporary security ligation was put around the distal site of the CCA prior the bifurcation of the ICA and ECA. The correct placement of the filament was monitored by BPU measurement resulting in decreased BPU on the ipsilateral side. Before insertion of the filament into the ICA, baseline BPU values were routinely monitored, also during the 2 h occlusion period until the sensors were removed again from the skull after filament withdrawal. Only those animals that showed a BPU drop of more than 50 % after MCAO and a return to nearly normal levels were included in the study. After 2 h of occlusion, the filament was removed and the security ligation was closed so that the CCA incision was flanked by permanent ligation to avoid bleeding. Next, the neck skin incision was sutured, the Laser-Doppler measuring sensors were removed and then, the head skin incision was finally sewed up with a 4-0 suture (B. Braun Melsungen AG, Germany). Sham-operated animals underwent the same anesthesia and surgical procedures with the exception of tMCAO. After tMCAO, animals were

monitored and kept under a heating lap until the animals finally woke up. Then, the animals were randomly assigned to the different experimental groups. Animals were allowed to recover for 6, 12, 24 or 72 h after tMCAO for time course studies and 24 or 72 h for steroid hormone treatment. Animal numbers and group strength are summarized in Table 1.

2.3. Hormone application

For hormone treatment, rats subjected to tMCAO received an application of vehicle (see below), E2 or P (Sigma Aldrich, Germany) in a randomized manner. Both steroids were initially diluted in pure ethanol as a solvent to a stock concentration of 1.25 µg/µL (E2) and 25 µg/µL (P). For application of the steroid hormones, a mixture of E2 (25 µg/kg body weight) or P (10 mg/kg body weight) in sesame oil in a final volume of 500 µL was given as a neck depot. Control animals received an appropriate amount of ethanol/sesame oil mixture (vehicle), where E2 or P was substituted with pure ethanol. The injection was given immediately after withdrawal of the filament and every 12 h after the occlusion until final sacrifice of the animal. All applications of hormones or ethanol/sesame oil mixtures were performed by a person blinded to the study after random assignment of the animal to an experimental group.

2.4. TTC staining

After ischemia, rats were sacrificed for tissue preparation at the indicated time points. Animals were deeply anesthetized with 5 % isoflurane followed by an intraperitoneal injection of a pentobarbital overdose (330 mg/kg). Then, the animals were transcardially perfused with ice-cold 0.9 % sodium chloride solution to remove the blood from the vascular system. After decapitation, brains were rapidly dissected out of the skull and placed into a brain matrix (stainless steel, 1 mm rat coronal 300 – 600 g, Harvard Apparatus, USA). Brains were cut into six consecutive 2 mm thick coronal sections and placed in 2 % 2,3,5-triphenyltetrazolium chloride (TTC, Fluka, Germany) solution in PBS to stain vital tissue for 15 min at 37 °C and 55 rpm on a rotary shaker (New Brunswick Scientific, Eppendorf, Germany). After that, slices were arranged in a frontal to occipital order and photographed using a digital camera (Canon Ixus 220HS). The unstained pale areas were defined as infarct area and further evaluated in a blinded manner using the open access image software ImageJ V1.48 (NIH, USA).

TTC staining delineates the transition zone from infarct to non-infarct area, thus representing the penumbra. This transition zone (for details see Figure 6) was dissected (micro-punches) and collected for further molecular and biochemical analysis. Samples of all consecutive slices (separated into ipsi- and contralateral side) were pooled.

2.5. Determination of the infarct volume

Infarct sizes were determined by measuring the whole area of the brain slice and separately the left and right hemisphere. Due to an appearing edema after stroke on the ipsilateral side, the infarct area was adjusted to remove the edema effect. Therefore, the area size was determined on each slice for the infarct area, the total brain area and the ipsilateral hemisphere. Then for each slice, the area of the contralateral side was divided by the area of the ipsilateral side and then multiplied with the infarct area. Finally, the infarct area was summed up of all slices and multiplied with the slice thickness (2 mm) to calculate the edema-adjusted infarct volume (EAIV, see formula 1, adjusted from [181]).

(1) $$EAIV = a_{IF} * \frac{(a_{tb} - a_i)}{a_i}$$

a_{IF}: area infarct volume
a_{tb}: area total brain slice
a_i: area of ipsilateral hemisphere

2.6. Tissue preparation

After slices were photographed, tissue samples were collected by micro-punching with a biopsy extractor (2 mm in diameter). The tissue biopsies were pooled separately for the ipsi- and contralateral side and immediately shock frozen in liquid nitrogen. For longer storage, samples were frozen at -80 °C. For RNA isolation, the phenol-chloroform extraction method was used. Samples were transferred into homogenization tubes containing homogenization beats (0.5 mm diameter, PeqLab, VWR, Germany) and 1 mL of peqGOLD RNA TriFast kit (PeqLab, VWR, Germany) was added. Samples were homogenized for 15 s at 5.000 rpm using the Precellys 24 homogenizer (PeqLab, VWR, Germany). Finally, 500 µL of the homogenate was transferred to a fresh 1.5 mL reaction tube (Sarstedt AG, Germany) and refilled with fresh TriFast to 1 mL. Samples were then placed on ice to proceed with total RNA-extraction (see section 2.11.1). The remaining 500 mL were frozen at -80 °C.

For protein isolation, 300 µL of radio immune precipitation assay (RIPA) buffer containing protease inhibitors (Roche, Switzerland) were added to tissue samples and homogenized following the same protocol described above (1 x 15 s at 5.000 rpm). After homogenization, samples were placed on ice for 30 min to reduce the foam, after that transferred into fresh 1.5 mL reaction tube and centrifuged for 30 min at 4 °C and 16.000 g to pelletize the cell debris. Then, the supernatant was transferred to a new tube and stored at -80 °C until further processing.

2.7. Cell culture cultivation

2.7.1. Primary astroglia cell cultures

Cerebral cortices were prepared from neonatal 1 to 2 day old mouse pups. The head was decapitated, the brain carefully removed and placed into preparation buffer to isolate both cortical hemispheres. All other parts of the brain as well as the meninges were removed. Then, cortices were minced and dispersed in Dulbecco's PBS (Gibco, USA) containing 1 % trypsin and 0.02 % EDTA (Gibco, USA) for 10 min. Afterwards, tissues were transferred into new tubes (Greiner Bio-One, Austria) containing Dulbecco's modified Eagle's medium (DMEM) supplemented with 10 % heat-inactivated fetal calf (FCS) serum (Gibco, USA), and streptomycin/penicillin (PS, 0.5 %, Invitrogen, Germany) and minced by pipetting several times up and down in sequence with a 10 mL serological pipette followed by a 5 mL pipette and an attached 1 mL tip on the 5 mL pipette. Finally, the cell suspension was filtered through a 40 µm nylon mesh and centrifuged at 400 g for 5 min. After discarding the supernatant, the cell pellet was re-suspended in culture medium and seeded on 75 cm^2 culture flasks coated with poly-L-ornithine (Sigma Aldrich, Germany) at a density of two mouse brains per flask. The cultures were grown at 37 °C in a humidified incubator with 5 % CO_2. After 3 to 4 days, the first medium change was performed and then every 3 days the procedure was repeated until the growth area was covered with a sealed cell layer. Then, cultures were splitted 1:3 after short incubation in 0.1 % trypsin and followed by a centrifugation step at 400 g for 5 min and growth again until the cell layer was confluent again. To split up astrocytes from other cell types, culture flasks were first shaken on a rotary shaker at 37 °C and 130 rpm for 120 min to detach microglia cells. After the microglia suspension was discarded, new culture medium was added and the culture flasks were shaken over night at 37 °C and 230 rpm to remove oligodendrocyte progenitor cells and other

debris. Finally, cells were seeded in the following cell densities. For gene expression 250.000 cells/well on 12 well culture plates and for immunocytochemistry (ICC) studies 50.000 cells/well on cover slips in 24 well culture plates and for FAM-FLICA Casp-1 activation 50.000 cells/well on 48 well culture plates were seeded. The final astroglia culture was characterized by >95 % homogeneity of glial fibrillary acidic protein (GFAP)-positive cells as it was routinely performed in our lab and has been described several times [182,183].

2.7.2. BV-2 cells

The BV-2 cell line, originally generated by Blasi and colleagues [184] by retroviral raf/myc-immortalization of neonatal murine microglia, was purchased from Banca biologica e cell factory (Centro di Risorse Biologiche, IRCCS Azienda Ospedaliera Universitaria, Genova, Italy). In previous work, we could show that this cell line is suitable for *in vitro* experiments and shows a similar reaction to hypoxic conditions like primary rat microglia cells [126,185].

BV-2 cells were maintained in a humidified environment at 37 °C and 5 % CO_2 and cultured in culture medium (see section 2.7.1, DMEM 10 % FCS 0.5 % PS). Due to the high proliferation rate of the cells, they were sub-cultured at the level of approx. 80-90 % confluence every other day. The supernatant was collected and the cell layer was washed once with PBS/EDTA buffer to remove all residues. Then, the cell layer was detached with 0.1 % trypsin and centrifuged at 400 g for 5 min. The cell pellet was re-suspended in culture medium and then re-seeded. For experiments, the cell pellet was re-suspended in Roswell Park Memorial Institute (RPMI, glutathione 0.001 mg/mL, l-glutamine 0.3 mg/mL, sodium bicarbonate 2.0 mg/mL, vitamins, amino acids, HEPES) medium 1640 without phenol red (Gibco, USA) adjusted to 1 mg/mL glucose and supplemented with 5 % hormone-free charcoal-stripped FCS (CSFCS, Gibco, USA) and 0.5 % PS. Finally, cells were seeded in the following cell densities. For gene expression and protein studies, 400.000 cells/well on 12 well culture plates and for ICC studies 50.000 cells/well on cover slips in 24 well culture plates were seeded. For FAM-FLICA Casp1 activity, 50.000 cells/well were seeded on a 48 well culture plate.

2.8. Steroid hormone treatment

One day before starting hypoxia, the culture medium was changed to the starving medium RPMI 1640 with decreased glucose containing 5 % CSFCS and 0.5 % PS

for both, astroglia and BV-2 cells. This nutrient-deprived exposure abated cell-specific basic mRNA expression stress- and immune-related parameters [118,185]. Therefore, gradually decreasing of glucose and FCS represents a prerequisite to configure a basal threshold to investigate potential up- or down-regulation of hypoxia-inducible factors. Note, that for steroid hormone treatment, FCS was exchanged to steroid-free charcoal-stripped fetal bovine serum during pre- and hormone treatment. For hormone treatment, water-soluble and cell culture tested E2 and P (both Sigma Aldrich, Germany) were initially diluted in pro analysis ethanol to yield a concentration of 10^{-2} M. Then they were further diluted in the treatment medium (RPMI 1640 1 % CSFCS 0.5 % PS) to a concentration of 10^{-4} M. In the last step, these pre-dilutions of E2 or P were diluted again in treatment medium to their final concentration of 10^{-7} M that corresponds to 27.24 ng/mL (E2) and 31.45 ng/mL (P). Controls were treated with the same concentration of ethanol in the treatment medium.

2.9. Hypoxic stimulation

Hypoxic conditions were set up in a cube-shaped hypoxia chamber that was flooded with inert nitrogen gas to replace the oxygen 15 min prior the experiment. Oxygen levels were continuously monitored using an oxygen detector (GOX 100T, Greisinger Electronic GmbH, Germany). The chamber was covered with a separate water jacket warmed up to 42 °C above an external water bath to maintain 37 °C within the chamber. This experimental set up was successfully used to create hypoxia and mimic ischemic conditions [185–187]. Additionally, minor modifications were made to the set up. First, the nitrogen gas was warmed up prior flooding the chamber by a respiflo (Covidien, Germany) placed in the water bath to compensate temperature fluctuations due to the nitrogen gas tanks were kept outside the building. Second, a further oxygen and temperature probe (FireStingO_2, PyroScience, Germany) was placed inside the chamber to measure the inner oxygen and temperature levels (see Figure 5 for detailed experimental set-up). Cells were exposed to

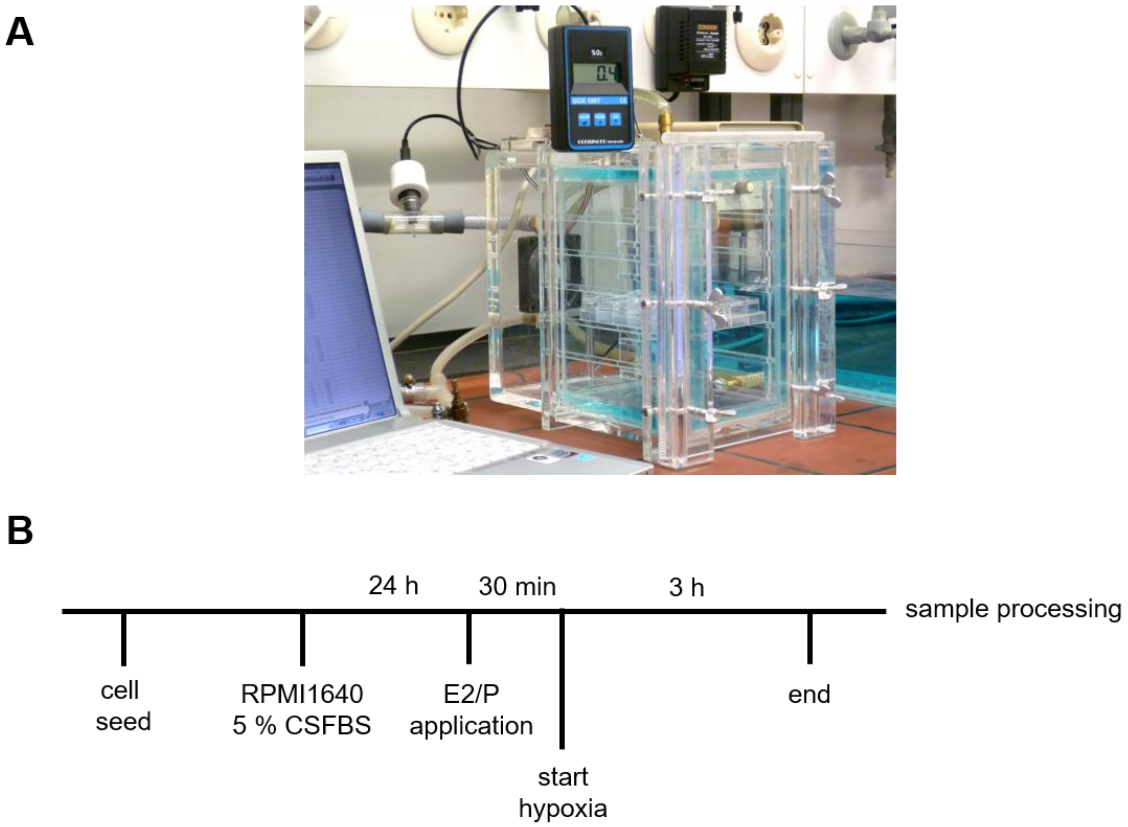

Figure 5: Experimental set-up of the hypoxic chamber used for *in vitro* experiments

(A) The chamber was tempered at 37 °C by using a water bath. The oxygen concentration was measured within the chamber and in the exhaust gas. All data were electronically monitored during the experiment. (B) Trial procedure for *in vitro* hypoxia experiments in astrocytes and BV-2 cells. To prevent cell proliferation, BV-2 cells were seeded in RPMI1640 5 % CSFBS, whereas astrocytes were maintained in culture medium until a sealed monolayer stopped cell proliferation. Then, astrocytes received RPMI1640 5 % CSFBS for 24 h. Prior hypoxia, cells received new RPMI1640 1 % CSFBS medium containing E2 or P. After 3 h hypoxia or the corresponding normoxia, controls samples were processed accordingly.

hypoxia for 3 h with or without hormone supplementation. After that, samples were subsequently processed for gene expression or protein analysis.

2.10. Sample preparation

After hypoxia experiments, astroglia and BV-2 cells were processed as follows. For gene expression studies, the supernatant was discarded and 333 µL of PeqGOLD TriFast was added per well on ice. After a short incubation time, three wells per group were pooled into a fresh tube and frozen at -80 °C for later RNA isolation. For

Table 2: List of rat primers

AT, annealing temperature; bp, base pair length

Primer	Sequence	bp	AT
AIM2		186	62 °C
s	TGCTACGGAGCTGGTGTTTT		
as	ACTCCGTCCTGTCTGCAATG		
CycloA		196	65 °C
s	GGCAAATGCTGGACCAAACAC		
as	TTAGAGTTGTCCACAGTCGGAGATG		
GAPDH		196	60 °C
s	AACCCATCACCATCTTCCAG		
as	GTGGTTCACACCCATCACAA		
IL1b		170	62 °C
s	TGGCAACTGTCCCTGAACTC		
as	GTCGAGATGCTGCTGTGAGA		
IL18		152	61 °C
s	GGACTGGCTGTGACCCTATC		
as	TGTCCTGGCACACGTTTCTG		
NLRC4		98	60 °C
s	GGCTGAGGCCCACGTATAAA		
as	CTCCTCTGGCTCTCTGGACT		
NLRP1b		102	60 °C
s	GGGGCAGCCAAATCAAGTTC		
as	TGAGCGGTCATTGCAACTCT		
NLRP3		314	65 °C
s	TCTGTTCATTGGCTGCGGAT		
as	GCCTTTTTCGAACTTGCCGT		
Pycard (ASC)		80	64 °C
s	GCTGCAGATGGACCCCATAG		
as	ACATTGTGAGCTCCAAGCCA		
TNFα		168	64 °C
s	GGAGGGAGAACAGCAACTCC		
as	TCTGCCAGTTCCACATCTCG		

immunocytochemistry, the supernatant was discarded and cells were fixed with 3.7 % formaldehyde solution in PBS for 20 min at room temperature. Then, cells were washed three times with PBS for 5 min at room temperature and finally placed in PBS at 4 °C for later processing.

2.11. Gene expression

2.11.1. Total RNA extraction

Total RNA was extracted from tissue or cell culture samples following the manufactures protocol. Briefly, samples incubated for 5 min at room temperature to achieve complete dissociation of nucleotide complexes. Then, samples were transferred on ice and 200 µL of chloroform was added to the samples. After samples were homogenized for 5 to 10 s, they were incubated for 10 min on ice for phase separation. Note that after incubation the clear aqueous phase should be the upper face. Otherwise, samples had to be homogenized and incubated again for 10 min on ice. To enhance this effect, samples were centrifuged at 4 °C and 12.000 g for 10 min. Next, the upper phase was transferred into a new tube and 500 µL of isopropyl alcohol was added to each sample followed by homogenizing. To achieve higher RNA precipitation, samples were stored at -20 °C overnight. Next day, samples were centrifuged at 4 °C at 16.000 g for 60 min to pelletize the RNA. The RNA pellet was washed twice with 75 % (v/v) ethanol by discarding the supernatant and adding fresh ethanol and centrifugation at 4 °C for 12.000 g for 10 min. After that, the supernatant was discarded and the pellet was air dried for 10 to 30 min. Finally, the RNA pellet was dissolved in 12 µL RNAase/DNAase-free ultrapure water (UP, Gibco, USA) and incubated on a thermal shaker (Eppendorf, Germany) at 55 °C and 800 rpm. RNA purity and concentration were measured with a NanoDrop 1000 device (PeqLab, VWR, Germany). RNA was clarified as pure when the ratio 260/280 nm was above 1.9 and the ratio 260/230 nm above 2.0. The extracted RNA could be stored for longer time at -80 °C.

2.11.2. cDNA synthesis and PCR

Complementary DNA (cDNA) was synthesized using the M-MLV reverse transcription (RT)-kit. One µg of total RNA was diluted with UP to a final volume of 11 µL and incubated in a thermal cycler (Eppendorf, Germany) at 95 °C for 5 min followed by

an incubation step on ice for 5 min. Then, 8.1 µL of a master mix (MM) which contained 5x first strand buffer, 100 mM DTT, 10 mM dNTPs (Bioline. Germany), random hexanucleotide primers and M-MLV reverse transcriptase (all Invitrogen, Germany) were added per sample. After gentle mixing, the reaction was started in a thermal cycler at 37 °C for 50 min followed by an inactivation step at 70 °C for

Table 3: List of mouse primers

AT: annealing temperature; bp: base pair length

Primer	Sequence	bp	AT
AIM2		229	60 °C
s	CGACGTGGCAGATAGGACAG		
as	GGCAGCAGAGCAGTTTTCAG		
HPRT		249	62 °C
s	GCTGGTGAAAAGGACCTCT		
as	CACAGGACTAGAACACCTGC		
lL1β		229	61 °C
s	GCCCATCCTCTGTGACTCAT		
as	AGGCCACAGGTATTTTGTCG		
IL18		122	62 °C
s	GCCTGTGTTCGAGGATATGACT		
as	CCTTCACAGAGAGGGTCACAG		
NLRC4		86	64 °C
s	ATCGTCATCACCGTGTGGAG		
as	GCCAGACTCGCCTTCAATCA		
NLRP1b		94	64 °C
s	AGTAATCTGGAGGGGTTGGAC		
as	GTTGGCAGCCAGGGTATATCA		
NLRP3		113	65 °C
s	CCTGGGGGACTTTGGAATCAG		
as	GATCCTGACAACACGCGGA		
Pycard (ASC)		229	60 °C
s	GTGGGTGGCTTTCCTTGATT		
as	TTGTCTTGGCTGGTGGTCTCT		

15 min. For checking successful cDNA synthesis, a PCR was performed with hypoxanthine-guanine phosphoribosyltransferase (HPRT) for *in vitro* samples or cyclophilin (CycloA) for *in vivo* samples as control genes. Therefore, a master mix was prepared containing 9.3 µL UP, 1.25 µL 10x NH_4 reaction buffer, 0.38 µL $MgCl_2$ (50 mM), 0.25 µL dNTPs (10 mM), 0.08 µL Taq-polymerase (all Bioline, Germany) and the respective sense and anti-sense primers (0.25 µL each, see Table 2 and Table 3). Then, 1 µL of sample was added to the MM (11.5 µL), and the PCR reaction was conducted using a thermal cycler (Eppendorf, Germany) starting at 95 °C for 3 min, followed by 40 cycles of DNA amplification (30 s at 95 °C, 30 s at 62 (HPRT) or 65 °C (CycloA), and 45 s at 72 °C) with final extension at 72 °C for 5 min and hold at 4 °C. Primers were designed with Primer-BLAST[1]. PCR products were separated by electrophoresis using 2 % (w/v) agarose gels containing ethidium bromide (Roth, Germany) and running at constant 140 V for 25 min. Every PCR experiment included negative (UP) and positive controls. For visualization of lanes, a UV transluminator chamber E-Box VX2 (PeqLab, Germany) was used. When only one lane appeared at the appropriate size, it was assumed that no DNA contamination was present in the samples.

2.11.3. MicroRNA/cDNA synthesis

Complementary DNA of total RNA was synthesized using the Qiagen miScript II RT kit following a slightly modified manufacture protocol. Briefly, one µg of total RNA was diluted with UP to a final volume of 6 µL. After addition of the MM containing 2 µL 5x miScript HiSpec Buffer, 1 µL 10x miScript Nucleotide Mix and 1 µL miScript Reverse Transcriptase Mix for each sample, the reaction mix was incubated in a thermal cycler at 37 °C for 60 min. Then, the RT was inactivated by incubating the samples at 95 °C for 5 min. Finally, samples were diluted with UP 1:20 and a check PCR with miRNA U6 was performed to check successful transcription of mature miRNAs. A MM was prepared according to section 2.11.2 with slight modifications. The MM contained 1.5 µL less of UP water and therefore, 0.5 µL of each primer (forward and reverse) and 2 µL of sample were added instead of 1 µL. The PCR reaction was conducted using a thermal cycler starting at 95 °C for 3 min, followed by 40 cycles of DNA amplification (40 s at 95 °C, 30 s at 55, and 30 s at 72 °C) with final extension at 72 °C for 1 min and hold at 4 °C. All primers for miRNA-PCR and

[1] http://www.ncbi.nlm.nih.gov/tools/primer-blast/

miRNA-semi-quantitative real time PCR (miRqrtPCR) were designed using the freely available software miRprimer developed by Peter Busk (Busk, 2014). Separation and visualization of PCR products was performed as described in section 2.11.2.

2.11.4. Semi-quantitative real time PCR

Gene expression studies were solely performed with tissues corresponding to the penumbra or isolated and transcribed cDNA from primary mouse astrocytes or BV-2 cells. For semi-quantitative real time PCR (qrtPCR) an external standard was generated by 7 time repeated 2-fold dilution of total sample pooling. Note, that each sample was diluted 10-fold to adjust concentration within the range of the external standard. Measurement of expression levels of target genes was performed with a mixture consisting of 2 µL reversed-transcribed cDNA, 2 µL UP, 5 µL 2x SensiMix plus SYBR & Fluorescein (Bioline, Germany), and 0.5 µL primers (10 pmol/µL) using the MyIQ RT-qrtPCR detection system (Bio-Rad, Germany) in special 96-well plates (BIOPlastics, Netherlands) under following conditions: 10 min enzyme activation at 95 °C, 15 s denaturation at 95 °C, 40 cycles of 30 s at primer-specific an-

Table 4: List of miRNA primers

AT: annealing temperature; S: species; m: mouse; r: rat

Primer	Sequence	S	AT
miR-103-3p		m+r	58 °C
s	GCAGAGCAGCATTGTACAG		
as	GGTCCAGTTTTTTTTTTTTTTTCATAG		
miR-107-3p		m+r	56 °C
s	GCAGAGCAGCATTGTACAG		
as	GGTCCAGTTTTTTTTTTTTTTTGATAG		
mmu-miR-223-3p		m	57 °C
s	CGCAGTGTCAGTTTGTCA		
as	CCAGTTTTTTTTTTTTTTTGGGGTA		
rno-miR-223-3p		r	56 °C
s	GCGTGTATTTGACAAGCTGAG		
as	GGTCCAGTTTTTTTTTTTTTTTCAAC		

nealing temperatures, 30 s amplification at 72 °C, and 5 s fluorescence measurement at 72 °C. The target and the housekeeping genes (see Table 2 and Table 3*)* were measured at cycle threshold (Ct-values) by qrtPCR. Relative quantification was calculated by the ΔΔCt-method using the qbase+ software (Biogazelle, Belgium). Data were expressed as relative amount of the target to the housekeepers. Up- or down-regulation of genes of interest after stroke were graphical illustrated by fold change subjected to sham animals, and hypoxia was illustrated by fold change subjected to normoxia, respectively. Note that sham and normoxia were set to 1.

2.11.5. MicroRNA semi-quantitative real time PCR

For miRqrtPCR, each sample was diluted 20-fold. Measurement of expression levels of target miRNA genes was performed with a mixture consisting of 2 µL reversed-transcribed cDNA, 1 µL UP, 5 µL 2x SensiMix plus SYBR & Fluorescein (Bioline, Germany), and 1 µL primers (10 pmol/µL) using the CFXconnect RT-qrtPCR detection system (Bio-Rad, Germany) in special 96-well plates (BIOPlastics, Netherlands). The following conditions were chosen: 10 min enzyme activation at 95 °C, 15 s denaturation at 95 °C, 40 to 50 cycles of 15 s at primer-specific annealing temperatures, 10 s amplification at 72 °C with fluorescence measurement. The target and the housekeeping genes (Table 4*)* were measured at cycle threshold (Ct-values) by qrtPCR. Relative quantification was calculated by the ΔΔCt-method using the qbase+ software (Biogazelle, Belgium). Data were expressed as relative amount of the target to the housekeepers. Graphical illustration was done as described under 2.11.4.

2.12. Western blotting

For Western Blot (WB) analysis of *in vivo* samples, protein concentration was determined using the Pierce BCA protein assay kit (ThermoFisher Scientific, USA) following the manufactures protocol. Briefly, 10 µL of sample or standard were measured as duplicate by adding of 200 µL BCA solution to the samples and after incubation at 60°C for 10 min in a thermal incubator, the extinction was measured using a Tecan infinite M200 microplate reader (Tecan, Switzerland).

Protein samples were separated by 8 % SDS-PAGE (NLRP1, NLRP3) and 14 % SDS-PAGE (ASC, IL1β, Casp1). Samples were diluted with 6-fold Laemmli and

Table 5: Used antibodies

WB, Western Blot; IHC, immunohistochemistry; IF, immunofluorescence

antibody	company	WB	IHC	IF
β-actin	Sigma Aldrich, USA	1:5,000		
ASC	Santa Cruz, USA	1:1,000	1:500	1:250
Casp1	Santa Cruz, USA	1:1,000		
GFAP	Santa Cruz, USA			1:300
Iba1	Abcam plc, UK			1:300
lL1β	Abcam plc, UK	1:500		
NeuN	Cell Signaling, USA			1:500
NLRP1b	Cell Signaling, USA	1:500		
NLRP3	Bioss, USA	1:1,000	1:750	1:300

RIPA+ buffer to a concentration of 20-50 µg per lane and incubated at 95 °C for 5 min. Then, samples and a protein ladder (Life Technologies, USA) were loaded onto a 4 % stacking gel. Samples were separated initially by constant 80 V for 10 min followed by 140 V for 50-60 min. Then, samples were transferred on a methanol-activated PVDF membrane (Roche, Germany) either with a semi-dry transblot chamber (transfer buffer 1, 25 V const. for 50 min) or a wet/tank blot transfer system (transfer buffer 2, 80 V const. for 2 h) (both Bio-Rad, Germany) depending on the protein size of the target. After blotting, the blotting efficiency was checked by placing the membrane in methanol followed by incubation in 0.1 % Ponceau solution for 30 s. Then, the Ponceau solution was discarded and the membrane was washed twice in distilled water followed by washing two times in TBS–Tween 0.01 % (TBST) for 5 min until the red staining disappeared. Afterwards, the membrane was placed in methanol and dried at room temperature for 1 h. Before blocking with either 5 % or 1 % (only Casp1) dry milk for 60 min, the membrane was reactivated by placing in it methanol for a short period followed by a washing step in TBST. Finally, the primary antibody diluted in the blocking solution placed on the membrane and incubated over night at 4 °C. A list of used antibodies and dilutions is given in Table 5.
Next day, after washing and incubating with horseradish peroxidase-conjugated secondary antibodies for 1 h, labeled proteins were visualized using ECL™ Plus kit

(Pierce, USA). β-actin served as a loading control marker. For control, spinal cord tissue from wild type (wt) and NLRP3$^{-/-}$ mice (strain B6.129S6-Nlrp3^{tm1Bhk}/J, Jackson Lab., USA, a kind gift by Prof. Dr. Trautwein, Clinic for Internal Medicine, RWTH Aachen, Germany) was used. The WB bands were densitometrically evaluated with the program Quantity One (Bio-Rad, Germany). Bands were adjusted with their respective β-actin-bands. Subsequently, the values were referred to control (=1).

2.13. Immunofluorescence staining

2.13.1. *In vivo* tissue staining

For immunofluorescence double-labeling, formalin-fixed and paraffin-embedded sections (5 μm) were used. After rehydration through a descending alcohol concentration, slices were heat-unmasked by Tris/EDTA pH 9.0 buffer for 10 min. Then, slices were washed three times in PBS for 5 min and blocked in PBS containing 2 % FCS and 1 % BSA (IFF buffer) for 1 h followed by primary antibody incubation in blocking solution over night at 4 °C. A list of the used antibodies is given in Table 5. The following antibodies, anti-GFAP, anti-neuronal nuclear antigen (NeuN) and ionized calcium-binding adapter molecule 1 (Iba1) were either combined with ASC or NLRP3. Next day, slices were washed three times with PBS, and the secondary antibodies fluorescent anti-rabbit antibody (1:500; Alexa Fluor 488, Invitrogen, Germany) and anti-mouse/anti-goat antibody (1:500; Alexa Fluor 598, Invitrogen, Germany) were applied for 2 h at room temperature. After a washing step, Hoechst 33342 (Invitrogen, Germany, diluted 1:10,000 in PBS) was used to counterstain the nuclei for 10 min. Finally, slices were mounted using ImmuMount (ThermoFisher Scientific, USA). Fluorescence images for qualitative expression analysis were acquired with a Leica DMI 6000 B, whereas the co-localization study was performed with a Zeiss LSM 7 DUO confocal fluorescence microscope.

2.13.2. Immunocytochemistry

After hypoxia, cover slips were washed once with PBS and afterwards the cells were fixed with 3.7 % paraformaldehyde (PFA) in PBS for 20 min at room temperature. Then, cover slips were washed three times with PBS to remove the PFA. Subsequently, cells were permeabilized by an incubation with 0.2 % Triton-X for 15 min at room temperature and then washed and blocked in IFF buffer for another 15 min followed by primary antibody incubation in blocking solution over night at 4 °C. A list

of the used antibodies is given in Table 5. The following antibodies GFAP and Iba1 were combined with ASC and NLRP3 or Casp1. Next day, the primary antibody solution was discarded and the cover slips were washed with PBS followed by subsequent incubation with the secondary antibodies fluorescent anti-rabbit antibody (1:500; Alexa Fluor 488) and anti-mouse/anti-goat antibody (1:500; Alexa Fluor 598) for 2 h at room temperature. After a washing step, Hoechst 33342 diluted 1:10,000 in PBS was used for counterstaining the nuclei for 10 min. Finally, cover slips were mounted using ImmuMount. Fluorescence images were acquired with a Leica DMI 6000 B fluorescence microscope.

2.13.3. FAM-FLICA Casp1 staining

For determination of Casp1 activation after hypoxia the FAM-FLICA *in vitro* Casp1 kit (ImmunoChemistry Technologies, USA) was used. After hypoxia, the supernatant was discarded and the FAM-FLICA dye diluted 1:150 in treatment medium (RPMI 1640, 1 % CSFCS, 0.5 % PS) was placed for 1 h at 37 °C in the dark. Then, the FAM-FLICA reagent was discarded and cells were washed with the washing buffer diluted in PBS twice. Immediately after washing, fluorescence images were acquired with the Leica DMI 6000 B fluorescence microscope.

2.14. Data analysis

Values were analyzed for normal distribution using the Shapiro-Wilk normality test putting all values in one group. When the normality test was significant, values were BOX-COX-transformed after calculation of the optimal lambda using the trial version of NCSS 10 Statistical Software (2015). NCSS, LLC. Kaysville, Utah, USA, (ncss.com/software/ncss) and used for statistical analysis according to the Handbook of Biological Statistics (McDonald, 2014). Note that no optimal lambda was found for NLRP3 expression data collected in astrocyte cells passing the Shapiro-Wilk normality test. Therefore, these data were analyzed with the non-parametric Friedman's test followed by Tukey's post-hoc test. Intergroup differences were tested by two-tailed unpaired t-test (Casp1 expression in BV-2 cells), ANOVA two-way or ANOVA one-way followed by Tukey post-hoc test (multiple groups). All statistical tests were performed using NCSS 10 or GraphPad Prism 5 (GraphPad Software Inc., USA). Data are given as arithmetic means ± SEM. The p-values are given as $p \leq 0.05$, $p \leq 0.01$, and $p \leq 0.001$. Asterisks indicating sham vs. tMCAO ± treatment

or normoxia control vs. hypoxia control/E2/P, letters indicating tMCAO or hypoxia control vs. treatment.

3. Results

3.1. Progression of the infarct zone after stroke and the effect of steroid hormones

In the first set of experiments, the progression of the infarct zone was determined at various time points after stroke using TTC-stained coronal sections. As shown in representative images in the upper panel of Figure 6A, the infarct zone was mainly

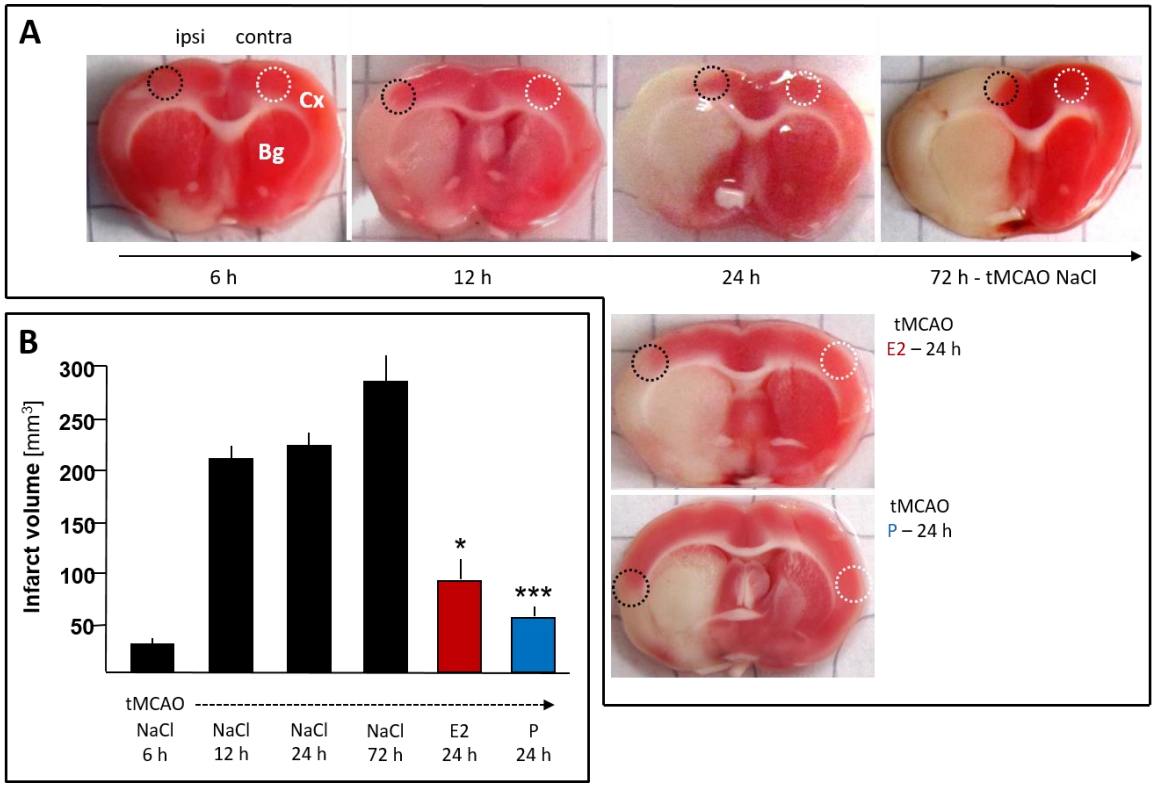

Figure 6: The effect of tMCAO and E2 or P treatment on the infarct volume in male rats

(A) Shows a series of TTC-stained 2 mm coronal sections at different post-hypoxic intervals taken at bregma +0.25 mm. Note the time-dependent spreading of the pale infarct zone and the reduced infarct area after E2 or P administration compared to untreated animals corresponding to 24 h post-stroke. Black and white circles indicate the micro-punched ipsilateral (peri-infarct area) and contralateral cortex areas, respectively, taken for molecular and biochemical analysis. These areas shifted according to the reduced infarct area after E2 or P administration. (B) Quantitative determination of the infarct volume and representative TTC-stained slices. E2 and P substitution significantly reduced the infarct volume mainly in the Cx. *p≤0.05, ***p≤0.001; E2 or P-24 h vs. NaCl-24 h. Data represent the means ± SEM. Abbreviations: Cx: cerebral cortex; Bg: basal ganglia. Modified from Lammerding et al. (2015) [188].

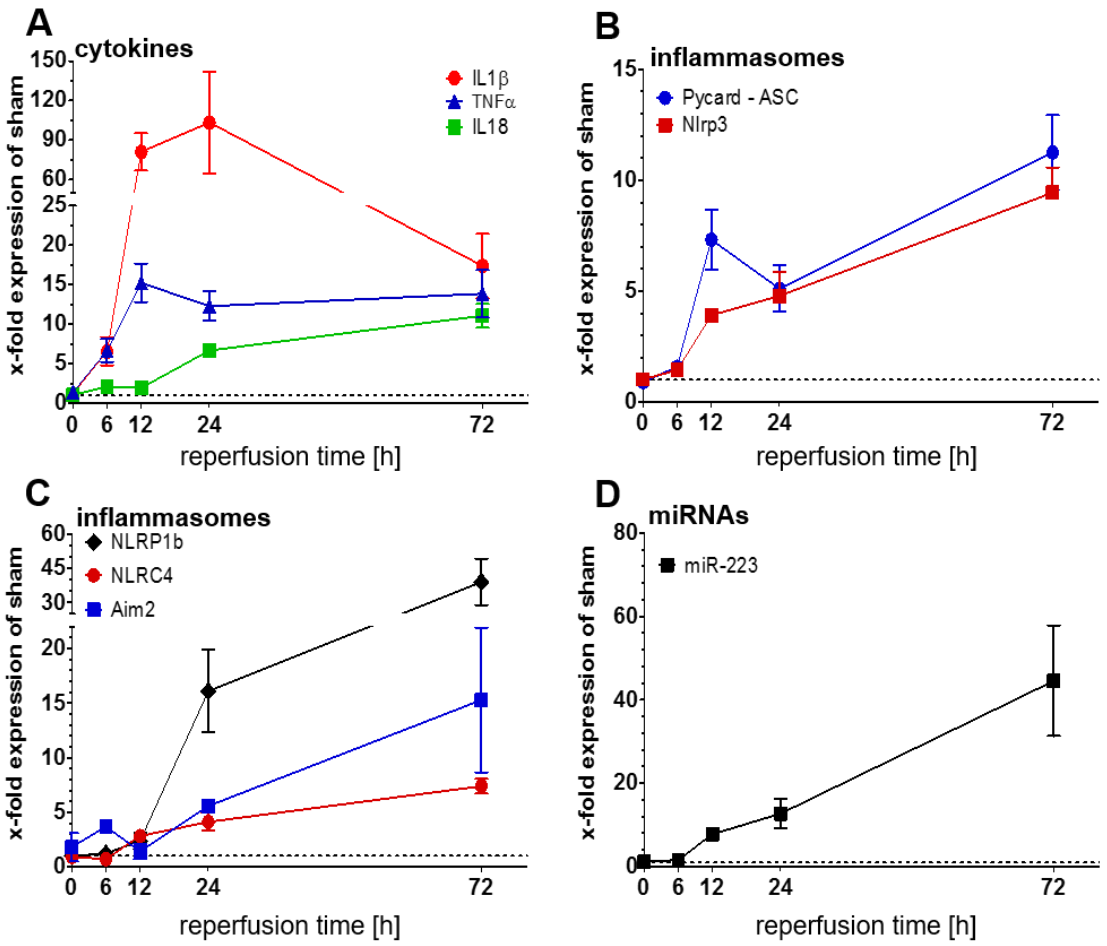

Figure 7: Time-course of cytokine (a), inflammasome (b, c) component gene and miRNA miR-223-3p (d) expression in the peri-infarct zone after tMCAO

(A) Quantitative qrtPCR revealed that IL1β and TNFα mRNA levels rapidly rose within 6-12 h after stroke, whereas IL18 mRNA levels increased between 12 and 24 h. NLRP3 (B), AIM2 and NLRC4 (C) showed a moderate but continuous rise after stroke. ASC (B) rapidly increased between 6 and 12 h and then remained at that level. NLRP1b (C) massively rose after 12 h and beyond. (D) Quantitative qrtPCR revealed that miR-223 levels were rapidly and steady increased during 12 to 72 h after stroke. Data represent the means ± SEM. Modified from Lammerding et al. (2015) [188].

extending to the basal ganglia (Bg) and the cortex (Cx). Only minor infarct signs were detectable in the Bg and Cx regions after 6 h of reperfusion. It then stepwise increased until 72 h post-stroke including large parts of the Bg and Cx, finally covering almost the whole cortex and resulting in a total infarct volume of approx. 300 mm^3. The application of E2 or P 1 h and 13 h after stroke onset significantly reduced the infarct volume by 50 to 60 % compared to the 24 h vehicle as shown in

the lower panel. The corresponding quantitative evaluation of infarct progression and steroid-dependent tissue protection are presented in Figure 6B.

3.2. Post-stroke expression of cytokines and inflammasome genes and miR-223 in the peri-infarct zone

In the next step, I examined the ipsilateral expression levels of inflammation related cytokines and inflammasome genes as well as miR-223 expression in the peri-infarct zone in a time-dependent manner. I aimed at directly comparing expression profiles and deriving from these data a better assignment of inflammatory pro-

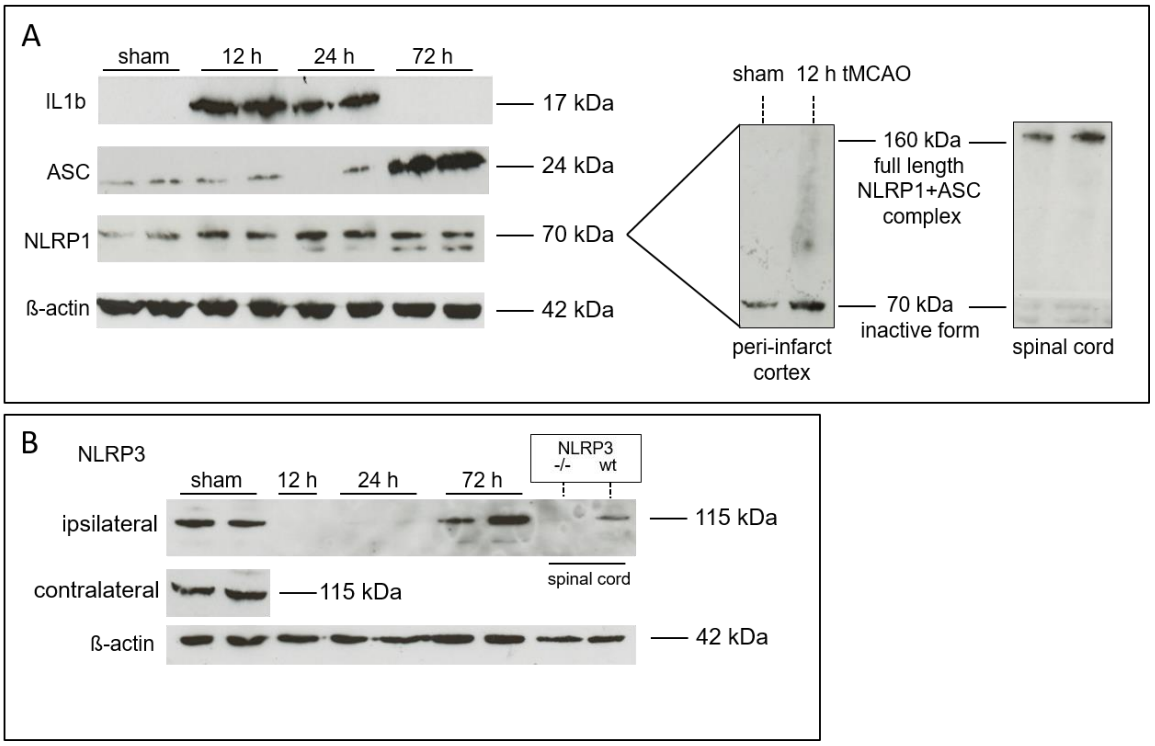

Figure 8: Western Blot analysis of IL1β, ASC, NLRP1 and NLRP3 levels in the peri-infarct zone during the first 72 h after stroke

(A) IL1β temporarily increased at 12 and 24 h. ASC protein levels were low until 24 h and thereafter massively increased at 72 h. NLRP1b augmented stepwise, but only the 70-kDa sized band was visible, whereas the band at approximately 165 kDa was absent at the investigated time points (the extract on the right view shows a comparison between sham and 12 h samples after tMCAO with spinal cord tissue samples where the full sized 165 kDa band was detectable). (B) Interestingly, NLRP3 was already found under sham control conditions in both hemispheres. It completely disappeared at 12 and 24 h and then returned to initial values. Tissues from NLRP3$^{-/-}$ and wild type (wt) mouse spinal cord were used as a negative and positive control, respectively. Modified from Lammerding et al. (2015) [188].

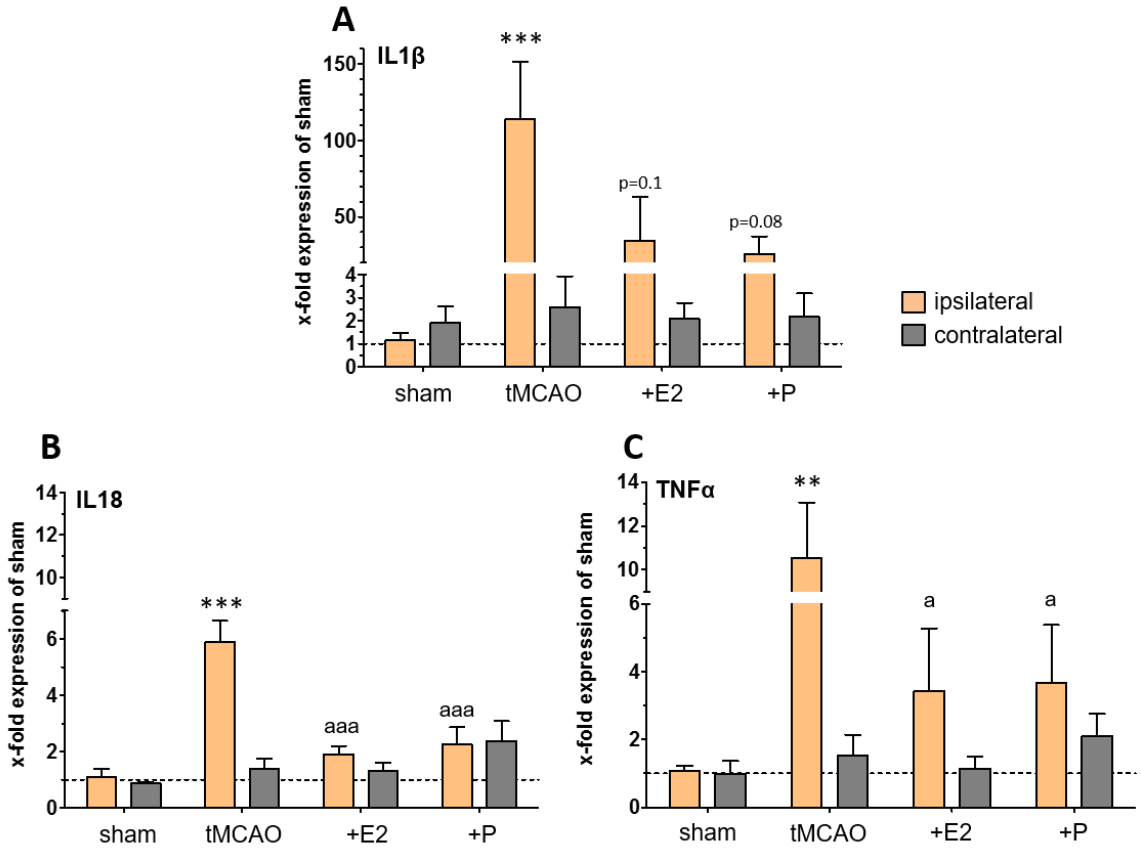

Figure 9: Regulation of gene expression of IL1β (A), IL18 (B) and TNFα (C) 24 h after stroke by gonadal steroids

All three cytokines were massively increased on the ipsilateral side after tMCAO. E2 and P significantly repressed the rise of IL18 and TNFα, whereas IL1β was reduced by approx. 50 % not reaching a significant level. a: p ≤ 0.05, **: p ≤ 0.01, ***/aaa: p ≤ 0.001, the asterisks indicate comparison of groups with ipsilateral sham, letters indicate E2 or P vs. tMCAO ipsilateral Data represent the means ± SEM. Modified from Lammerding et al. (2015) [188].

cesses to cellular and cell type-specific responses and, in case of testing neuroprotective factors, to therapeutic strategies. Figure 7A summarizes the time course of cytokine expression. I found a massive up-regulation of IL1β and TNFα during the first 12 h after stroke onset and persisting level until 72 h. In contrast, IL18 showed a delayed and milder up-regulation after 24 h with a peak at 72 h. The expression profiles of inflammasome components varied to that of cytokines and showed an initial lag followed by a moderate and selective increase between 12 and 24 h (see Figure 7B and C). AIM2 showed a fluctuation with a peak at 6 and 72 h and decreased levels reaching almost basal level at 12 h (Figure 7C). In contrast, all other inflammasome components, such as NLRP3, NLRP1b, NLRC4 and Pycard (ASC),

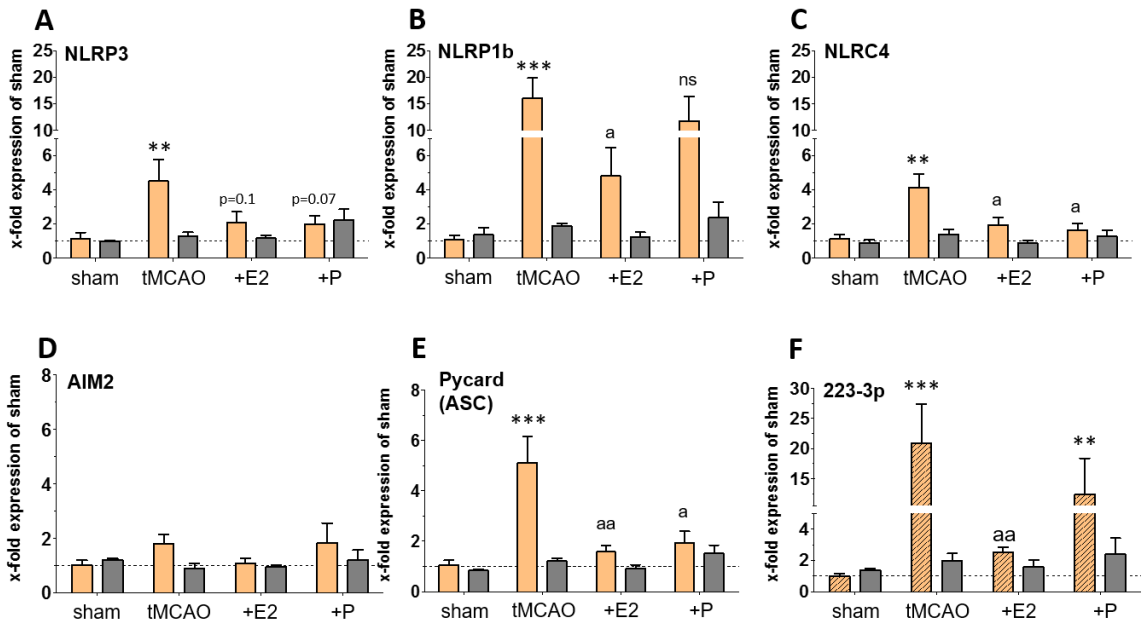

Figure 10: Regulation of gene expression of NLRP3 (A), NLRP1b (B), NLRC4 (C), AIM2 (D), Pycard (ASC) (E) and miR-223-3p (F) 24 h after stroke by gonadal steroids

Besides AIM2 (D), all inflammasomes significantly increased on the ipsilateral side after tMCAO. E2 and P significantly abolished the induction of NLRC4 (C) and Pycard (ASC) (E), whereas only E2 effectively reduced NLRP1b (B). NLRP3 (A) was apparently reduced after E2 and P but failed to reach a significant level. A massive increase of miRNA-223 (F) on the ipsilateral side was measured using the qrtPCR approach. This effect was attenuated only by E2, but not P, administration significantly. ns: not significant, a: $p \leq 0.05$, **/aa: $p \leq 0.01$, *** $p \leq 0.001$, the asterisks indicate comparison of groups with ipsilateral sham, letters indicate E2 or P vs. tMCAO ipsilateral. Data represent the means ± SEM. Modified from Lammerding et al. (2015) [188].

were up-regulated after 12 h of reperfusion. NLRP1b expression reached highest values compared to the others at 24 and 72 h (Figure 7C). The expression of the Pycard (ASC) inflammasome adapter fits right in the other inflammasome expression patterns with a stepwise increase until 72 h. The expression pattern analysis of miR-223-3p revealed that this particular miRNA steadily increased during the initial 72 h post-stroke (Figure 7D).

3.3. Post-stroke expression of IL1β and inflammasome proteins in the peri-infarct zone

In order to further characterize inflammatory processes within the peri-infarct zone, I have examined protein levels of IL1β, ASC and NLRP1b (Figure 8A) or NLRP3

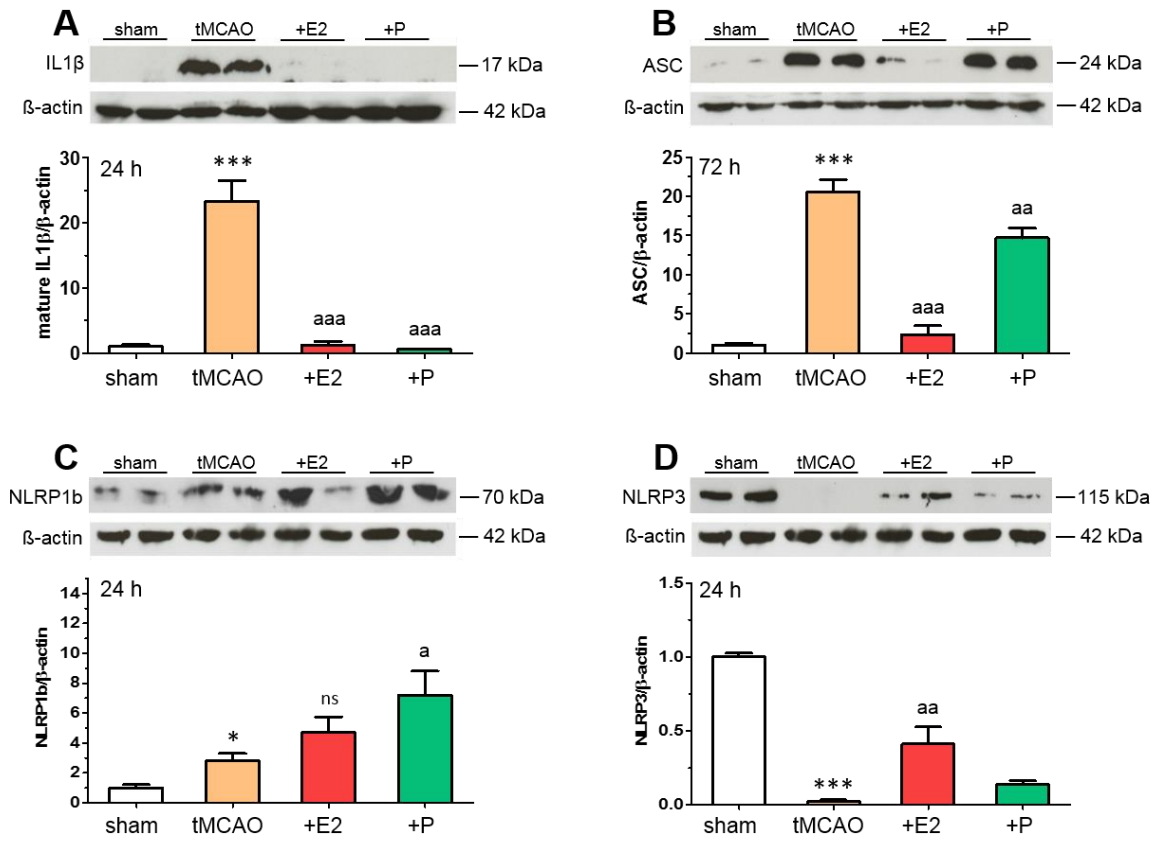

Figure 11: Effect of E2 and P treatment on protein expression levels of IL1β (A) after 24 h, ASC (B) after 72 h, NLRP1b (C) and NLRP3 (D) both after 24 h in the peri-infarct zone of the cortex

WB lanes represent two representative protein examples per group, whereas all samples of animals per treatment were used for the quantitative assessment. (A) IL1β protein levels were highly elevated after 24 h post tMCAO induction. Both steroid hormones inhibited this effect significantly. (B) tMCAO boosted ASC levels not until 72 h, where both hormones impeded these effect. Note, that E2 restored ASC levels almost to the sham level, whereas P administration showed lower capabilities to hamper ASC levels. (C) NLRP1b protein levels were slightly increased 24 h after tMCAO. NLRP1b was further significantly boosted by P administration, as well as E2, but not reaching a significant level. (D) The NLRP3 protein uniquely disappeared after tMCAO compared to the other components. E2 inhibited this effect significantly, whereas P administration slightly elevated the rare NLRP3 levels (not significant). ns: not significant, *: $p \leq 0.05$, **/aa: $p \leq 0.01$, ***/aaa: $p \leq 0.001$, the asterisks indicate comparison of groups with ipsilateral sham; letters indicate E2 or P vs. tMCAO ipsilateral. Data represent the means ± SEM. Modified from Lammerding et al. (2015) [188].

(Figure 8B) by using a WB approach The IL1β protein was detectable after 12 and 24 h and disappeared after 72 h. During the first 24 h, ASC levels were similar to sham levels and massively increased after 72 h of reperfusion time. The NLRP1 inflammasome protein was weakly expressed in sham animals. Then it increased during the time course with a peak at 24 h. Noteworthy, the inactive form with approx. 70 to 75 kDa but not the full complex with a size of approx. 165 kDa was detectable. In contrast, by using spinal cord tissue as a reference, we observed that in the spinal cord, the full complex consisting of NLRP1 and ASC was detected at approx. 165 kDa compared to the inactive form at approx. 70 kDa. With respect to NLRP3, high levels of this protein were detected on both, the ipsi- and contralateral site. After stroke, NLPR3 protein disappeared during the initial 12 to 24 h and reappeared at 72 h after reperfusion (Figure 8B). In order to validate the specificity of the

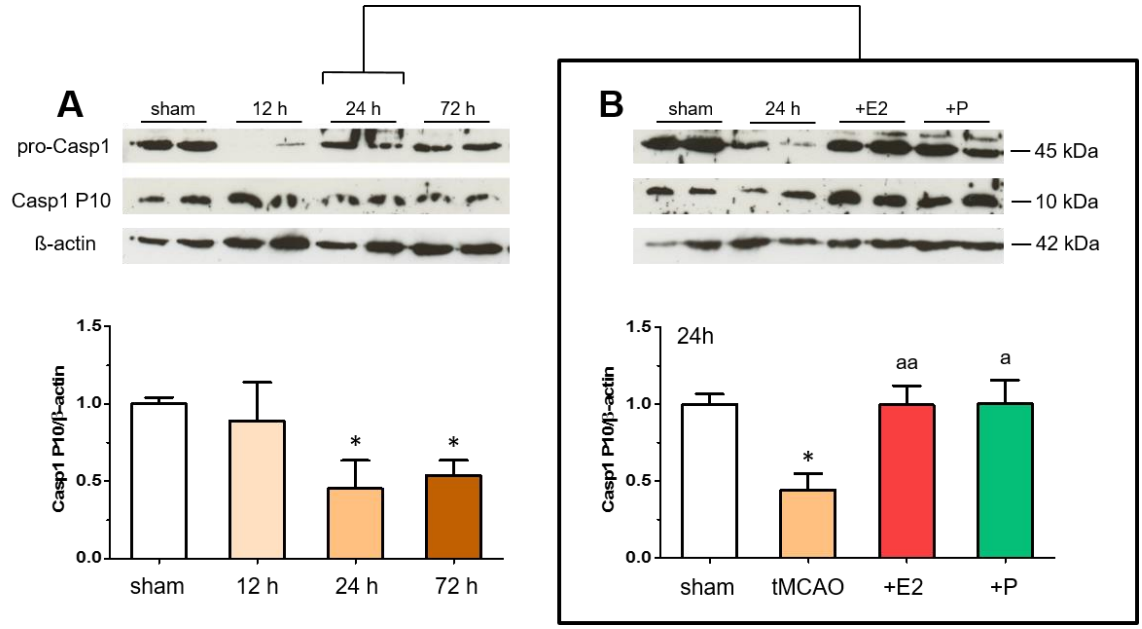

Figure 12: Western Blot analysis of Casp1 levels in the peri-infarct zone during the first 72 h after stroke (A) and 24 h after stroke with hormone treatment (B)
Representative WB lanes of pro-Casp1 (45 kDa) and the active form P10 of Casp1 (10 kDa) normalized to β-actin are demonstrated in the upper panels. (A) Protein levels of the active Casp1 form P10 decreased significantly during extended reperfusion time of 24 and 72 h post stroke. (B) Reduction of Casp1 P10 levels was hampered by E2 and P administration compared to tMCAO levels after 24 h of reperfusion. */a: $p \leq 0.05$, aa: $p \leq 0.01$, the asterisk indicates comparison of groups with ipsilateral sham, letters indicate E2 or P vs. tMCAO ipsilateral. Data represent the means ± SEM. Modified from Lammerding et al. (2015) [188].

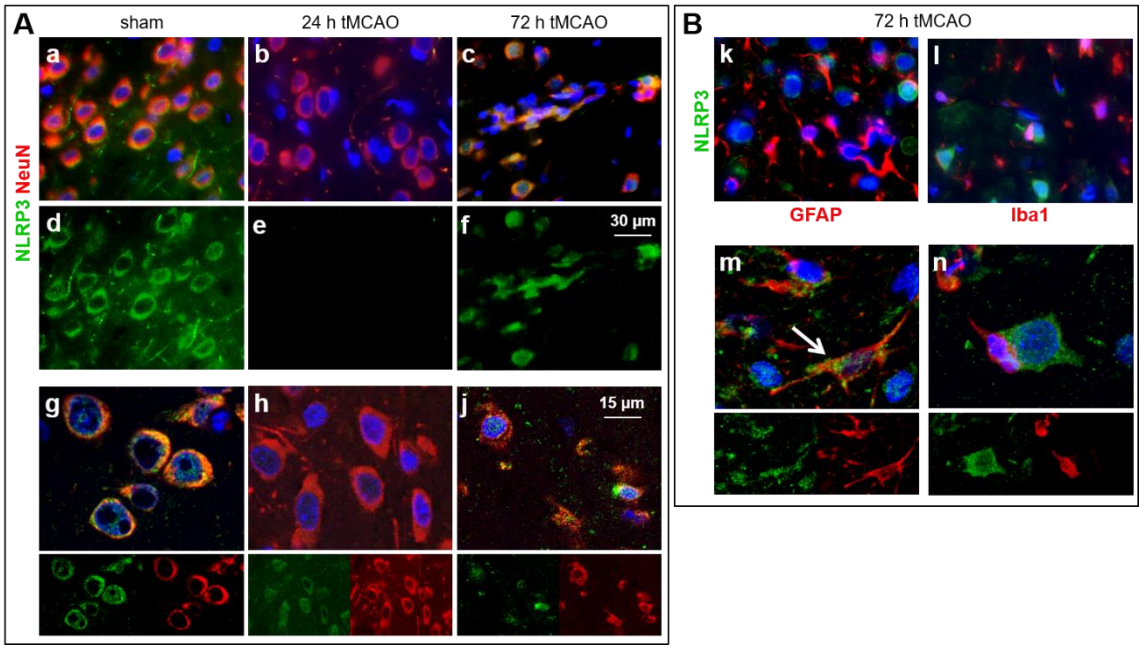

Figure 13: Immunofluorescence double staining of NLRP3 with NeuN (neurons), GFAP (astroglia) and Iba1 (microglia)

(A) In the upper panel, time-dependent expression of NLRP3 is demonstrated. In control animals (sham), NLRP3 was strongly expressed in the cerebral cortex and mainly co-labeled with NeuN+ neurons (a, d). After tMCAO and 24 h reperfusion, NLRP3 almost completely disappeared (b, e) and reappeared during the prolonged reperfusion time of 72 h (c, f). In the lower panel, representative confocal images are presented. (B) At a closer look, only few GFAP+ astrocytes co-labeled with NLRP3 (k, m), whereas NLRP3 was not found in Iba1+ microglial cells (l, n). Scale bars represent 30 µm (a-f and k-l) and 15 µm (g-j and m–n). Modified from Lammerding et al. (2015) [188].

used antiserum, samples from wild type (wt) and NLRP3$^{-/-}$ knockdown mice were used as controls. No immune-reactive band was detectable at the indicated size of 115 kDa in the knockdown mice compared to the wt littermate.

3.4. Effect of steroid hormones on gene expression of cytokine and inflammasome components and miR-223 expression in the peri-infarct zone

Since the steroid hormones E2 and P were found in previous studies to be neuroprotective in the tMCAO stroke model, I aimed at investigating the molecular mechanisms of protective steroid action. Therefore, I investigated the effect of both hormones on the expression levels of cytokines and inflammasome components genes

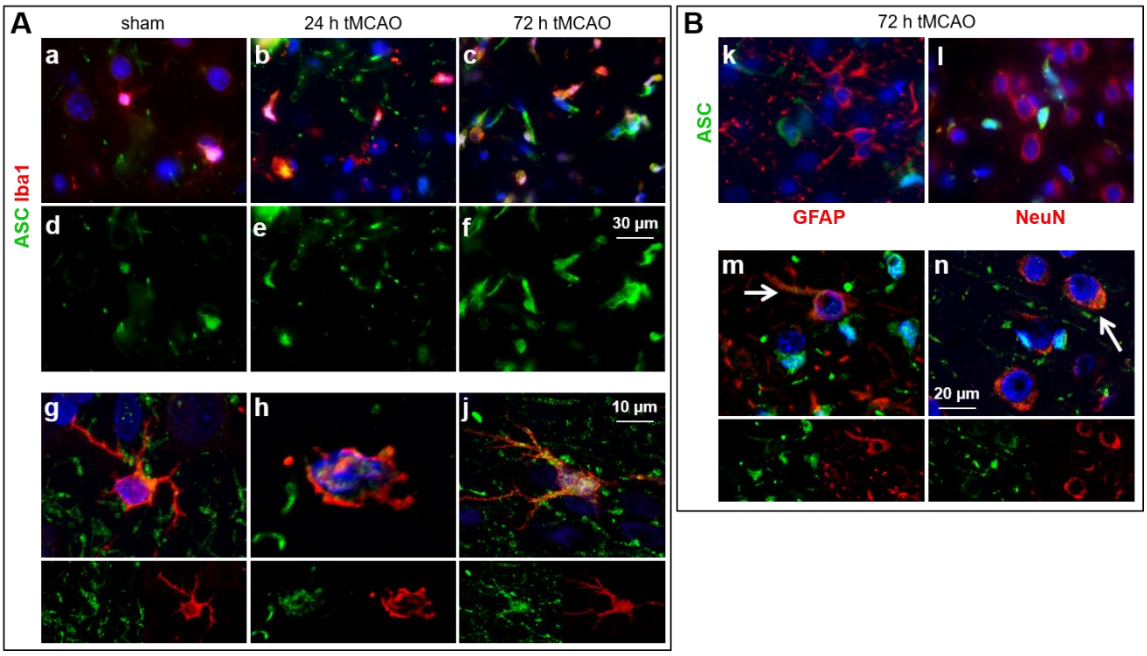

Figure 14: Immunofluorescence double staining of ASC with Iba1 (microglia), GFAP (astroglia) and NeuN (neurons)

(A) In the upper panel, time dependent expression of ASC is shown. In control animals (sham, a, d) and 24 h after tMCAO (b, e), ASC was weakly expressed. Higher ASC levels were seen at 72 h after tMCAO (c, f). Thereby, ASC mainly co-labeled with Iba1+ microglia. In the lower panel, representative confocal images are presented. (B) Beside microglia, ASC occasionally co-labeled with GFAP+ (k) or NeuN+ (l) cells (white arrows in m and n). Scale bars represent 30 µm (a–f and k-l), 10 µm (g-j) and 20 µm (m-n). Modified from Lammerding et al. (2015) [188].

as well as miR-223. I have selectively chosen the time point of 24 h after stroke onset, since most of the studied genes revealed then a maximum expression level. As demonstrated in Figure 9A, IL1β expression was significantly elevated after stroke. Both hormones slightly but not significantly inhibited this effect. In the case of IL18 and TNFα, which were both induced after stroke, both E2 and P significantly, reduced the up-regulation of these cytokines to a similar extent (Figure 9B-C).

All inflammasome complexes with the exception of AIM2 were significantly elevated in the ipsilateral cerebral cortex 24 h after stroke. Whereas the administration of both hormones could inhibit the up-regulation of NLRP3, values did not reach significant levels ($p=0.1$ for E2 and $p=0.07$ for P, Figure 10A). With NLRP1b, only E2 significantly antagonized the up-regulation of this inflammasome (Figure 10B). In contrast, both steroid hormones E2 and P significantly reduced NLRC4 and Pycard

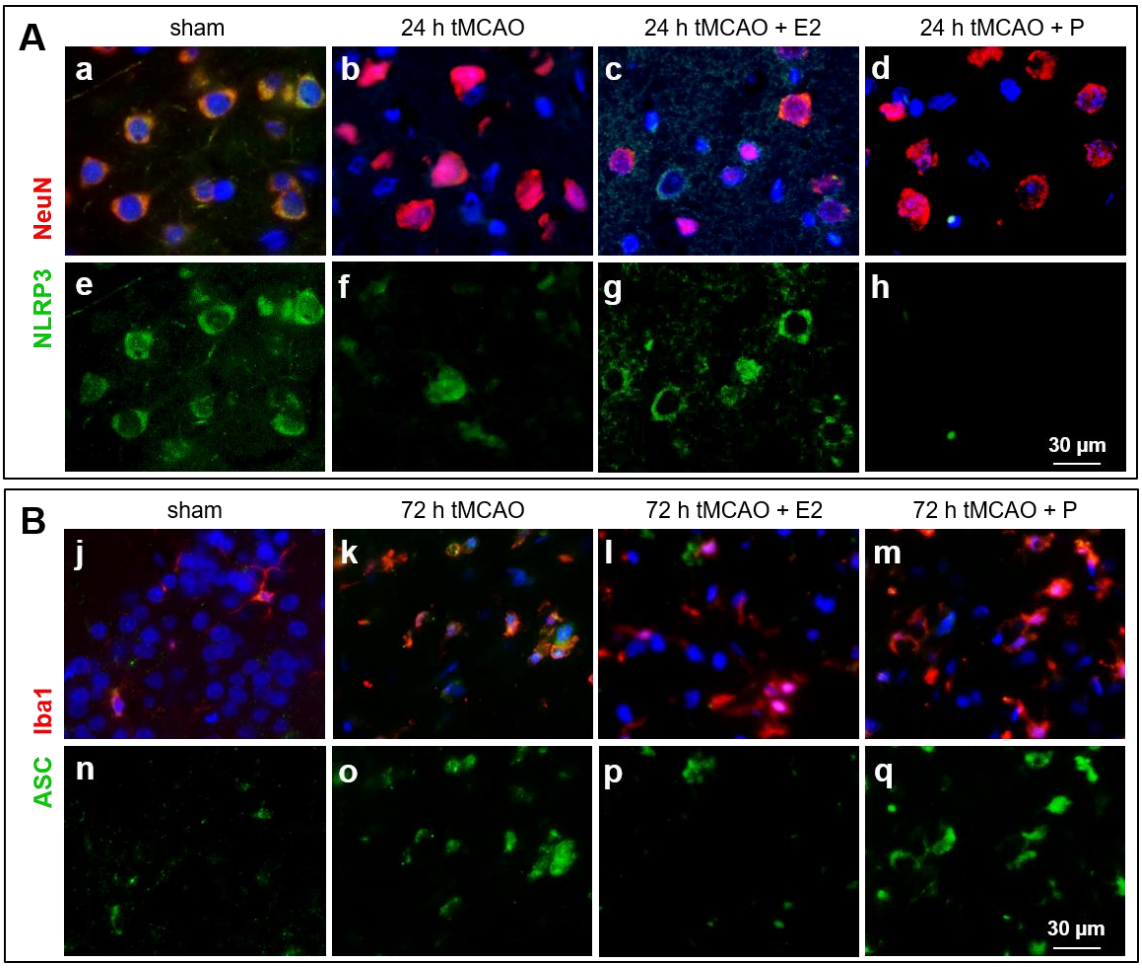

Figure 15 Immunofluorescence double staining of NLRP3 with NeuN (neurons, panel A) and ASC with Iba1 (microglia, panel B) following steroid hormone treatment

(A) In sham animals (a, e), NLRP3 was mainly expressed in NeuN+ neurons and disappeared in the peri-infarct zone following stroke (b, f). E2 administration partially restored NLRP3+ signals in (c, g), whereas P treatment showed no effect (d, h). (B) tMCAO boosted ASC expression 72 h after onset of ischemia (k, o) compared to sham animals (j, n). This effect was mainly inhibited by E2 administration (l, p). P treatment showed almost no impact on ASC protein levels (m, q). Scale bars represent 30 µm. Modified from Lammerding et al. (2015) [188].

(ASC) expression compared to the vehicle group (Figure 10C and E). I have additionally studied the influence of stroke and steroid hormone substitution on miR-223 expression (Figure 10F). Under stroke conditions, miR-223 levels were significantly elevated after 24 h post stroke. E2 application reduced miR-223 mRNA levels in a statistical significant way, whereas P showed no influence on miR-223 expression.

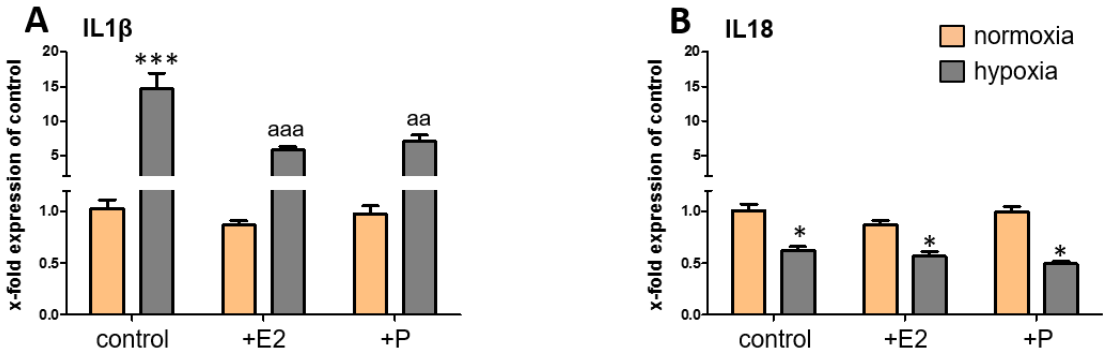

Figure 16: Regulation of gene expression of IL1β (A) and IL18 (B) after hypoxia in BV-2 cells

(A) Hypoxic conditions yielded an up-regulation of IL1β in BV-2 cells that was altered by both steroid hormones. (B) In contrast, IL18 significantly dropped. No effects of E2 or P were observed on IL18 levels after hypoxia. *: $p \leq 0.05$, aa: $p \leq 0.01$, ***/aaa: $p \leq 0.001$, the asterisks indicate comparison of groups with normoxia control, letters indicate E2 or P vs. hypoxia control. Data represent the means ± SEM.

3.5. Effect of steroid hormones on protein levels of IL1β, inflammasome components and Casp1

I used a WB approach to test the impact of E2 and P on the protein level of IL1β, inflammasomes and to demonstrate Casp1 in its active form. As shown in Figure 11A, IL1β protein levels were extremely boosted after tMCAO. This effect was almost completely inhibited by E2 and P administration. A similar picture was found for ASC (Figure 11B) with a massive up-regulation after tMCAO and a strong and significant prevention of this effect by E2 and to a lower extent by P. Both hormone effects were significantly different from each other. On the translational level, I could only detect the “inactive” form of NLRP1b at approx. 70 kDa as already shown in Figure 8A. Here, E2 and P appeared to increase the levels of the small-sized NLRP1b further compared to tMCAO, whereas only P administration reached a significant level (Figure 11C). NLRP3 was expressed under control conditions at high levels and disappeared almost completely after tMCAO (Figure 11D). Hormone administration partly restored NLRP3 levels by E2 but not by P. As a marker for active inflammasome complexes leading to Casp1 processing, the pro-active (pro-Casp1) and active (Casp1 P10) forms were analyzed during prolonged reperfusion time (Figure 12A) and after steroid hormone application (Figure 12B). The pro-active form was high at beginning, then completely disappeared and slightly returned to half-maximal levels. The active 10 kDa form decreased and revealed lowest levels

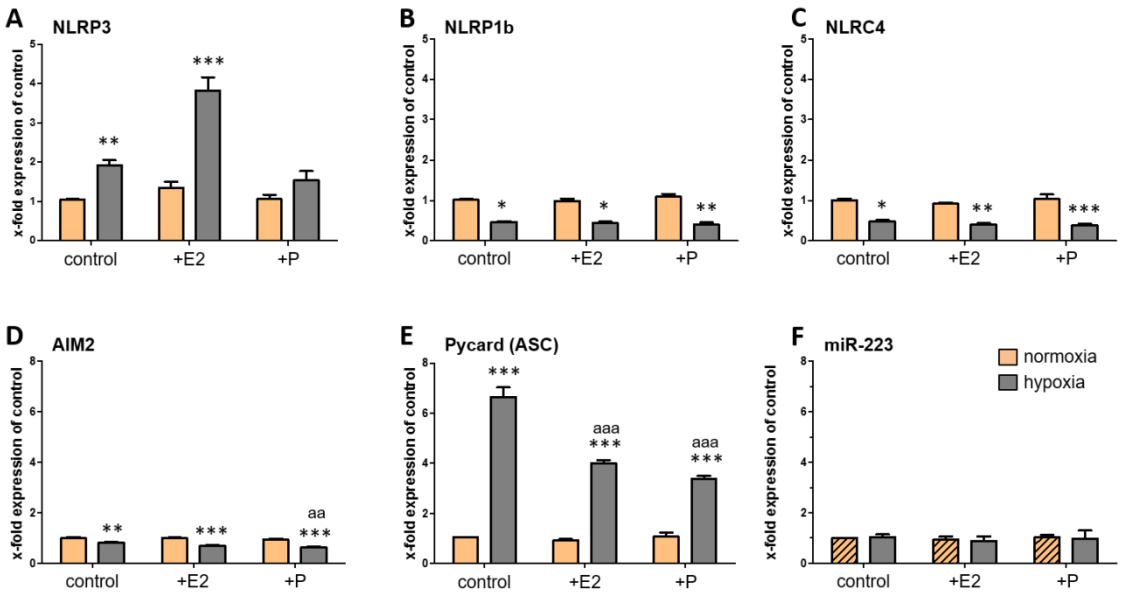

Figure 17: Regulation of gene expression of NLRP3 (A), NLRP1b (B), NLRC4 (C), AIM2 (D), Pycard (ASC) (E) and miR-223-3p (F) after hypoxia in BV-2 cells

Hypoxic conditions regulated all inflammasome components in BV-2 cells revealing either an increase (NLRP3, Pycard (ASC)) or decrease (NLRP1b, AIM2, NLRC4). E2 administration boosted NLRP3 expression. This effect did not reach a significant level. Only P selectively reduced AIM2 further. Both steroid hormones dampened ASC expression. Neither hypoxia nor steroid hormone treatment showed any effect on miR-223 expression in BV-2 cells. *: $p \leq 0.05$, **/aa: $p \leq 0.01$, ***/aaa: $p \leq 0.001$, the asterisks indicate comparison of groups with normoxia control, letters indicate E2 or P vs. hypoxia control. Data represent the means ± SEM.

at 24 h post stroke. Both steroid hormones prevented this decline of Casp1 p10 levels.

3.6. Immunofluorescence double-labeling of inflammasomes in neural cells in the peri-infarct zone

In order to attribute the different inflammasome components to cell types within the penumbra, I have performed double-immunofluorescence staining with GFAP, Iba1 and NeuN as astroglial, microglial and neuronal marker, respectively and co-labeled with NLRP3 or ASC antibodies. As demonstrated in Figure 13d-f, the NLRP3 protein was highly expressed in sham animals under control conditions. Then, NLRP3 disappeared at 24 h after tMCAO and appeared again at 72 h (Figure 13g-j and m-n representative confocal images are shown). These findings are in good agreement with previous WB data. Co-labeling revealed that mainly neurons also express

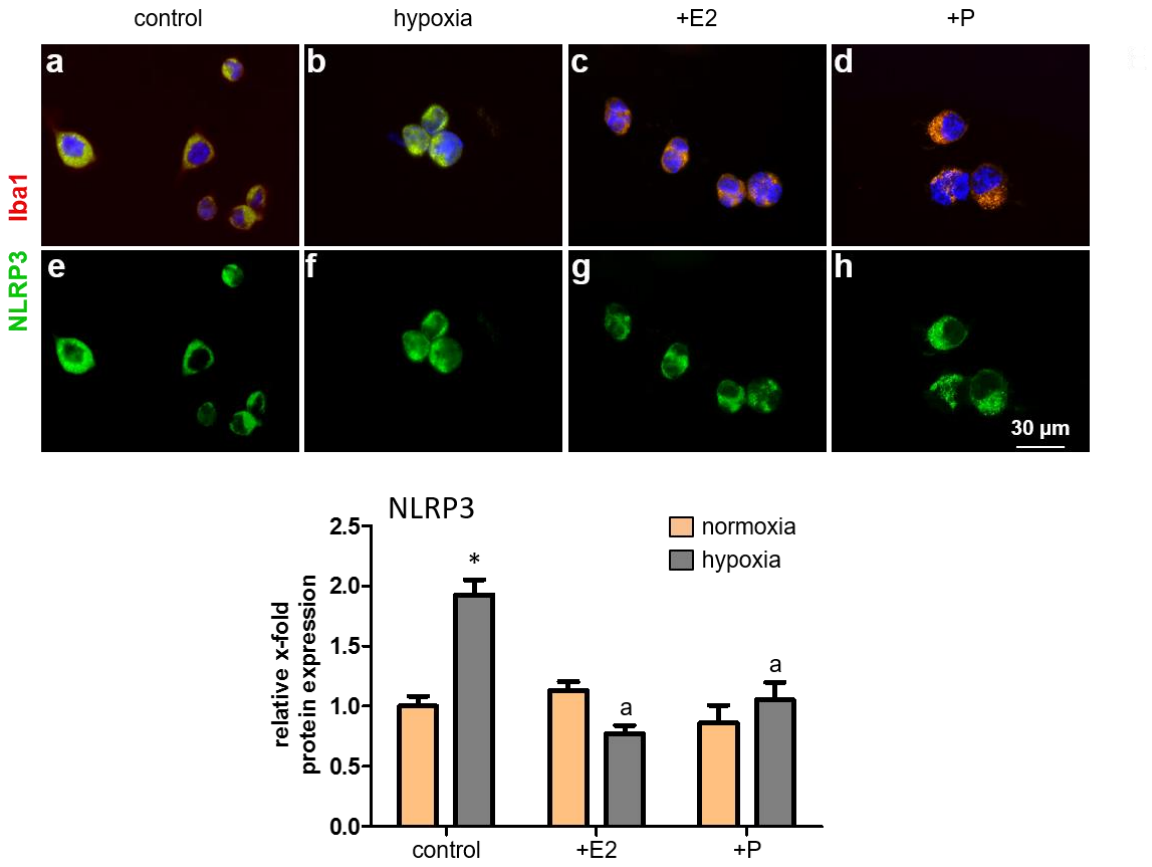

Figure 18: Immunofluorescence double staining of NLRP3 with Iba1 in BV-2 cells
In BV-2 cells, brighter fluorescence signals were measured after hypoxia (b, f) compared to normoxia conditions (a, e). Both, E2 (c, g) and P (d, h), attenuated this effect. The lower panel shows the quantification of the mean fluorescence values with regard to Iba1+ cells. */a: $p \leq 0.05$, the asterisk indicates comparison of groups with normoxia control, letters indicate E2 or P vs. hypoxia control. Scale bars represent 30 µm (A–H). Data represent the means ± SEM.

NLRP3 (Figure 13a-c), whereas NLRP3 was hardly detectable in Iba1+ microglia cells (Figure 13l and n) and only in some cases in GFAP+ astrocytes (Figure 13k and m). ASC protein was expressed at low levels in sham animals. After tMCAO, ASC was increased at 24 h and further after 72 h (Figure 14d-f and g-j). These findings coincide well with WB data. Whereas only few Iba1+ microglial cells were double-labeled with ASC in sham animals and 24 h post stroke, most Iba1+ microglia co-expressed ASC (Figure 14a-c). Further, ASC was sporadically co-expressed in neurons (Figure 14n) and astroglia (Figure 14m). We have also analyzed the effect of E2 and P on co-localization of NLRP3 and ASC in neurons and microglia,

since these cell types were shown to be the main sources of the respective inflammasome components in the used animal model. These data are summarized in Figure 15. As shown in panels a-h, E2 but not P restored NLRP3 expression in neurons which was absent after tMCAO. Further, increased ASC levels occurring after tMCAO were diminished by E2 administration, whereas P showed only minor effects on ASC levels (Figure 15j-q).

3.7. Cytokine and inflammasome component gene- and miR-223-expression in the microglia cell line BV-2 after hypoxia

To investigate the impact of hypoxia on inflammasome components, an *in vitro* hypoxia approach was used. For hypoxia experiments, I used the murine microglia-like cell line BV-2 which has been previously shown to share many functional and

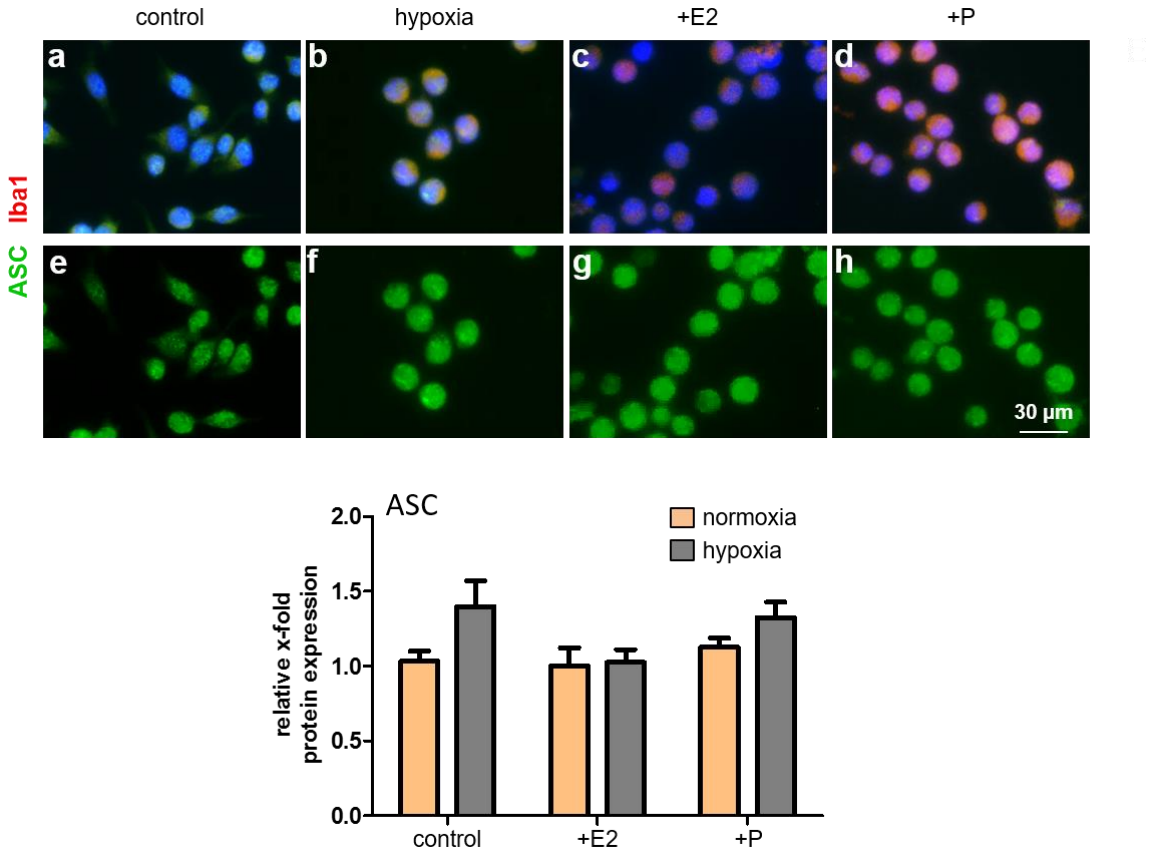

Figure 19: Immunofluorescence double staining of ASC with Iba1 in BV-2 cells
ASC protein levels were selectively increased after hypoxia (b, f) compared to normoxia controls (a, e) but did not reach significant levels (lower panel). Steroid hormone application showed no effect on ASC levels (c, g and d, h). Scale bars represent 30 µm (A–H). Data represent the means ± SEM.

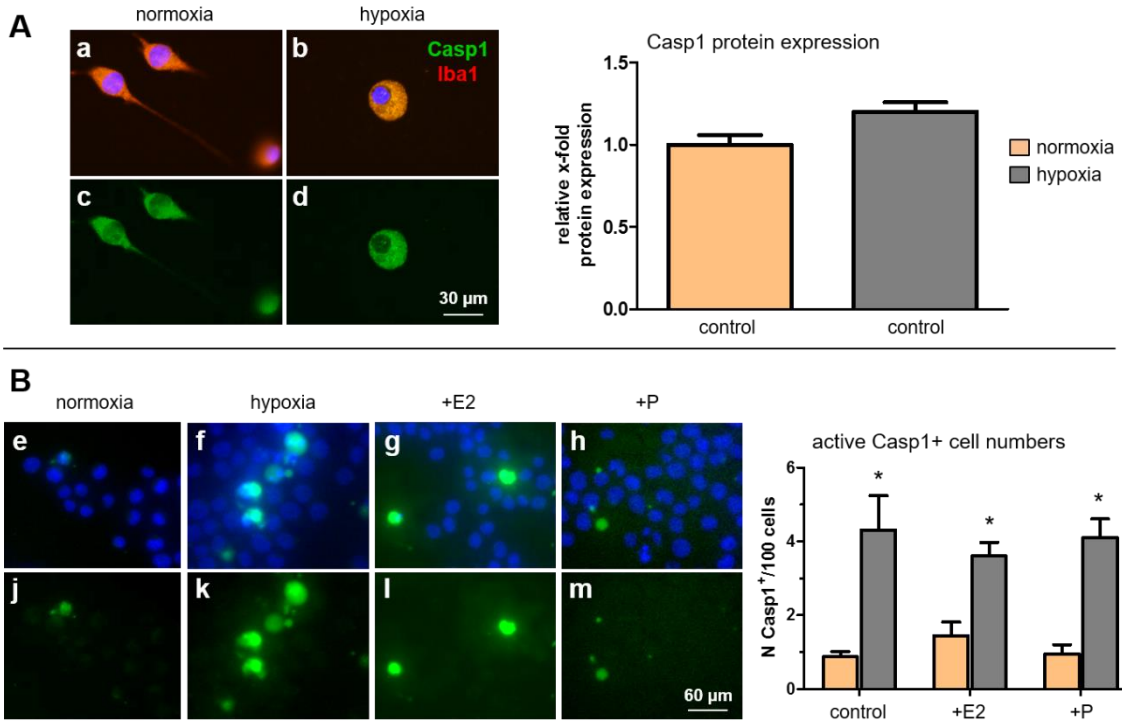

Figure 20: Casp1 expression and activity after hypoxia in BV-2 cells

In panel (A), Casp1 expression is shown. Similar levels were found under normoxia (C, E) and hypoxia (D, F). The right panel gives the quantitative results. In panel (B), Casp1-activity is demonstrated by green fluorescence. Under normoxia, few cells are positive, whereas positive labeled numbers were increased after hypoxia. No clear effect of hormonal treatment was observed. Scale bars represent 30 µm (a-d) or 60 µm (e-m). *: $p \leq 0.05$, the asterisk indicates comparison of groups with normoxia control. Data represent the means ± SEM. N: cell number.

morphological similarities to primary murine microglia cells [126,185,187]. The experimental procedure for *in vitro* experiments is summarized in Figure 5B. In the first step, the expression profiles of the cytokines IL1β (Figure 16A) and IL18 (Figure 16B) with and without hormone supplementation were determined. Hypoxia for 3 h caused a massive up-regulation of IL1β. This effect was significantly dampened by both steroid hormones. In contrast, hypoxia evoked a significant down-regulation of IL18 and no effect of E2 or P was observed.

Hypoxia affected all measured inflammasome component genes which were either significantly up-regulated (NLRP3, Pycard/ASC) or down-regulated (AIM2, NLRP1b and NLRC4, see Figure 17A-E). Interestingly, E2 supplementation further boosted NLRP3 expression, whereas P showed no effect on NLRP3 expression. In addition, both steroid hormones significantly reduced the level of Pycard (ASC) or selectively

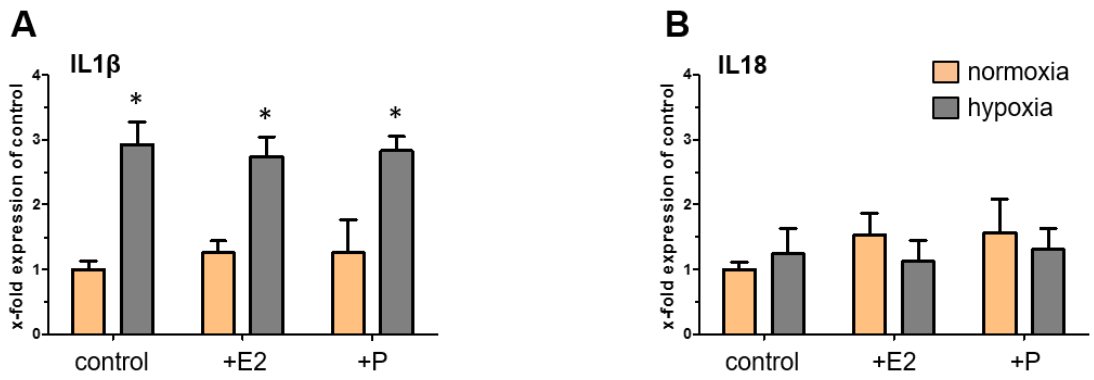

Figure 21: Regulation of gene expression of IL1β (A) and IL18 (B) after hypoxia in astroglia cells

(A) Hypoxic conditions led to an up-regulation of IL1β expression in astroglia cells. This effect was not inhibited by steroid hormone application. (B) IL18 expression was not affected by hypoxia or by the treatment with E2 or P. *: $p \leq 0.05$, the asterisk indicates comparison of groups with normoxia control. Data represent the means ± SEM.

for P further decreased AIM2 levels following hypoxia. On the other hand, E2 and P administration showed no effect on reduced mRNA levels of NLRP1b and NLRC4 following hypoxia.

By investigating miR-223 expression in BV-2 cells, we found that the hypoxic stimulus caused no obvious changes in miRNA levels. Treatment with both steroid hormones did not change these levels (Figure 17F).

3.8. Immunofluorescence double-labeling of NLRP3 and ASC in BV-2 cells after hypoxia

In a next step, I have examined the expression pattern of NLRP3 and ASC and their co-expression with Iba1 after 3 h hypoxia using immunofluorescence double-labeling (Figure 18 and Figure 19). As demonstrated in Figure 18a-h, NLRP3 expression was moderate under normoxia conditions and increased after hypoxia. E2 and P treatment diminished the up-regulation resulting in weaker fluorescence signals. Determination of the mean fluorescence intensity revealed a significant increase of NLRP3 levels and a reduction by both steroid hormones back to basic levels.

In contrast, ASC protein levels were slightly increased after hypoxia indicated by a higher fluorescence signal as demonstrated in panels a-h of Figure 19. The fluorescence signal appeared weaker as compared to hypoxia after steroid hormone supplementation.

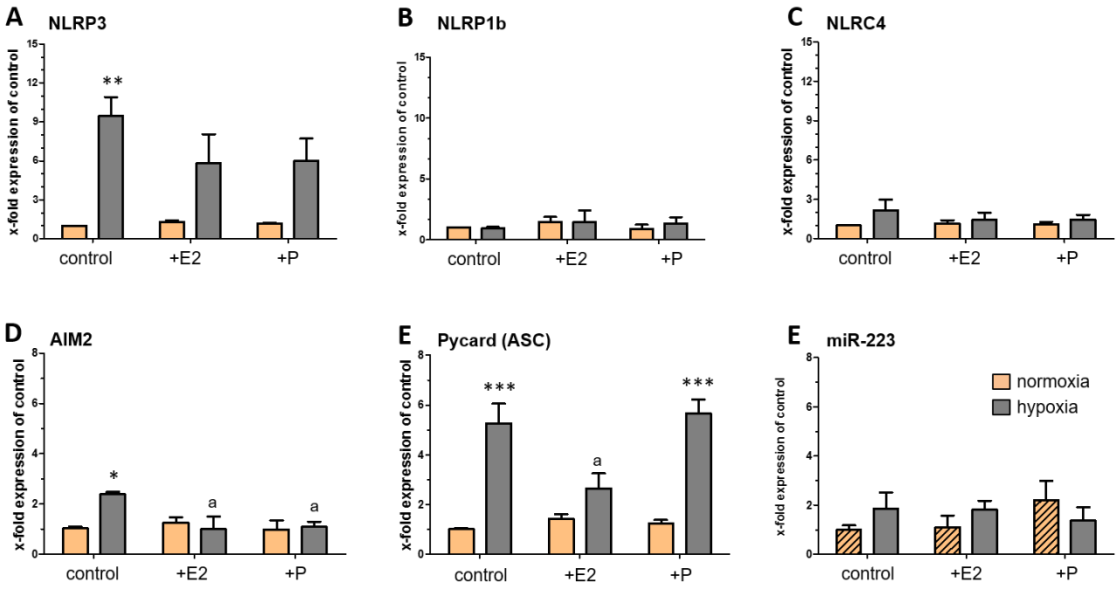

Figure 22: Regulation of gene expression of NLRP3 (A), NLRP1b (B), NLRC4 (C), AIM2 (D), Pycard (ASC) (E) and miR-223-3p after hypoxia in astrocytes

Except of NLRP1b and NLRC4, the other inflammasome components genes, namely NLRP3, AIM2 and Pycard (ASC), were boosted after hypoxia. E2 or P administration selectively dampened these effect significantly for Pycard (ASC) (+E2, E), both E2 and P for AIM2 (D) or not reaching a significant level for NLRP3 (A). Further, no effect was detected on NLRP1b (B) or NLRC4 (C) expression. Neither hypoxia nor steroid hormone treatment showed any effect on miR-223 expression in astrocytes. */a: $p \leq 0.05$, **: $p \leq 0.01$, ***: $p \leq 0.001$, the asterisks indicate comparison of groups with normoxia control, letters indicate E2 or P vs. hypoxia control. Data represent the means ± SEM.

3.9. Casp1 activation after hypoxia and effect of steroid hormone supplementation in BV-2 cells

The final step in the intracellular inflammasome cascade is the activation of Casp1 and, in consequence, the synthesis and release of mainly IL1β. Therefore, I have investigated the protein expression of active Casp1 in BV-2 cells under hypoxia and after hormone supplementation. As demonstrated in Figure 20A, hypoxic conditions showed per se no clear effect on Casp1 protein levels. On the other hand, hypoxia led to significant more green-labeled cells compared to normoxia conditions indicating higher Casp1 activity (Figure 20B). None of these effects was altered by E2 or P administration.

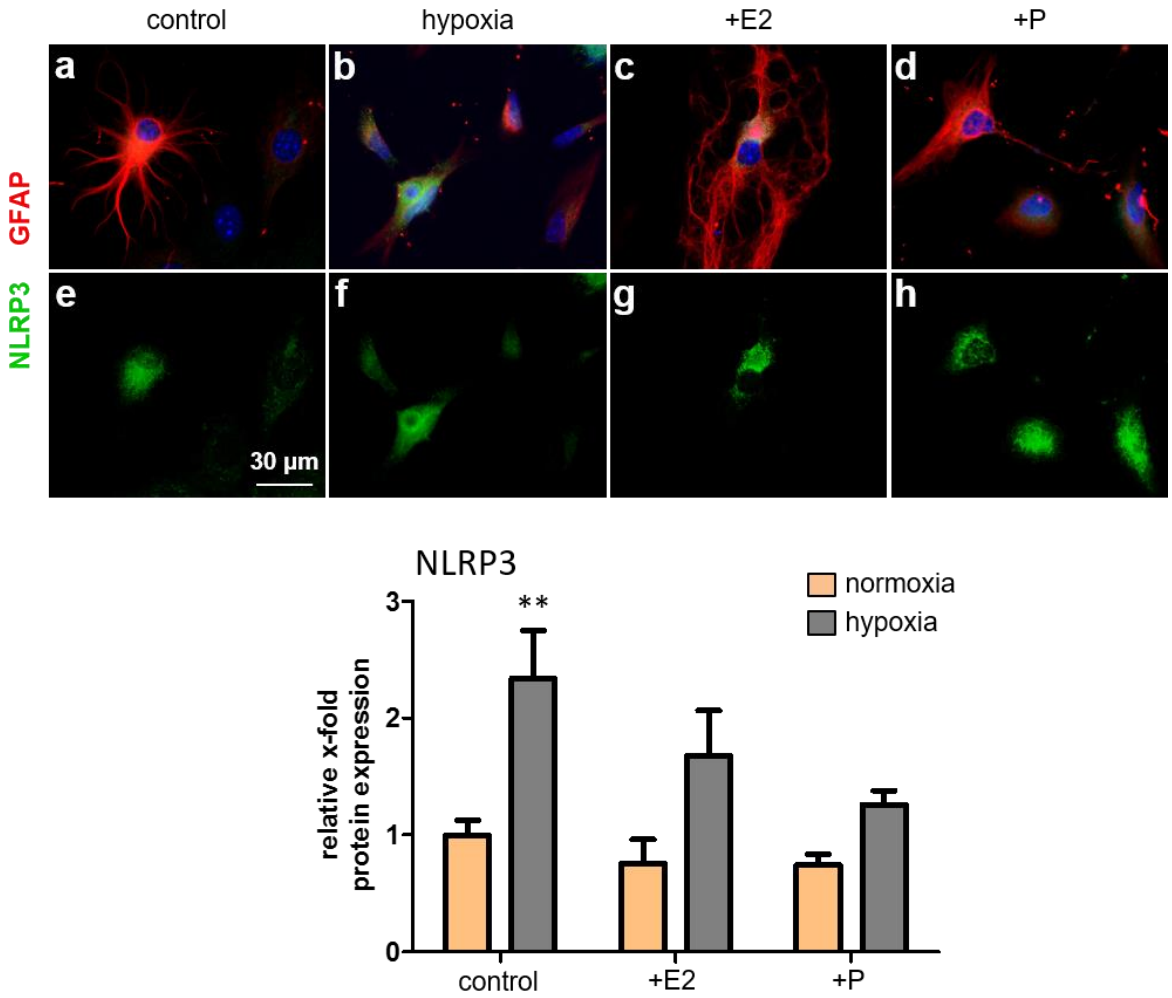

Figure 23: Immunofluorescence double staining of NLRP3 with GFAP in astrocyte after hypoxia

After hypoxia, higher numbers of NLRP3 (green) fluorescence labeled signals were found in GFAP+ astrocytes (b, f) as compared to normoxia controls (a, e). After E2 (c, g) or P (d, h) administration, lower signals were found. These effects did not reach a significant level. **: $p \leq 0.05$, the asterisks indicate comparison of groups with normoxia control. Scale bars represent 30 µm (a–h). Data represent the means ± SEM.

3.10. Expression of cytokine and inflammasome component genes and miR-223 in murine primary astrocytes

Besides brain-intrinsic microglia, local astrocytes in the hypoxia-damaged brain region are important regulators of tissue degradation and neuronal death. Therefore, I have further analyzed the capacity of astrocytes either to synthesize cytokines and inflammasome components as well as miR-223 and the efficacy of steroid hormones to regulate these inflammatory processes. First, I have addressed the expression of

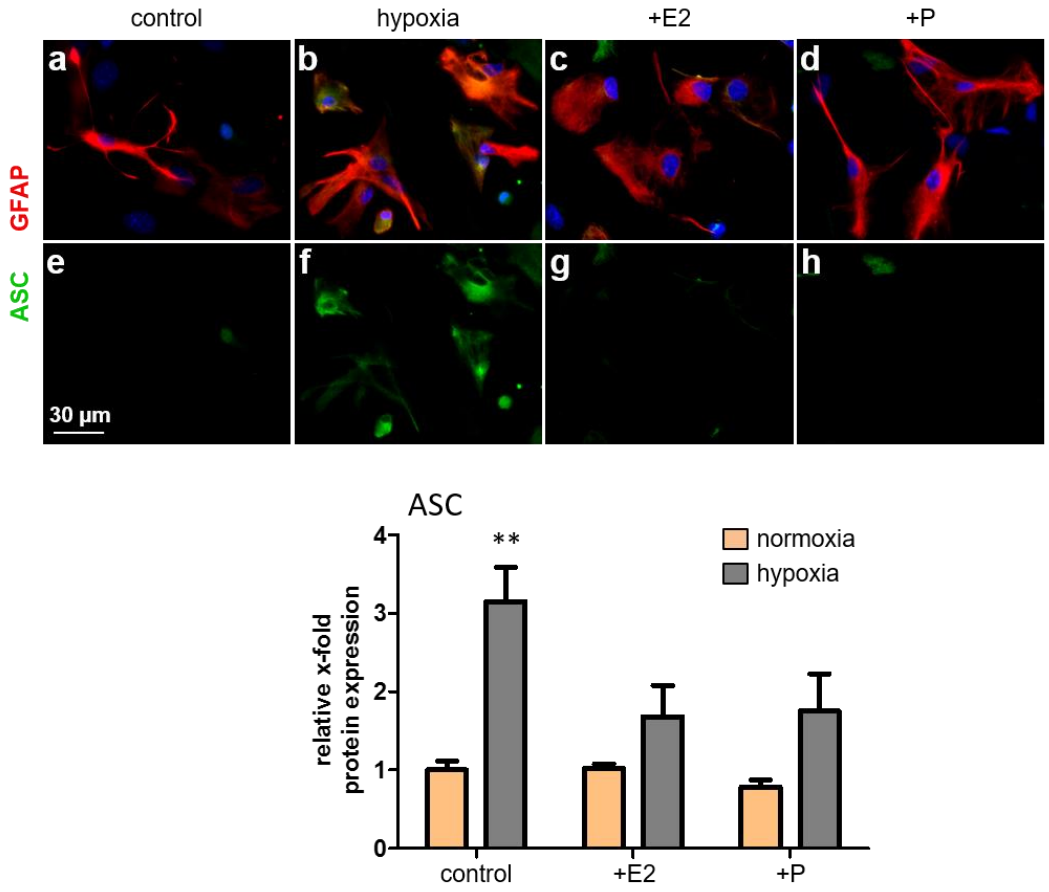

Figure 24: Immunofluorescence double staining of ASC with GFAP in astrocytes after hypoxia

After hypoxic conditions, more ASC (green) fluorescence signals were found in GFAP+ astrocytes (b, f) as compared with normoxia controls (a, e). After E2 (c, g) or P (d, h) administration, lower signals were found. These effects did not reach a significant level. **: $p \leq 0.05$, the asterisks indicate comparison of groups with normoxia control. Scale bars represent 30 µm (A–H). Data represent the means ± SEM.

the cytokines IL1β and IL18 after a hypoxia. IL1β was significantly up-regulated (Figure 21A), and E2 and P supplementation showed no effect on IL1β expression. There was no detectable impact of hypoxia and hormone application on IL18 gene expression (Figure 21B).

With the exception of NLRP1b and NLRC4, hypoxia induced a significant up-regulation of NLRP3, AIM2 and Pycard (ASC) (Figure 22A-E). Whereas E2 or P selectively dampened the effect on Pycard (ASC, +E2) expression followed hypoxia, both hormones significantly reduced expression levels of AIM2. NLRP3 expression was slightly attenuated but did not reach a significant level. With regard to miR-223 levels, hypoxic conditions did not show any impact on the expression pattern. Steroid hormones did not show any effects, too (Figure 22F).

3.11. Immunofluorescence double-labeling of NLRP3 and ASC in astrocytes after hypoxia

Further, I have evaluated the immunofluorescence labeling index of NLRP3 (Figure 23) and ASC (Figure 24) in astroglia after hypoxia and the effect of steroid hormone supplementation. As shown in the Figure 23a-h, NLRP3 expression was low under normoxia and increased after hypoxia. E2 and P treatment diminished the upregulation resulting in weaker fluorescence signals. Determination of the mean fluorescence revealed a significant increase of NLRP3 levels and a slight but not statistically significant reduction achieved by both steroid hormones.

ASC data showed a similar trend with increased fluorescence signals after hypoxia and a reduction after steroid hormone supplementation (Figure 24a-h).

3.12. Casp1 activation after hypoxia and regulation by steroid hormones in astrocytes

Finally, I have examined the influence of hypoxia and steroid hormone supplementation on Casp1 expression and activity in astrocytes (Figure 25). As demonstrated in Figure 25a-h, Casp1 fluorescence signals increased after hypoxia in GFAP+ astrocytes. Neither E2 nor P administration dampened the fluorescence intensity. These findings were confirmed by mean value determination of the fluorescence signal. Measurement of Casp1 activity in astrocytes (Figure 25B) revealed that under hypoxic conditions a comparable number of cells were Casp1+ in comparison with normoxia conditions. Only P was able to decrease Casp1 activity (Figure 25B).

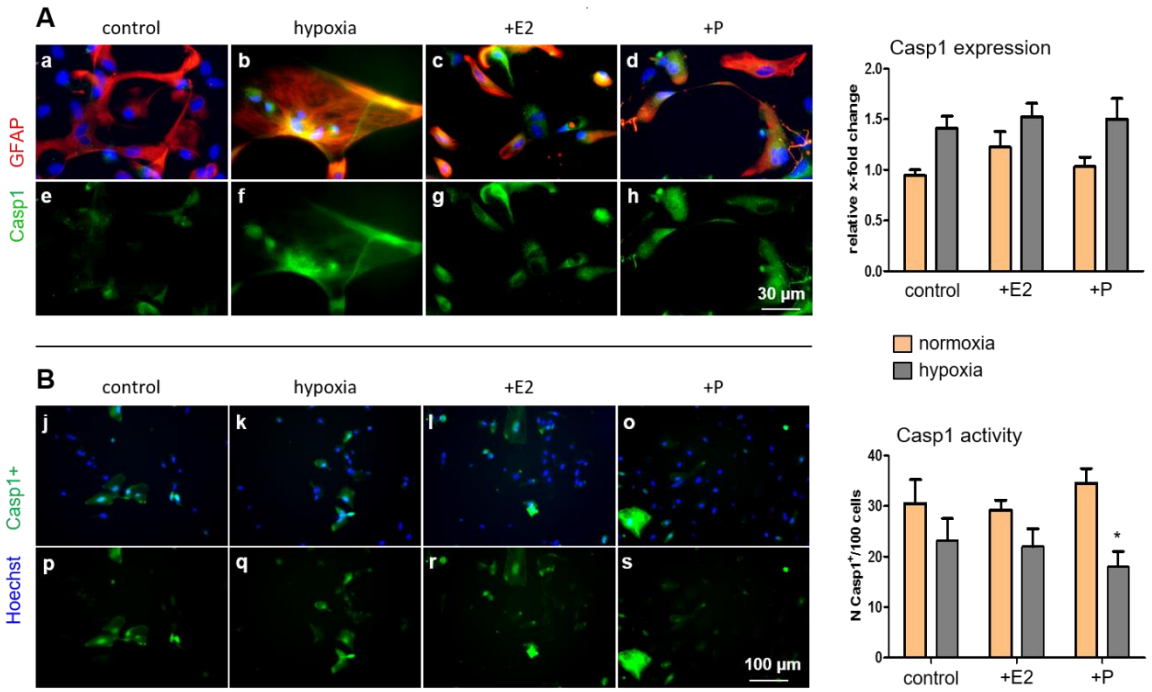

Figure 25: Casp1 expression and activity after hypoxia in astrocytes

(A) Expression of Casp1 was measured by fluorescence double-staining of green-labeled Casp1 with red-labeled GFAP. Stimulated by hypoxic conditions, selectively more Casp1 signals were found in GFAP+ astrocytes (b, f) as compared with normoxia controls (a, e). However, this effect was not significant. E2 (c, g) or P (d, h) administration did not affect Casp1 levels after hypoxia. (B) Measurement of Casp1 activity. Note that P treatment reduced Casp1 activity. Counting of Casp1+ cells revealed high numbers under normoxia, whereas hypoxia caused a decrease. Selective P administration diminished Casp1+ cell numbers. Scale bars represent 30 µm (a-h) or 100 µm (j-s). *: $p \leq 0.05$, the asterisks indicate comparison of groups with normoxia. Data represent the means ± SEM.

4. Discussion

4.1. General

Transient MCAO in rats is a valid an well-accepted experimental model for studying ischemia-related neuropathological processes including neuronal death, cerebral inflammation, and BBB damage in the affected brain area [189]. In a first setting, I attempted to reassure whether this animal and stroke model is also suited for investigating inflammasomes. I slightly modified our tMCAO model by replacing the prior used tip of a human heart catheter by silicone rubber-coated monofilaments. This intraluminal suture method is characterized by its high reproducibility when an appropriate suture size according to the animal weight is selected [190,191]. In this study, I used a size of 0.41 mm diameter, which resulted in a low animal number, which had to be excluded throughout this study. I used Wistar rats to be able to compare previous data with the present and because this strain shows a very low variability of infarct sizes [192]. Three animals of totally 54 rats had to be excluded from the study because the animals did not survive the next 72 h after stroke onset. All other animals developed typical ischemic brain pathologies including ipsilateral hemisphere tissue death and related neurobehavioral deficits. Neuroprotective effects of E2 and P in the experimental stroke models such as tMCAO are well-documented by several other studies [117,118,148,150,193]. Neuroprotection is dose- and time dependent [194]. An early application and appropriate concentrations (25 mg/kg for E2 and 10 mg/kg for P) are needed to dampen stroke pathophysiological and other side effects like increased survival rates after tMCAO [117,194,195].

Irrespective of the particular brain disorder, i.e. ischemia, acute brain trauma, neurodegeneration, there are common mechanisms discussed by which gonadal steroids might execute their neuroprotective role. Brain-derived neurotrophic factor (BDNF) is involved in neuronal survival, synaptic plasticity, learning and memory, and neuroplasticity. Exogenous application of BDNF promoted improvement of motor skills in a rat stroke model [196]. An important mechanism by which E2 and P affect neuronal survival in the CNS is the increase of endogenous BDNF protein levels [197]. Excitotoxicity is another mechanism mediating neuronal cell loss through an excess of extracellular glutamate after an ischemic insult. The damaging

effects result in the activation of downstream intracellular signaling pathways including the influx of calcium ions into neuronal cells, which finally orchestrate pro-apoptotic cascades [198]. One possibility of E2 action to attenuate glutamate-induced neurotoxicity might be to increase glutamate transporters activity/expression in astrocytes [183,199,200]. In contrast, the neuroprotective potential of P and its metabolites could be related to a direct blocking of calcium entry through voltage-gated calcium channels into neurons [201]. The apoptotic activity in cells finally can be suppressed by E2 through activation of the transcription factor signal transducer and activator of transcription 3 (STAT3) and inhibition of Akt phosphorylation by P [202,203]. Another decisive pathological process after stroke is mitochondrial impairment which results in ROS release [204]. It has been shown that E2 and P directly improve mitochondrial function and diminish ROS release in neurons, activated primary rat microglia, microglia cell lines and astrocytes [166,186,205–207]. Mitochondria-released ROS represents an important trigger for the expression of a number of pro-inflammatory genes such as NF-κB, Hif1, TNFα or IL1β [21,22]. TNFα and IL1β are pro-inflammatory cytokines that contribute to stroke pathology. A particular anti-inflammatory action of both steroids has also been shown *in vivo* and *in vitro* and could be confirmed as part of this work [117,152,182,205,208]. Generally, the reduction of inflammatory processes is mainly responsible for dampening the devastating non-physiological post-stroke scenario and finally protects cells.

4.2. Inflammasome components and miR-223 *in vivo* after tMCAO and steroid hormone treatment

4.2.1. Impact of steroid hormones on cytokines after tMCAO

After stroke, the expression pattern of cytokines, inflammasome components and miR-223 reveal a robust time-dependent profile. Cytokines showed a fast reaction with highest levels appearing at 12 to 24 h post ischemia, and inflammasomes showed a peak expression at 72 h. The application of E2 or P ameliorate the expression of stroke-induced IL18 and TNFα. IL1β expression was also reduced by E2 (~70 %) and P (~77 %) but did not reach a significant level, whereas IL1β protein was ameliorated completely by both steroid hormones. Both steroids also regulated NRLC4, ASC at the mRNA level, and E2 selectively NLRP1b and miR-223. Casp1 was regulated by both steroids and other components were selectively modified by E2 (ASC and NLRP3) or P (NLRP1).

Exemplarily, WB analysis partially confirmed the qrtPCR data. Due to the limitations of antibody specificity, only the mature IL1ß protein could be confidently evaluated. Since the pro-forms of IL1β and IL18 are cleaved by the same enzyme [209], therefore a similar maturation process for IL18 might be expected. IL1β maturation shows the same processing mechanism as described for NLRP3 activation. The regulatory scenario of inflammasome activation requires a first stimulus which primes the system and induces mRNA expression of distinct target genes (i.e. pro-IL1β) and the maturation of the translated pro-IL1β into its mature form. Afterwards, this cytokine is secreted by the cell to act as a signal for neighboring cells [210]. During the maturation of IL1β and IL18, additional factors are necessary which carry the CARD domain, the specific interaction side with caspases [40]. It is unclear whether IL-18 plays an important role for neuropathological changes in the early phase of stroke. IL-18-silencing in mice had no effect on the infarct volume and improvement of neurological scoring after tMCAO [211,212]. On the other hand, Hedtjarn et al. and colleagues demonstrated in postnatal rats at P7 and mice at P9 using a gas supply hypoxia system with reduced oxygen concentrations that the infarct size and the behavioral scoring were significantly lower in IL-18 knockout animals compared to wt littermates [213]. The contribution of IL18 to ischemic pathology in the immature brain was allocated to microglia cells. Hypothermia decreased IL18 expression and suppressed microglia activation [214]. At later stages in life, IL18 might lose its significance in the acute phase of stroke and might gain other functions such as its participation in the prediction of the development of post-stroke depression [215].

4.2.2. Regulation of NLRP1 by steroid hormones after tMCAO

NLRP1b is an inflammasome member with a CARD domain and, in contrast to other inflammasomes, interacts directly with caspases without the adaptor ASC [70]. The protein size of NLRP1 is considered as approx. 165 kDa with five known isoforms which lack several amino acids in the LRR domain and result in smaller sized NLRP1 isoforms of approx. 150 kDa [216]. I was only able to detect the 70 kDa isoform in the cerebral cortex penumbra. This small form of NLRP1 completely lacks the LRR domain and has already been described in the thymus and Jurkat T cell line [217,218]. Since the short NLRP1b isoform is also detectable in sham animals, I assume that under non pathological conditions low numbers of T cells could be present. This is supported by a recent work, where regulatory T cells were found in healthy rat brains and participating in the suppression of inflammation [219]. In

stroke pathogenesis, leukocytes pass through the disturbed BBB and infiltrate the brain parenchyma. Beside neutrophils, T cells enter the CNS with inflammatory and protective roles in the acute phase [220]. This might be an explanation of increased 70 kDa-NLRP1b protein in the penumbra after ischemia. As the amount of this small isoform of NLRP1b was further increased after E2 (not significant) and P, it might represent an additional aspect how these steroid hormones could support hampered tissue by recruiting a supportive T cell subpopulation. T cell recruitment seems to be a fast responses after ischemia, where different immune cell populations are seen 3 to 24 h after stroke onset [220]. Information relating to the impact of E2 and/or P impact on T cell recruitment is sparse. The action of NLRP1b on the migration/function of different T cell subpopulations might give new insights into stroke pathology and steroid hormone-dependent neuroprotective abilities. Another possible theory is a switching of NLRP1b between an active or inactive form. The 70 kDa isoform may be considered as an inactive form. Through conformational changes, it might be transformed into the active form. This concept however seems less likely, since after tMCAO two bands of NLRP1b should be detectable or at least a shift from the 70 kDa to the approx. 165 kDa lane should occur. The presence of increased levels of this small isoform after E2 and P application could support this theory. The possibility of a complex consisting of NLRP1 and ASC at approx. 165 kDa is also doubtful. Non-covalent protein interactions are split by the denaturing conditions of the WB approach and there is no evidence so far about ASC fusion with NLRP1. This is emphasized by the detection of only one ASC lane at approx. 24 kDa. In general, the suppression of NLRP1b appears to be beneficial in stroke and other models [60,71,221]. Thus, the anti-inflammatory action of E2 and P might be linked with pathways involving NLRP1b signaling.

4.2.3. Impact of steroid hormones on NLRC4 and AIM2 after tMCAO

Casp1 can directly interact with inflammasome components containing a CARD domain and omit the ASC adaptor, so that other inflammasome components increasingly move to the fore [40]. The same research group also found smaller infarct sizes and an improved neurological score in NLRC4$^{-/-}$- and AIM2$^{-/-}$-knockout mice but not in NLRP3$^{-/-}$ animals [70]. In contrast to AIM2, NLRC4 can interact with Casp1 with or without needing to interfere with the ASC adaptor, both leading to cell death [40]. They proposed a contribution of NLRC4 and AIM2 independently of NLRP3 in stroke

pathology. NLRC4 expression was boosted after tMCAO, which indicates the involvement of NLRC4 in this model. Both hormones attenuated the mRNA expression of NLRC4 *in vivo.* However, due to the fact, that appropriate antisera for NLRC4 were not available at the time, I performed these experiments, I cannot provide information about the respective protein values. The analysis of newly synthetized NLRC4 or AIM2 protein after ischemia could help us to draw a more precise picture of NLRC4 and AIM2 contention in stroke pathology.

4.2.4. Impact of steroid hormones on NLRP3 and miR223 after tMCAO

Interestingly, NLRP3 protein was already present at high amounts in both the ipsi- and contralateral hemispheres in sham animals and almost disappeared during the early phase after stroke although gene expression was still elevated and only returned to basal levels at 72 h. E2 but not P administration inhibited the drop in protein levels after tMCAO. These data are somehow contradict to other findings, where Fann et al. attributed NLRP3 a predominant role in stroke-induced cell death [60]. The FDA approved immunoglobulins (IVIg), through suppressing NLRP3 activity, rescued cortical neurons from cell death in a murine tMCAO model [60]. However, other reports show that tMCAO-related effects in NLRP3$^{-/-}$ knockout mice were not different from wt controls [70]. Since NLRP3 was predominantly expressed by neurons, we speculate that neurons are equipped with NLRP3 for fast reactions in response to vulnerable conditions. The influence of E2 by restoring the drop of NLRP3 after tMCAO is correlated positively with an up-regulation of miR-223 under steroid hormone therapy. MiR-223 is evidently a strong suppressor of NLRP3 [102,222]. In human and mice studies, circulating miR-223 in the blood and brain were elevated in human stroke patients and tMCAO mice [223]. In these studies, elevated miR-223 correlated with smaller infarct sizes and lower NIHSS scores (lower scores mean smaller infarcts). The neuroprotective potency of miR-223 is further highlighted by increasing the infarct volume in miR-223 knockout mice and decreasing after the application of a miR-223 mimic [103]. In my study, I observed that 24 h post reperfusion, levels of NLRP3 and miR-223 mRNAs were increased but NLRP3 protein was absent. Therefore, miR-223 might inhibit the translation of NLRP3 leading to a stepwise reduction of NLRP3 protein which results in a complete absence at 24 h post tMCAO. After prolonged survival, miR-223 expression might further increase, whereas NLRP3 protein returned to sham levels. NLRP3 is not the only target of miR-223. Recently, Turner et al. demonstrated additional targets of miR-223, such

as the glutamate receptor subunits GluR2 and NR2B [103]. They showed that protein levels of both subunits were elevated after a bilateral common carotid artery occlusion in miR-223 knockout mice. This implicates that miR-223 affects different target genes in a randomly manner or in a still unknown process only selectively. Therefore, a yet unknown regulatory mechanism could sense protein levels of the specifically regulated miRNA target genes to guide the miRNA to its specific targets. This seems quite unusual and would need many sensors. So far, no further information regarding such regulatory mechanism is available. A novel miRNA, miR-BART15 derived from Epstein-Barr Virus, was recently shown to target the same 3'-UTR side as miR-223 does [224]. Even when this specific miRNA not naturally occurs in mammalians, it shows that other miRNAs might also regulate NLRP3. Supplementary, using an *in situ* hybridization approach could help us to verify the dominant neural cell types which express miR-223 after tMCAO. Overall, I have to note that miR-223 expression and NLRP3 protein levels were opposed. This underlines our hypothesis about E2-mediated action through miR-223 on NLRP3. I would expect higher NLRP3 protein and lower or unchanged miR-223 expression post tMCAO and *vice versa* lower NLRP3 and induced miR-223 expression following E2 administration. Nevertheless, my data indicate that NLRP3 is regulated by E2 through miR-223 in neurons.

4.2.5. Impact of steroid hormones on ASC after tMCAO

It is thought that under normal conditions, the CNS is fully supplied with all inflammasome components to assure that inflammasomes can easily assemble and cleave the pro-forms of IL1β and IL18 under pathological conditions. The transcription of the Pycard gene and translation into ASC adaptor protein appears to be delayed in our experimental model. Highest protein amounts were found at 72 h post stroke and Pycard expression peaked at 12 h and at 72 h. This delay might be due to a regulatory mechanism, such as miRNA regulation/inhibition. Taking the effects of steroid hormone treatment in consideration, different pathways might be involved in ASC up-regulation. P dampened ASC at mRNA but not protein level. A prolonged pathophysiological condition might overcome initial P action at later reperfusion stage in comparison to E2. Beyond this, a possible switch in ASC expression in different neural cells could be a reason. It is imaginable that P attenuates mRNA levels in cell type A, whereas expression of the ASC gene is elevated in cell type B, which is not influenced by P. As an argument against such an idea, PR are widely

expressed in the CNS with no restriction to specific cell types [145,146]. A research group recently assigned ASC a dominant role during tMCAO. They indicated that $ASC^{-/-}$-knockout mice show a significant reduction in infarct volume and a better neurological outcome after ischemia [70]. It is however questionable whether a complete missing of ASC in the CNS is generally neuroprotective or reduced cytokine secretion from glial cells is the impetus to neuroprotection due to inhibited inflammasome assembly. My data indicate that at least E2 potentially execute neuroprotection by dampening ASC.

4.2.6. Impact of steroid hormones on Casp1 after tMCAO

A surprising finding in my study was the diminution of the cleaved 10 kDa active Casp1 form. E2 and P diminished the decrease after tMCAO. Casp1 is cleaved from its pro-form into 10 and 20 kDa subunits. Active Casp1 includes two heterodimers and interacts with its CARD domain to form the inflammasome [209]. Increased IL1β levels lead to the assumption of higher amounts of the active Casp1 subunit, which is assembled by other components resulting in inflammasome activation. This process did not occur in our model. The amount of Casp1 P10 decreased at 24 h and 72 h post ischemia in comparison to sham animals. In contrast, the pro-form almost completely disappeared at 12 h and returned to the initial values at 24 h and 72 h post tMCAO. Since this issue can be explained by a rapid cleavage of the pro-Casp1 into the active subunits followed by expression and translation of new pro-Casp1, the withdrawal of P10 leaves room for speculations. I would expect an increase of the active P10 isoform following cerebral ischemia as demonstrated in *in vitro* OGD and *in vivo* tMCAO experiments [60]. However, reduced P10 levels correlate with decreased NLRP3 following tMCAO and selectively increased post E2 or P administration. I assume that Casp1 P10 mainly restricts to neurons. To support this, IL1β maturation can take place in the cytosol or in lysosomal exocytotic vesicles. A part of Casp1 is released and due to its short half-life finally degraded [225,226]. It was demonstrated that apoptosis occurs after an ischemic insult predominantly in the hypoxic penumbra, whereas the ischemic core is characterized by necrotic cell death due to complete lack of oxygen and nutrients [227]. It is generally accepted that endogenous Casp1 is not involved in apoptosis [228,229] but rather inducing pyroptotic cell death [228]. Therefore, lower Casp1 protein levels could be the result of reduced cell numbers in the penumbra due to apoptotic cells and Casp1 con-

sumption after IL1β maturation. On the other hand, the peri-infarct zone is characterized by microgliosis, which might be the main source of IL1β release [117]. A more detailed investigation of Casp1 expression and allocation to intrinsic brain cell types might contribute to a better understanding of Casp1 regulation and activity in the peri-infarct zone. Another model to explain the ambiguity of Casp1 function might evolve from the fact that Casp1 has a low substrate specificity at high concentrations which was changed by lowering Casp1 concentrations [225]. This is supported by other studies which show the dependency of the transcription factors sterol regulatory element binding proteins (SREBPs) of active Casp1 and the involvement in N-methyl-D-aspartate receptor (NMDAR)-mediated excitotoxic neuronal death in *in vivo* and *in vitro* models of hypoxia [229–232]. This attributes Casp1 a role in the control of neuronal survival. On the contrary, IL1β maturation might be Casp1 independent as IL1β levels raise in parallel by an elevation of gelatinolytic activity in a rat tMCAO model [233]. Since in stroke manifold stimuli are present in the extra as well as in the stressed intracellular compartment, it seems plausible that more signaling pathways contribute to IL1ß processing and activation. At the end, I suggest that predominant amounts of NLRP3, miR-223 and Casp1 are allocated to neurons and these are involved in neuronal loss. How astrocytes and BV-2 cells react to *in vitro* hypoxia and how these components are involved will be discussed in the next section.

4.3. Inflammasome components and miR-223 in astrocytes and BV-2 cells after *in vitro* hypoxia and steroid hormone treatment

Next, the impact of *ex vivo*-hypoxia on glial cells with or without steroid hormone supplementation will be discussed. Neuronal cell death in stroke is mainly impressed by oxidative stress (ROS) and excitotoxicity [234], principally when cerebral blood flow is temporarily occluded [37]. Further, inflammation triggered by activated microglia cells strongly contributes to the aggravation of hypoxic cell death [235]. To generate hypoxic conditions, a self-constructed cube-shaped hypoxia chamber was flooded with nitrogen gas to mimic hypoxic conditions *in vitro* comparable to the *in vivo* situation. Our hypoxia model mimics hypoxic conditions for a short period, so that cell death is limited but cellular processes mediated by hypoxic factors are triggered [185–187]. I used primary murine astrocytes and a murine microglia-like cell

line BV-2, due to the limited amount of primary microglia cells. In response to hypoxia, BV-2 cells show similar morphological changes and expression profiles when comparted to primary microglia cells [126].

4.3.1. Impact of steroid hormones on cytokine expression in glial cells after hypoxia

Hypoxia induced a similar cytokine expression profile in both BV-2 cells and astrocytes. IL1β was elevated, whereas IL18 dropped (BV-2) or remained unmodified (astrocytes). E2 and P substitution altered only IL1β in BV-2 cells. E2 and P supplementation failed to inhibit hypoxia-induced IL1β secretion in BV-2 cells similar to previously reported data [185].

Since IL18 and IL1β have similar schematic profiles of inflammasome activation, the discrepancy between both cytokine expressions are an unexpected finding. Hanamsager et al. and colleagues presented similar data and independent behavioral reactions of IL1β from IL18 [47]. Depletion of NLRP3 and ASC attenuated IL1β secretion, whereas IL18 secretion was not affected. They discussed the existence of NLRP3 independent pathways contributing to IL18 processing and secretion. Other inflammasomes could also take part in IL18 processing. A possible candidate is NLRC4. But besides NLRC4, further stimuli are required for IL18 processing. As shown for IL1β secretion, different pathways play a role in monocytes and macrophages [236]. Casp1 is constitutively active in monocytes and a single stimulation with a TLR ligand leads to the release of the active IL1β form. In contrast, macrophages need two signals for IL1β secretion: (i), TLR-ligands induce IL1β transcription; (ii) a separate signal that provokes inflammasome activation. Similar distinctive pathways for IL18 processing are imaginable. My data indicate no clear-cut role for IL18 in our acute model. This supports the idea of the participation of IL18 at a later stage after stroke, thereby contributing to the development of depression.

Taking together, it can be safely concluded that microglial cells are a considerable source of IL1ß as an acute response to brain injury [185,187]. Using BV-2 cells, we have shown that this cell line closely resembles the *in vivo* microglia phenotype in many functional and pathophysiological responses. These cells secrete a large portion of cytokines into the supernatant. Notwithstanding the value of IL1ß for neuroinflammatory processes in the CNS, it needs to be mentioned that microglial cells and BV-2 cells also secrete a variety of other cytokines after stimulation such as TNFα, CCL5, or IL10 [185]. In contrary to *in vivo*, the administration of E2 or P did not

reduce IL1β amounts in the supernatant of hypoxic BV-2 cells or gene expression in astrocytes. This is surprising and unexpected. From previous studies, I know that both, BV-2 cells and astrocytes, are fully equipped with the necessary ERs and PRs [185,186]. Further, non-classical steroid receptors, which play also a role in the physiological and pathophysiological activation of cells, are also expressed under normoxia conditions. One idea of the lack of effects is that E2 and P influence the up-stream maturation cascade but not the final steps of IL1β processing. On the other hand, synthesis, processing and release of mature IL1β is tightly regulated as shown in monocytes and macrophages [237]. Pro-IL1β was generally not detectable in unstimulated monocytes and only stimuli lead to its expression. In that case, E2 and P have the potential to diminish IL1β expression [238]. Even other signaling pathways have taken into consideration as shown in human trophoblasts, where IL1β secretion was induced without the participation of NLRP3 and ASC [239]. Here, NOD1 was the driving factor for IL1β maturation besides Casp1.

4.3.2. Impact of steroid hormones on NLRP1, NLRC4 and AIM2 in glial cells after hypoxia

Hypoxia resulted in the down-regulation of NLRP1b, NLRC4 and AIM2 mRNA levels in BV-2 cells, whereas only AIM2 was up-regulated astrocytes. Treatment with E2 and P did not considerably affect these expression patterns in BV-2 cells and only reduced AIM2 in astroglia. These results clearly demonstrate different reactions of glial subtypes to hypoxia. I assume (and have preliminary evidence) that all CNS cells are fully equipped with inflammasome components to be assembled after a toxic/hypoxic stimulus [40]. Thus, reduced mRNA levels do not affect acute inflammasome assembly or function. This suggests that these inflammasome components do not necessarily participate in BV-2 cell-mediated inflammation. On the other hand, my data suggest that astrocytes are a major source of NLRC4 and AIM2 after cerebral ischemia. This is supported by findings which show that NLRC4, AIM2 and IL1β protein do not co-localize in microglia cells [70].

4.3.3. Impact of steroid hormones on NLRP3 and miR-223 in glial cells after hypoxia

NLRP3 expression at the gene and protein level was elevated following hypoxia in BV-2 cells and astrocytes. E2 and P selectively regulated these accretions. E2 boosted and P did not affect NLRP3 at the mRNA level in BV-2 cells but NLRP3

protein levels were reduced by E2 and P in both cell types. MiR-223 expression was not affected by hypoxia or steroid hormone supplementation. This implies that miR-223 has not a decisive impact as NLRP3 suppressor in both glial cells. Despite, other miR-223 targets could be regulated which were not in the focus of this study (see section 4.2.4). In our focus, ROS might be a key player for NLRP3 stimulation. Previously, we have shown that ROS production is increased *in vitro* by hypoxia and inhibited by both steroid hormones [185,186]. It is still under debate whether ROS is a common and pivotal effector in NLRP3 regulation [170]. At least in our chosen experimental *in vitro* model, this seems to be true. Thus, protective E2 and P action could be in part transmitted via an inhibition of ROS synthesis and thereby affecting NLRP3.The discrepancy between E2 and P effects *in vivo* (only E2 effective on NLRP3 protein) vs. *in vitro* (both E2 and P effective) might be explained by the absence of any cell-cell communication in culture. Future experiments using ROS inhibitors might answer this issue.

4.3.4. Impact of steroid hormones on ASC in glial cells after hypoxia

The ASC protein is required for interactions between inflammasomes and Casp1, with the exception of NLRC4 which interacts directly with Casp1-domain [40]. E2 and P have a regulatory effect on ASC expression *in vitro* (E2 attenuated ASC mRNA expression and both steroids decreased ASC protein in astrocytes and ASC mRNA expression in BV-2 cells). *In vivo*, ASC only significantly increased after 72 h *in vivo* and mainly co-localized with Iba1-positive cells. This indicates that microglia/macrophages are the main source of ASC which was also proposed by others [218]. BV-2 cells are furnished with sufficient amounts of ASC to build inflammasome complexes and initiate Casp1-mediated cytokine maturation. A prolonged hypoxia period or reperfusion duration might lead to significantly elevated ASC protein levels in BV-2 cells. On the other hand, the discrepancy between mRNA and the protein level might indicate an additional and unknown regulatory mechanism for ASC translation or differences in RNA/protein stability and/or turnover. The delayed massive increase suggest a switch of microglia cell function to an apoptotic or pyroptotic pathway mediated via ASC [240]. Co-localization studies of ASC with pro-apoptotic or pro-pyroptotic markers would be helpful to understand this dual reaction of microglia. In my *in vitro* hypoxia experiments, BV-2 and astrocytes were stressed but still not forced to enter cell death cascades [185–187]. The importance of ASC

in triggering inflammasome action was shown recently. An ASC knockdown improved neurological scores and reduced the infarct size in a mouse tMCAO model [70]. Therefore, I suggest that E2 regulatory effects on inflammasome involve ASC. P seems not to arbitrate its neuroprotective effects by this adaptor protein.

4.3.5. Impact of steroid hormones on Casp1 in glial cells after hypoxia

Finally, the role of Casp1 in glial cells following hypoxia and its possible regulation by E2 and P will be in the focus. Casp1 protein was neither after hypoxia nor by E2 or P regulated in BV-2 cells and astrocytes. Casp1 activity was elevated after hypoxia in BV-2. Steroid supplementation failed to regulate this activity. Surprisingly, Casp1 activity was higher in astrocytes and not influenced by hypoxia. P administration lowered Casp1 activity after hypoxia in astrocytes. Here, I have to consider that by using ICC, we are not able to discriminate between active Casp1 P10 and the inactive-forms. Therefore, I have used another experimental approach to determine the activity of Casp1, i.e. binding of active Casp1 to a green fluorescence labeled Casp1 inhibitor. Hypoxia led to a higher Casp1 activity. I further determined higher numbers of positive Casp1 signals in BV-2 cell cultures. E2 and P substitution did not reduce Casp1 activity. These results are in accordance with data from earlier measured IL1β concentrations in hypoxia-stimulated BV-2 cells. It underlines our hypothesis that E2 and P influence IL1β processing at an earlier stage but not the final maturation and release. In another study, Li et al. showed in primary mixed glia cultures and BV-2 cells in separate experiments that mimicking hypoxia with cobalt chloride ($CoCl_2$) or OGD failed to activate Casp1 [241]. On the contrary, OGD/$CoCl_2$-induced hypoxia led to activated Casp1 in bone marrow-derived macrophages. In primary mouse microglia cells, NLRP3 but not AIM2 activity was inhibited by OGD/$CoCl_2$-induced hypoxia. Increased Casp1 indicates an upstream mechanism that is responsible for Casp1 cleavage; AIM2 could be such a possible candidate. Further, information about AIM2 protein levels and its co-localization are needed to determine which components interact with Casp1. In astrocytes, neither Casp1 protein levels were increased nor Casp1 activity significantly changed. This indicates that even under conditions with elevated NLRP3 and ASC levels, Casp1 activity has not been boosted further by hypoxia. Co-localization studies might help to investigate sufficient inflammasome assembly after hypoxia and function of inflammasomes. Overall, I have shown that under normoxia the number of Casp1-positive astrocytes cells was significantly higher than for BV2 cells. Three hours hypoxia did

not affect the LDH release (marker for pyroptosis) [186]. It is known from other studies that LDH release requires a much longer hypoxic conditions [242]. Therefore, the analysis of Casp1 activity and LDH release after prolonged hypoxia or reperfusion might better indicate whether pyroptosis takes place at these later stages.

4.4. Translation

An important point to be addressed when working with animal models is that there are several differences between human and rodent stroke pathology. Gonadal steroid hormones showed neuroprotection in different experimental stroke studies [117–119]. The benefit of these steroids in human clinical trials are critically discussed [16]. First off all, anatomical structures of the CNS and brain blood supply in rodents differ from humans. Thus, the primary ischemic core after tMCAO may recover and a secondary delayed injury may evolve after a free interval of up to 12 h, which is not seen in human [190]. In experimental studies, most therapeutic drugs are applied directly after removal of the occluding filament or after tMCAO operation, which are most effective at this time point to protect the undersupplied penumbra region. Another issue occurs due to temperature management of the operated animals. For instance, hypothalamic ischemia develops always in rats following a 60 min period of tMCAO [243], whereas hypothalamic involvement rarely occurs in human stroke. The involvement of the hypothalamus in rat tMCAO models results from a hypothermic response, which persist for at least one day and may affect further analysis [243]. Mice also reveal hypothalamic involvement but due to the smaller surface/volume ratio of the mouse, temperature loss in the postoperative period leads to higher death rates. This implies to keep operated mice after tMCAO under a heating lamp to improve their survival [244]. Interactions between these CNS regions might influence each other, so that all other analyses may be affected.

Many different processes and factors hamper translation from animal science to human pathology. Since stroke mostly occurs in elderly patients who often show comorbidity, other pathophysiological processes can influence neuroprotective properties of tested drugs. Further, human samples are typically taken post mortem, were pathophysiological processes may be progressed and not reflecting initial cell damage and physiology.

4.5. Conclusion

In the present study, I could demonstrate novel aspects of neuroinflammatory processes after ischemia using a stroke animal model. In particular, I have profiled the activation and expression pattern of different inflammasomes and their allocation to specific cell types. Furthermore, I have demonstrated that sex steroids such as E2 and P are capable of modulating/dampening neuroinflammation in that way that tissue damage has reduced.

Beside neurons, I could clearly verify that inflammasome components are release by microglia and astroglial cells. This indicates the interaction of both cell types for the initiation and perpetuation of the neuroinflammatory cascade after stroke. The positive impact of steroid hormones on neuroinflammation appears selective by only regulating distinct inflammasome components and even the downstream regulatory role of miR-223 which is particularly important for NLRP3 activation. I conclude that my data contribute to a better understanding of pathophysiological processes in the brain after an ischemic insult and will help to design and test novel drugs for that devastating disease.

5. **References**

[1] World Health Organization, The Atlas of Heart Disease and Stroke, available at http://www.who.int/cardiovascular_diseases/resources/atlas/en/.

[2] M.A. Moskowitz, E.H. Lo, C. Iadecola, The science of stroke: mechanisms in search of treatments, Neuron 67 (2010) 181–198.

[3] E.C. Jauch, J.L. Saver, H.P. Adams, A. Bruno, J.J.B. Connors, B.M. Demaerschalk, P. Khatri, P.W. McMullan, A.I. Qureshi, K. Rosenfield, P.A. Scott, D.R. Summers, D.Z. Wang, M. Wintermark, H. Yonas, Guidelines for the early management of patients with acute ischemic stroke: a guideline for healthcare professionals from the American Heart Association/American Stroke Association, Stroke; a journal of cerebral circulation 44 (2013) 870–947.

[4] The Internet Stroke Center, available at http://www.strokecenter.org.

[5] U. Dirnagl, M. Endres, Found in translation: preclinical stroke research predicts human pathophysiology, clinical phenotypes, and therapeutic outcomes, Stroke; a journal of cerebral circulation 45 (2014) 1510–1518.

[6] National Heart, Lung and Blood Institute, What is a Stroke?, available at http://www.nhlbi.nih.gov/health/health-topics/topics/stroke.

[7] D. Mozaffarian, E.J. Benjamin, A.S. Go, D.K. Arnett, M.J. Blaha, M. Cushman, S. de Ferranti, J.-P. Després, H.J. Fullerton, V.J. Howard, M.D. Huffman, S.E. Judd, B.M. Kissela, D.T. Lackland, J.H. Lichtman, L.D. Lisabeth, S. Liu, R.H. Mackey, D.B. Matchar, D.K. McGuire, E.R. Mohler, C.S. Moy, P. Muntner, M.E. Mussolino, K. Nasir, R.W. Neumar, G. Nichol, L. Palaniappan, D.K. Pandey, M.J. Reeves, C.J. Rodriguez, P.D. Sorlie, J. Stein, A. Towfighi, T.N. Turan, S.S. Virani, J.Z. Willey, D. Woo, R.W. Yeh, M.B. Turner, Heart disease and stroke statistics--2015 update: a report from the American Heart Association, Circulation 131 (2015) 322.

[8] K.K. Andersen, T.S. Olsen, C. Dehlendorff, L.P. Kammersgaard, Hemorrhagic and ischemic strokes compared: stroke severity, mortality, and risk factors, Stroke; a journal of cerebral circulation 40 (2009) 2068–2072.

[9] P.L. Kolominsky-Rabas, C. Sarti, P.U. Heuschmann, C. Graf, S. Siemonsen, B. Neundoerfer, A. Katalinic, E. Lang, K.G. Gassmann, T.R. von Stockert, A prospective community-based study of stroke in Germany--the Erlangen

Stroke Project (ESPro): incidence and case fatality at 1, 3, and 12 months, Stroke; a journal of cerebral circulation 29 (1998) 2501–2506.

[10] U. Dirnagl, C. Iadecola, M.A. Moskowitz, Pathobiology of ischaemic stroke: an integrated view, Trends in Neurosciences 22 (1999) 391–397.

[11] A.R. Xavier, A.I. Qureshi, J.F. Kirmani, A.M. Yahia, R. Bakshi, Neuroimaging of stroke: a review, Southern medical journal 96 (2003) 367–379.

[12] L.R. Caplan, Are terms such as completed stroke or RIND of continued usefulness?, Stroke 14 (1983) 431–433.

[13] G.C. Fonarow, E.E. Smith, J.L. Saver, M.J. Reeves, D.L. Bhatt, M.V. Grau-Sepulveda, D.M. Olson, A.F. Hernandez, E.D. Peterson, L.H. Schwamm, Timeliness of tissue-type plasminogen activator therapy in acute ischemic stroke: patient characteristics, hospital factors, and outcomes associated with door-to-needle times within 60 minutes, Circulation 123 (2011) 750–758.

[14] L. Wechsler, P. Lyden, For how long is brain tissue salvageable? Thrombolysis-based evidence, Journal of stroke and cerebrovascular diseases the official journal of National Stroke Association 9 (2000) 21–23.

[15] A.R. Young, O. Touzani, J.-M. Derlon, G. Sette, E.T. MacKenzie, J.-C. Baron, Early Reperfusion in the Anesthetized Baboon Reduces Brain Damage Following Middle Cerebral Artery Occlusion: A Quantitative Analysis of Infarction Volume, Stroke 28 (1997) 632–638.

[16] D.J. Gladstone, S.E. Black, A.M. Hakim, Toward Wisdom From Failure: Lessons From Neuroprotective Stroke Trials and New Therapeutic Directions, Stroke 33 (2002) 2123–2136.

[17] P. Lipton, Ischemic cell death in brain neurons, Physiological reviews 79 (1999) 1431–1568.

[18] R. Brouns, P.P. de Deyn, The complexity of neurobiological processes in acute ischemic stroke, Clinical neurology and neurosurgery 111 (2009) 483–495.

[19] F.C. Choy, T.S. Klarić, S.A. Koblar, M.D. Lewis, The Role of the Neuroprotective Factor Npas4 in Cerebral Ischemia, International journal of molecular sciences 16 (2015) 29011–29028.

[20] J. Silver, J.H. Miller, Regeneration beyond the glial scar, Nature reviews. Neuroscience 5 (2004) 146–156.

[21] K. Ruscher, N. Isaev, G. Trendelenburg, M. Weih, L. Iurato, A. Meisel, U. Dirnagl, Induction of hypoxia inducible factor 1 by oxygen glucose deprivation is attenuated by hypoxic preconditioning in rat cultured neurons, Neuroscience Letters 254 (1998) 117–120.

[22] S.J. Hopkins, N.J. Rothwell, Cytokines and the nervous system I: Expression and recognition, Trends in Neurosciences 18 (1995) 83–88.

[23] Q. Wang, X.N. Tang, M.A. Yenari, The inflammatory response in stroke, Journal of Neuroimmunology 184 (2007) 53–68.

[24] P.L. Wood, Microglia as a unique cellular target in the treatment of stroke: potential neurotoxic mediators produced by activated microglia, Neurological Research 17 (1995) 242–248.

[25] K. Rupalla, P.R. Allegrini, D. Sauer, C. Wiessner, Time course of microglia activation and apoptosis in various brain regions after permanent focal cerebral ischemia in mice, Acta Neuropathologica 96 (1998) 172–178.

[26] A. Günther, L. Küppers-Tiedt, P.-M. Schneider, I. Kunert, J. Berrouschot, D. Schneider, S. Rossner, Reduced infarct volume and differential effects on glial cell activation after hyperbaric oxygen treatment in rat permanent focal cerebral ischaemia, The European journal of neuroscience 21 (2005) 3189–3194.

[27] N. Zhang, M. Komine-Kobayashi, R. Tanaka, M. Liu, Y. Mizuno, T. Urabe, Edaravone reduces early accumulation of oxidative products and sequential inflammatory responses after transient focal ischemia in mice brain, Stroke; a journal of cerebral circulation 36 (2005) 2220–2225.

[28] A. Denes, R. Vidyasagar, J. Feng, J. Narvainen, B.W. McColl, R.A. Kauppinen, S.M. Allan, Proliferating resident microglia after focal cerebral ischaemia in mice, Journal of cerebral blood flow and metabolism official journal of the International Society of Cerebral Blood Flow and Metabolism 27 (2007) 1941–1953.

[29] K. Nakajima, S. Kohsaka, Microglia: Neuroprotective and Neurotrophic Cells in the Central Nervous System, CDTCHD 4 (2004) 65–84.

[30] W.J. Streit, Microglia as neuroprotective, immunocompetent cells of the CNS, Glia 40 (2002) 133–139.

[31] Y. Zhao, D.A. Rempe, Targeting astrocytes for stroke therapy, Neurotherapeutics the journal of the American Society for Experimental NeuroTherapeutics 7 (2010) 439–451.

[32] M. Pekny, M. Nilsson, Astrocyte activation and reactive gliosis, Glia 50 (2005) 427–434.

[33] S.J. Hewett, J.K. Muir, D. Lobner, A. Symons, D.W. Choi, M.A. Moskowitz, C. Ayata, Potentiation of Oxygen-Glucose Deprivation Induced Neuronal Death After Induction of iNOS, Stroke 27 (1996) 1586–1591.

[34] G. Singhal, E.J. Jaehne, F. Corrigan, C. Toben, B.T. Baune, Inflammasomes in neuroinflammation and changes in brain function: a focused review, Frontiers in neuroscience 8 (2014) 315.

[35] A. Slowik, C. Beyer, Inflammasomes are neuroprotective targets for sex steroids, The Journal of Steroid Biochemistry and Molecular Biology 153 (2015) 135–143.

[36] M.T. Heneka, M.P. Kummer, E. Latz, Innate immune activation in neurodegenerative disease, Nature reviews. Immunology 14 (2014) 463–477.

[37] C.D. Savage, G. Lopez-Castejon, A. Denes, D. Brough, NLRP3-Inflammasome Activating DAMPs Stimulate an Inflammatory Response in Glia in the Absence of Priming Which Contributes to Brain Inflammation after Injury, Front. Immun. 3 (2012).

[38] A. Stutz, D.T. Golenbock, E. Latz, Inflammasomes: too big to miss, The Journal of clinical investigation 119 (2009) 3502–3511.

[39] F. Martinon, K. Burns, J. Tschopp, The inflammasome: a molecular platform triggering activation of inflammatory caspases and processing of proIL-beta, Molecular Cell 10 (2002) 417–426.

[40] J.G. Walsh, D.A. Muruve, C. Power, Inflammasomes in the CNS, Nat. Rev. Neurosci. 15 (2014) 84–97.

[41] L.-C. Hsu, S.R. Ali, S. McGillivray, P.-H. Tseng, S. Mariathasan, E.W. Humke, L. Eckmann, J.J. Powell, V. Nizet, V.M. Dixit, M. Karin, A NOD2-NALP1 complex mediates caspase-1-dependent IL-1beta secretion in response to Bacillus anthracis infection and muramyl dipeptide, Proc. Natl. Acad. Sci. U.S.A. 105 (2008) 7803–7808.

[42] J.P. de Rivero Vaccari, W.D. Dietrich, R.W. Keane, Activation and regulation of cellular inflammasomes: gaps in our knowledge for central nervous system injury, J Cereb Blood Flow Metab 34 (2014) 369–375.

[43] T. Fernandes-Alnemri, J.-W. Yu, P. Datta, J. Wu, E.S. Alnemri, AIM2 activates the inflammasome and cell death in response to cytoplasmic DNA, Nature 458 (2009) 509–513.

[44] Y. Yin, Y. Yan, X. Jiang, J. Mai, N.C. Chen, H. Wang, X.-F. Yang, Inflammasomes are differentially expressed in cardiovascular and other tissues, Int J Immunopathol Pharmacol 22 (2009) 311–322.

[45] de Rivero Vaccari, Juan Pablo, G. Lotocki, A.E. Marcillo, W.D. Dietrich, R.W. Keane, A molecular platform in neurons regulates inflammation after spinal cord injury, J. Neurosci. 28 (2008) 3404–3414.

[46] de Rivero Vaccari, Juan Pablo, G. Lotocki, O.F. Alonso, H.M. Bramlett, W.D. Dietrich, R.W. Keane, Therapeutic neutralization of the NLRP1 inflammasome reduces the innate immune response and improves histopathology after traumatic brain injury, Journal of cerebral blood flow and metabolism official journal of the International Society of Cerebral Blood Flow and Metabolism 29 (2009) 1251–1261.

[47] R. Hanamsagar, V. Torres, T. Kielian, Inflammasome activation and IL-1β/IL-18 processing are influenced by distinct pathways in microglia, J. Neurochem. 119 (2011) 736–748.

[48] Y. Jamilloux, R. Pierini, M. Querenet, C. Juruj, A.-L. Fauchais, M.-O. Jauberteau, S. Jarraud, G. Lina, J. Etienne, C.R. Roy, T. Henry, N. Davoust, F. Ader, Inflammasome activation restricts Legionella pneumophila replication in primary microglial cells through flagellin detection, Glia 61 (2013) 539–549.

[49] S.E. Adamczak, de Rivero Vaccari, Juan Pablo, G. Dale, F.J. Brand, D. Nonner, M.R. Bullock, G.P. Dahl, W.D. Dietrich, R.W. Keane, Pyroptotic neuronal cell death mediated by the AIM2 inflammasome, Journal of cerebral blood flow and metabolism official journal of the International Society of Cerebral Blood Flow and Metabolism 34 (2014) 621–629.

[50] F.G. Bauernfeind, G. Horvath, A. Stutz, E.S. Alnemri, K. MacDonald, D. Speert, T. Fernandes-Alnemri, J. Wu, B.G. Monks, K.A. Fitzgerald, V. Hornung, E. Latz, Cutting edge: NF-kappaB activating pattern recognition and cytokine receptors license NLRP3 inflammasome activation by regulating

NLRP3 expression, Journal of immunology (Baltimore, Md. 1950) 183 (2009) 787–791.

[51] E. Latz, T.S. Xiao, A. Stutz, Activation and regulation of the inflammasomes, Nature reviews. Immunology 13 (2013) 397–411.

[52] J. Minkiewicz, de Rivero Vaccari, Juan Pablo, R.W. Keane, Human astrocytes express a novel NLRP2 inflammasome, Glia 61 (2013) 1113–1121.

[53] H. Peng, B. Chang, C. Lu, J. Su, Y. Wu, P. Lv, Y. Wang, J. Liu, B. Zhang, F. Quan, Z. Guo, Y. Zhang, H. Clarke, Nlrp2, a Maternal Effect Gene Required for Early Embryonic Development in the Mouse, PloS one 7 (2012) e30344.

[54] G. Trendelenburg, Molecular regulation of cell fate in cerebral ischemia: role of the inflammasome and connected pathways, Journal of cerebral blood flow and metabolism official journal of the International Society of Cerebral Blood Flow and Metabolism 34 (2014) 1857–1867.

[55] F. Yang, Z. Wang, X. Wei, H. Han, X. Meng, Y. Zhang, W. Shi, F. Li, T. Xin, Q. Pang, F. Yi, NLRP3 deficiency ameliorates neurovascular damage in experimental ischemic stroke, Journal of cerebral blood flow and metabolism official journal of the International Society of Cerebral Blood Flow and Metabolism 34 (2014) 660–667.

[56] S.S. Iyer, W.P. Pulskens, J.J. Sadler, L.M. Butter, G.J. Teske, T.K. Ulland, S.C. Eisenbarth, S. Florquin, R.A. Flavell, J.C. Leemans, F.S. Sutterwala, Necrotic cells trigger a sterile inflammatory response through the Nlrp3 inflammasome, Proceedings of the National Academy of Sciences of the United States of America 106 (2009) 20388–20393.

[57] C. Jin, R.A. Flavell, Innate sensors of pathogen and stress: linking inflammation to obesity, The Journal of allergy and clinical immunology 132 (2013) 287–294.

[58] M. Rabuffetti, C. Sciorati, G. Tarozzo, E. Clementi, A.A. Manfredi, M. Beltramo, Inhibition of caspase-1-like activity by Ac-Tyr-Val-Ala-Asp-chloromethyl ketone induces long-lasting neuroprotection in cerebral ischemia through apoptosis reduction and decrease of proinflammatory cytokines, The Journal of neuroscience the official journal of the Society for Neuroscience 20 (2000) 4398–4404.

[59] J. Ross, D. Brough, R.M. Gibson, S.A. Loddick, N.J. Rothwell, A selective, non-peptide caspase-1 inhibitor, VRT-018858, markedly reduces brain damage induced by transient ischemia in the rat, Neuropharmacology 53 (2007) 638–642.

[60] D.Y.-W. Fann, S.Y. Lee, S. Manzanero, S.C. Tang, M. Gelderblom, P. Chunduri, C. Bernreuther, M. Glatzel, Y.L. Cheng, J. Thundyil, A. Widiapradja, K.Z. Lok, S.L. Foo, Y.C. Wang, Y.I. Li, G.R. Drummond, M. Basta, T. Magnus, D.G. Jo, M.P. Mattson, C.G. Sobey, T.V. Arumugam, Intravenous immunoglobulin suppresses NLRP1 and NLRP3 inflammasome-mediated neuronal death in ischemic stroke, Cell death & disease 4 (2013) e790.

[61] D.P. Abulafia, de Rivero Vaccari, Juan Pablo, J.D. Lozano, G. Lotocki, R.W. Keane, W.D. Dietrich, Inhibition of the inflammasome complex reduces the inflammatory response after thromboembolic stroke in mice, Journal of cerebral blood flow and metabolism official journal of the International Society of Cerebral Blood Flow and Metabolism 29 (2009) 534–544.

[62] F. Bauernfeind, E. Bartok, A. Rieger, L. Franchi, G. Núñez, V. Hornung, Cutting edge: reactive oxygen species inhibitors block priming, but not activation, of the NLRP3 inflammasome, Journal of immunology (Baltimore, Md. 1950) 187 (2011) 613–617.

[63] J. Dang, L.-O. Brandenburg, C. Rosen, A. Fragoulis, M. Kipp, T. Pufe, C. Beyer, C.J. Wruck, Nrf2 expression by neurons, astroglia, and microglia in the cerebral cortical penumbra of ischemic rats, Journal of molecular neuroscience MN 46 (2012) 578–584.

[64] A.Y. Shih, P. Li, T.H. Murphy, A small-molecule-inducible Nrf2-mediated antioxidant response provides effective prophylaxis against cerebral ischemia in vivo, The Journal of neuroscience the official journal of the Society for Neuroscience 25 (2005) 10321–10335.

[65] C. Zhao, D.D. Gillette, X. Li, Z. Zhang, H. Wen, Nuclear factor E2-related factor-2 (Nrf2) is required for NLRP3 and AIM2 inflammasome activation, The Journal of biological chemistry 289 (2014) 17020–17029.

[66] A. Cauwels, E. Rogge, B. Vandendriessche, S. Shiva, P. Brouckaert, Extracellular ATP drives systemic inflammation, tissue damage and mortality, Cell death & disease 5 (2014) e1102.

[67] R. Muñoz-Planillo, P. Kuffa, G. Martínez-Colón, B.L. Smith, T.M. Rajendiran, G. Núñez, K^+ efflux is the common trigger of NLRP3 inflammasome activation by bacterial toxins and particulate matter, Immunity 38 (2013) 1142–1153.

[68] V. Pétrilli, S. Papin, C. Dostert, A. Mayor, F. Martinon, J. Tschopp, Activation of the NALP3 inflammasome is triggered by low intracellular potassium concentration, Cell death and differentiation 14 (2007) 1583–1589.

[69] W.R. Silverman, de Rivero Vaccari, Juan Pablo, S. Locovei, F. Qiu, S.K. Carlsson, E. Scemes, R.W. Keane, G. Dahl, The pannexin 1 channel activates the inflammasome in neurons and astrocytes, The Journal of biological chemistry 284 (2009) 18143–18151.

[70] A. Denes, G. Coutts, N. Lénárt, S.M. Cruickshank, P. Pelegrin, J. Skinner, N. Rothwell, S.M. Allan, D. Brough, AIM2 and NLRC4 inflammasomes contribute with ASC to acute brain injury independently of NLRP3, Proceedings of the National Academy of Sciences of the United States of America 112 (2015) 4050–4055.

[71] D.Y.-W. Fann, S.-Y. Lee, S. Manzanero, P. Chunduri, C.G. Sobey, T.V. Arumugam, Pathogenesis of acute stroke and the role of inflammasomes, Ageing research reviews 12 (2013) 941–966.

[72] C. Iadecola, J. Anrather, The immunology of stroke: from mechanisms to translation, Nature medicine 17 (2011) 796–808.

[73] A. Kaczmarek, P. Vandenabeele, D.V. Krysko, Necroptosis: the release of damage-associated molecular patterns and its physiological relevance, Immunity 38 (2013) 209–223.

[74] G. Ziegler, V. Prinz, M.W. Albrecht, D. Harhausen, U. Khojasteh, W. Nacken, M. Endres, U. Dirnagl, W. Nietfeld, G. Trendelenburg, Mrp-8 and -14 mediate CNS injury in focal cerebral ischemia, Biochimica et biophysica acta 1792 (2009) 1198–1204.

[75] D.P. Bartel, MicroRNAs, Cell 116 (2004) 281–297.

[76] Y. Zhao, J.F. Ransom, A. Li, V. Vedantham, M. von Drehle, A.N. Muth, T. Tsuchihashi, M.T. McManus, R.J. Schwartz, D. Srivastava, Dysregulation of cardiogenesis, cardiac conduction, and cell cycle in mice lacking miRNA-1-2, Cell 129 (2007) 303–317.

[77] M. Carleton, M.A. Cleary, P.S. Linsley, MicroRNAs and cell cycle regulation, Cell cycle (Georgetown, Tex.) 6 (2007) 2127–2132.

[78] Y. Lee, K. Jeon, J.-T. Lee, S. Kim, V.N. Kim, MicroRNA maturation: stepwise processing and subcellular localization, The EMBO journal 21 (2002) 4663–4670.

[79] V.N. Kim, J. Han, M.C. Siomi, Biogenesis of small RNAs in animals, Nature reviews. Molecular cell biology 10 (2009) 126–139.

[80] J. Winter, S. Jung, S. Keller, R.I. Gregory, S. Diederichs, Many roads to maturity: microRNA biogenesis pathways and their regulation, Nature cell biology 11 (2009) 228–234.

[81] Y. Lee, M. Kim, J. Han, K.-H. Yeom, S. Lee, S.H. Baek, V.N. Kim, MicroRNA genes are transcribed by RNA polymerase II, The EMBO journal 23 (2004) 4051–4060.

[82] X. Cai, C.H. Hagedorn, B.R. Cullen, Human microRNAs are processed from capped, polyadenylated transcripts that can also function as mRNAs, RNA (New York, N.Y.) 10 (2004) 1957–1966.

[83] Y. Lee, C. Ahn, J. Han, H. Choi, J. Kim, J. Yim, J. Lee, P. Provost, O. Rådmark, S. Kim, V.N. Kim, The nuclear RNase III Drosha initiates microRNA processing, Nature 425 (2003) 415–419.

[84] V.N. Kim, MicroRNA precursors in motion: exportin-5 mediates their nuclear export, Trends in cell biology 14 (2004) 156–159.

[85] U.A. Ørom, F.C. Nielsen, A.H. Lund, MicroRNA-10a binds the 5'UTR of ribosomal protein mRNAs and enhances their translation, Molecular Cell 30 (2008) 460–471.

[86] Y. Tay, J. Zhang, A.M. Thomson, B. Lim, I. Rigoutsos, MicroRNAs to Nanog, Oct4 and Sox2 coding regions modulate embryonic stem cell differentiation, Nature 455 (2008) 1124–1128.

[87] S. Jalali, G.K. Ramanathan, P.T. Parthasarathy, S. Aljubran, L. Galam, A. Yunus, S. Garcia, R.R. Cox, R.F. Lockey, N. Kolliputi, Mir-206 regulates pulmonary artery smooth muscle cell proliferation and differentiation, PloS one 7 (2012) e46808.

[88] A. Krek, D. Grün, M.N. Poy, R. Wolf, L. Rosenberg, E.J. Epstein, P. MacMenamin, I. da Piedade, K.C. Gunsalus, M. Stoffel, N. Rajewsky, Combinatorial microRNA target predictions, Nature genetics 37 (2005) 495–500.

[89] Ricarte Filho, Júlio C M, E.T. Kimura, MicroRNAs: nova classe de reguladores gênicos envolvidos na função endócrina e câncer, Arquivos brasileiros de endocrinologia e metabologia 50 (2006) 1102–1107.

[90] C. Wang, B. Ji, B. Cheng, J. Chen, B. Bai, Neuroprotection of microRNA in neurological disorders (Review), Biomedical reports 2 (2014) 611–619.

[91] L.F. Sempere, S. Freemantle, I. Pitha-Rowe, E. Moss, E. Dmitrovsky, V. Ambros, Expression profiling of mammalian microRNAs uncovers a subset of brain-expressed microRNAs with possible roles in murine and human neuronal differentiation, Genome biology 5 (2004) R13.

[92] X. HE, Q. ZHANG, Y. LIU, X. PAN, Cloning and Identification of Novel MicroRNAs from Rat Hippocampus, Acta Biochim Biophys Sinica 39 (2007) 708–714.

[93] M. Lagos-Quintana, R. Rauhut, A. Yalcin, J. Meyer, W. Lendeckel, T. Tuschl, Identification of Tissue-Specific MicroRNAs from Mouse, Current Biology 12 (2002) 735–739.

[94] K.S. Tan, A. Armugam, S. Sepramaniam, K.Y. Lim, K.D. Setyowati, C.W. Wang, K. Jeyaseelan, Expression profile of MicroRNAs in young stroke patients, PloS one 4 (2009) e7689.

[95] A. Dharap, R. Vemuganti, Ischemic pre-conditioning alters cerebral microRNAs that are upstream to neuroprotective signaling pathways, Journal of neurochemistry 113 (2010) 1685–1691.

[96] W. Sun, W. Shen, S. Yang, F. Hu, H. Li, T.-H. Zhu, miR-223 and miR-142 attenuate hematopoietic cell proliferation, and miR-223 positively regulates miR-142 through LMO2 isoforms and CEBP-β, Cell research 20 (2010) 1158–1169.

[97] J.B. Johnnidis, M.H. Harris, R.T. Wheeler, S. Stehling-Sun, M.H. Lam, O. Kirak, T.R. Brummelkamp, M.D. Fleming, F.D. Camargo, Regulation of progenitor cell proliferation and granulocyte function by microRNA-223, Nature 451 (2008) 1125–1129.

[98] F. Fazi, S. Racanicchi, G. Zardo, L.M. Starnes, M. Mancini, L. Travaglini, D. Diverio, E. Ammatuna, G. Cimino, F. Lo-Coco, F. Grignani, C. Nervi, Epigenetic silencing of the myelopoiesis regulator microRNA-223 by the AML1/ETO oncoprotein, Cancer cell 12 (2007) 457–466.

[99] V. Fulci, G. Scappucci, G.D. Sebastiani, C. Giannitti, D. Franceschini, F. Meloni, T. Colombo, F. Citarella, V. Barnaba, G. Minisola, M. Galeazzi, G. Macino, miR-223 is overexpressed in T-lymphocytes of patients affected by rheumatoid arthritis, Human immunology 71 (2010) 206–211.

[100] J.-f. Wang, M.-l. Yu, G. Yu, J.-j. Bian, X.-m. Deng, X.-j. Wan, K.-m. Zhu, Serum miR-146a and miR-223 as potential new biomarkers for sepsis, Biochemical and biophysical research communications 394 (2010) 184–188.

[101] C.-H. Yu, C.-F. Xu, Y.-M. Li, Association of MicroRNA-223 expression with hepatic ischemia/reperfusion injury in mice, Digestive diseases and sciences 54 (2009) 2362–2366.

[102] F. Bauernfeind, A. Rieger, F.A. Schildberg, P.A. Knolle, J.L. Schmid-Burgk, V. Hornung, NLRP3 Inflammasome Activity Is Negatively Controlled by miR-223, The Journal of Immunology 189 (2012) 4175–4181.

[103] M.M. Harraz, S.M. Eacker, X. Wang, T.M. Dawson, V.L. Dawson, MicroRNA-223 is neuroprotective by targeting glutamate receptors, Proceedings of the National Academy of Sciences of the United States of America 109 (2012) 18962–18967.

[104] R.T. Turner, B.L. Riggs, T.C. Spelsberg, Skeletal effects of estrogen, Endocrine reviews 15 (1994) 275–300.

[105] H.J. Teede, Sex hormones and the cardiovascular system: effects on arterial function in women, Clinical and experimental pharmacology & physiology 34 (2007) 672–676.

[106] P. Appelros, B. Stegmayr, A. Terént, Sex differences in stroke epidemiology: a systematic review, Stroke; a journal of cerebral circulation 40 (2009) 1082–1090.

[107] T.B. Wyller, Stroke and gender, The journal of gender-specific medicine JGSM the official journal of the Partnership for Women's Health at Columbia 2 (1999) 41–45.

[108] C. Behl, Oestrogen as a neuroprotective hormone, Nature reviews. Neuroscience 3 (2002) 433–442.

[109] V.R. Feeser, R.M. Loria, Modulation of traumatic brain injury using progesterone and the role of glial cells on its neuroprotective actions, Journal of Neuroimmunology 237 (2011) 4–12.

[110] R. Saunders-Pullman, Estrogens and Parkinson Disease: Neuroprotective, Symptomatic, Neither, or Both?, ENDO 21 (2003) 81–88.

[111] H. Xu, G.K. Gouras, J.P. Greenfield, B. Vincent, J. Naslund, L. Mazzarelli, G. Fried, J.N. Jovanovic, M. Seeger, N.R. Relkin, F. Liao, F. Checler, J.D. Buxbaum, B.T. Chait, G. Thinakaran, S.S. Sisodia, R. Wang, P. Greengard, S. Gandy, Estrogen reduces neuronal generation of Alzheimer beta-amyloid peptides, Nature medicine 4 (1998) 447–451.

[112] G. Candore, C.R. Balistreri, M.P. Grimaldi, S. Vasto, F. Listì, M. Chiappelli, F. Licastro, D. Lio, C. Caruso, Age-related inflammatory diseases: role of genetics and gender in the pathophysiology of Alzheimer's disease, Annals of the New York Academy of Sciences 1089 (2006) 472–486.

[113] W.B. Kannel, Menopause and Risk of Cardiovascular Disease, Ann Intern Med 85 (1976) 447.

[114] A.J. Mhyre, D.M. Dorsa, Estrogen activates rapid signaling in the brain: role of estrogen receptor alpha and estrogen receptor beta in neurons and glia, Neuroscience 138 (2006) 851–858.

[115] M. Kipp, C. Beyer, Impact of sex steroids on neuroinflammatory processes and experimental multiple sclerosis, Frontiers in neuroendocrinology 30 (2009) 188–200.

[116] I. Merchenthaler, T.L. Dellovade, P.J. Shughrue, Neuroprotection by estrogen in animal models of global and focal ischemia, Annals of the New York Academy of Sciences 1007 (2003) 89–100.

[117] J. Dang, B. Mitkari, M. Kipp, C. Beyer, Gonadal steroids prevent cell damage and stimulate behavioral recovery after transient middle cerebral artery occlusion in male and female rats, Brain, behavior, and immunity 25 (2011) 715–726.

[118] C. Ulbrich, A. Zendedel, P. Habib, M. Kipp, C. Beyer, J. Dang, Long-term cerebral cortex protection and behavioral stabilization by gonadal steroid hormones after transient focal hypoxia, The Journal of Steroid Biochemistry and Molecular Biology 131 (2012) 10–16.

[119] N.J. Alkayed, I. Harukuni, A.S. Kimes, E.D. London, R.J. Traystman, P.D. Hurn, P.A. Grady, Gender-Linked Brain Injury in Experimental Stroke Editorial Comment, Stroke 29 (1998) 159–166.

[120] L.M. Garcia-Segura, F. Naftolin, J.B. Hutchison, I. Azcoitia, J.A. Chowen, Role of astroglia in estrogen regulation of synaptic plasticity and brain repair, Journal of neurobiology 40 (1999) 574–584.

[121] C. Beyer, Estrogen and the developing mammalian brain, Anatomy and embryology 199 (1999) 379–390.

[122] B. McEwen, Estrogen actions throughout the brain, Recent progress in hormone research 57 (2002) 357–384.

[123] T. Numakawa, T. Matsumoto, Y. Numakawa, M. Richards, S. Yamawaki, H. Kunugi, Protective Action of Neurotrophic Factors and Estrogen against Oxidative Stress-Mediated Neurodegeneration, Journal of toxicology 2011 (2011) 405194.

[124] V.V. Chaban, A.J. Lakhter, P. Micevych, A membrane estrogen receptor mediates intracellular calcium release in astrocytes, Endocrinology 145 (2004) 3788–3795.

[125] D. Lebesgue, V. Chevaleyre, R.S. Zukin, A.M. Etgen, Estradiol rescues neurons from global ischemia-induced cell death: multiple cellular pathways of neuroprotection, Steroids 74 (2009) 555–561.

[126] P. Habib, C. Beyer, Regulation of brain microglia by female gonadal steroids, The Journal of Steroid Biochemistry and Molecular Biology 146 (2015) 3–14.

[127] G. Mor, J. Nilsen, T. Horvath, I. Bechmann, S. Brown, L.M. Garcia-Segura, F. Naftolin, Estrogen and microglia: A regulatory system that affects the brain, Journal of neurobiology 40 (1999) 484–496.

[128] C.M. Klinge, Estrogen receptor interaction with co-activators and co-repressors☆, Steroids 65 (2000) 227–251.

[129] O.K. Rønnekleiv, A. Malyala, M.J. Kelly, Membrane-initiated signaling of estrogen in the brain, Seminars in reproductive medicine 25 (2007) 165–177.

[130] C.D. Toran-Allerand, X. Guan, N.J. MacLusky, T.L. Horvath, S. Diano, M. Singh, E.S. Connolly, I.S. Nethrapalli, A.A. Tinnikov, ER-X: a novel, plasma membrane-associated, putative estrogen receptor that is regulated during development and after ischemic brain injury, The Journal of neuroscience the official journal of the Society for Neuroscience 22 (2002) 8391–8401.

[131] E. Brailoiu, S.L. Dun, G.C. Brailoiu, K. Mizuo, L.A. Sklar, T.I. Oprea, E.R. Prossnitz, N.J. Dun, Distribution and characterization of estrogen receptor G

protein-coupled receptor 30 in the rat central nervous system, The Journal of endocrinology 193 (2007) 311–321.

[132] H. Sakamoto, K.-i. Matsuda, K. Hosokawa, M. Nishi, J.F. Morris, E.R. Prossnitz, M. Kawata, Expression of G protein-coupled receptor-30, a G protein-coupled membrane estrogen receptor, in oxytocin neurons of the rat paraventricular and supraoptic nuclei, Endocrinology 148 (2007) 5842–5850.

[133] S.A. Laredo, R. Villalon Landeros, B.C. Trainor, Rapid effects of estrogens on behavior: environmental modulation and molecular mechanisms, Frontiers in neuroendocrinology 35 (2014) 447–458.

[134] V. Naderi, M. Khaksari, R. Abbasi, F. Maghool, Estrogen provides neuroprotection against brain edema and blood brain barrier disruption through both estrogen receptors alpha and beta following traumatic brain injury, Iranian journal of basic medical sciences 18 (2015) 138–144.

[135] J.G. Elzer, S. Muhammad, T.M. Wintermantel, A. Regnier-Vigouroux, J. Ludwig, G. Schütz, M. Schwaninger, Neuronal estrogen receptor-alpha mediates neuroprotection by 17beta-estradiol, Journal of cerebral blood flow and metabolism official journal of the International Society of Cerebral Blood Flow and Metabolism 30 (2010) 935–942.

[136] K. Saijo, J.G. Collier, A.C. Li, J.A. Katzenellenbogen, C.K. Glass, An ADIOL-ERβ-CtBP transrepression pathway negatively regulates microglia-mediated inflammation, Cell 145 (2011) 584–595.

[137] J. Sun, G. Nan, The Mitogen-Activated Protein Kinase (MAPK) Signaling Pathway as a Discovery Target in Stroke, Journal of molecular neuroscience MN (2016).

[138] R.C. Melcangi, S. Giatti, D. Calabrese, M. Pesaresi, G. Cermenati, N. Mitro, B. Viviani, L.M. Garcia-Segura, D. Caruso, Levels and actions of progesterone and its metabolites in the nervous system during physiological and pathological conditions, Allopregnanolone: State of the Art 113 (2014) 56–69.

[139] C.J. Prestigiacomo, S.C. Kim, E.S. Connolly, H. Liao, S.F. Yan, D.J. Pinsky, CD18-mediated neutrophil recruitment contributes to the pathogenesis of reperfused but not nonreperfused stroke, Stroke; a journal of cerebral circulation 30 (1999) 1110–1117.

[140] I. Sayeed, D.G. Stein, Progesterone as a neuroprotective factor in traumatic and ischemic brain injury, in: J. Verhaagen (Ed.), Neurotherapy: Progress in

restorative neuroscience and neurology proceedings of the 25th international summer school of brain research, held at the Royal Netherlands Academy of Arts and Sciences, Amsterdam, The Netherlands, August 25-28, 2008 / ed-ited by Joost Verhaagen … [et al.], Elsevier, Amsterdam, London, 2009, pp. 219–237.

[141] A. Ardeshiri, M.H. Kelley, I.P. Korner, P.D. Hurn, P.S. Herson, Mechanism of progesterone neuroprotection of rat cerebellar Purkinje cells following oxy-gen–glucose deprivation, European Journal of Neuroscience 24 (2006) 2567–2574.

[142] Y. Pang, J. Dong, P. Thomas, Characterization, Neurosteroid Binding and Brain Distribution of Human Membrane Progesterone Receptors δ and ϵ (mPRδ and mPRϵ) and mPRδ Involvement in Neurosteroid Inhibition of Apoptosis, Endocrinology 154 (2013) 283–295.

[143] M. Singh, C. Su, Progesterone-induced neuroprotection: Factors that may predict therapeutic efficacy, Brain research 1514 (2013) 98–106.

[144] D. Belelli, J.J. Lambert, Neurosteroids: endogenous regulators of the GABAA receptor, Nature Reviews Neuroscience 6 (2005) 565–575.

[145] C. Guerra-Araiza, O. Villamar-Cruz, A. González-Arenas, R. Chavira, I. Camacho-Arroyo, Changes in Progesterone Receptor Isoforms Content in the Rat Brain During the Oestrous Cycle and After Oestradiol and Progester-one Treatments, Journal of neuroendocrinology 15 (2003) 984–990.

[146] R.D. Brinton, R.F. Thompson, Foy, M. Baudry, J. Wang, C.E. Finch, T.E. Morgan, F.Z. Stanczyk, C.J. Pike, J. Nilsen, Progesterone Receptors: Form and Function in Brain, Frontiers in neuroendocrinology 29 (2008) 313–339.

[147] J. Nilsen, R.D. Brinton, Divergent impact of progesterone and medroxypro-gesterone acetate (Provera) on nuclear mitogen-activated protein kinase sig-naling, Proceedings of the National Academy of Sciences of the United States of America 100 (2003) 10506–10511.

[148] M. Liu, M.H. Kelley, P.S. Herson, P.D. Hurn, Neuroprotection of sex steroids, Minerva endocrinologica 35 (2010) 127–143.

[149] J. Chen, M. Chopp, Y. Li, Neuroprotective effects of progesterone after tran-sient middle cerebral artery occlusion in rat, Journal of the neurological sci-ences 171 (1999) 24–30.

[150] D.G. Stein, Progesterone exerts neuroprotective effects after brain injury, Brain research reviews 57 (2008) 386–397.

[151] J. Wang, Y. Zhao, C. Liu, C. Jiang, C. Zhao, Z. Zhu, Progesterone inhibits inflammatory response pathways after permanent middle cerebral artery occlusion in rats, Molecular medicine reports 4 (2011) 319–324.

[152] R. Aggarwal, B. Medhi, A. Pathak, V. Dhawan, A. Chakrabarti, Neuroprotective effect of progesterone on acute phase changes induced by partial global cerebral ischaemia in mice, The Journal of pharmacy and pharmacology 60 (2008) 731–737.

[153] W. Cai, Y. Zhu, K. Furuya, Z. Li, M. Sokabe, L. Chen, Two different molecular mechanisms underlying progesterone neuroprotection against ischemic brain damage, Neuropharmacology 55 (2008) 127–138.

[154] C.L. Gibson, D. Constantin, M.J.W. Prior, P.M.W. Bath, S.P. Murphy, Progesterone suppresses the inflammatory response and nitric oxide synthase-2 expression following cerebral ischemia, Experimental neurology 193 (2005) 522–530.

[155] V.H. Ozacmak, H. Sayan, The effects of 17beta estradiol, 17alpha estradiol and progesterone on oxidative stress biomarkers in ovariectomized female rat brain subjected to global cerebral ischemia, Physiological research / Academia Scientiarum Bohemoslovaca 58 (2009) 909–912.

[156] R.L. Roof, R. Duvdevani, D.G. Stein, Gender influences outcome of brain injury: progesterone plays a protective role, Brain research 607 (1993) 333–336.

[157] K.M. Webster, D.K. Wright, M. Sun, B.D. Semple, E. Ozturk, D.G. Stein, T.J. O'Brien, S.R. Shultz, Progesterone treatment reduces neuroinflammation, oxidative stress and brain damage and improves long-term outcomes in a rat model of repeated mild traumatic brain injury, Journal of neuroinflammation 12 (2015) 238.

[158] S. Kovats, Estrogen receptors regulate an inflammatory pathway of dendritic cell differentiation: mechanisms and implications for immunity, Hormones and behavior 62 (2012) 254–262.

[159] G. Nalbandian, S. Kovats, Understanding sex biases in immunity: effects of estrogen on the differentiation and function of antigen-presenting cells, Immunologic research 31 (2005) 91–106.

[160] E. Giannoni, L. Guignard, M. Knaup Reymond, M. Perreau, M. Roth-Kleiner, T. Calandra, T. Roger, Estradiol and progesterone strongly inhibit the innate immune response of mononuclear cells in newborns, Infection and immunity 79 (2011) 2690–2698.

[161] L. Su, Y. Sun, F. Ma, P. Lü, H. Huang, J. Zhou, Progesterone inhibits Toll-like receptor 4-mediated innate immune response in macrophages by suppressing NF-kappaB activation and enhancing SOCS1 expression, Immunology letters 125 (2009) 151–155.

[162] S. Muñoz-Cruz, C. Togno-Pierce, J. Morales-Montor, Non-reproductive effects of sex steroids: their immunoregulatory role, Current topics in medicinal chemistry 11 (2011) 1714–1727.

[163] M. Cunningham, G. Gilkeson, Estrogen Receptors in Immunity and Autoimmunity, Clinic Rev Allerg Immunol 40 (2011) 66–73.

[164] K.C. Williams, N.E. Renthal, R.D. Gerard, C.R. Mendelson, The microRNA (miR)-199a/214 cluster mediates opposing effects of progesterone and estrogen on uterine contractility during pregnancy and labor, Molecular endocrinology (Baltimore, Md.) 26 (2012) 1857–1867.

[165] S.M. Cutler, M. Cekic, D.M. Miller, B. Wali, J.W. VanLandingham, D.G. Stein, Progesterone improves acute recovery after traumatic brain injury in the aged rat, Journal of neurotrauma 24 (2007) 1475–1486.

[166] A. Grimm, K. Schmitt, U.E. Lang, A.G. Mensah-Nyagan, A. Eckert, Improvement of neuronal bioenergetics by neurosteroids: Implications for age-related neurodegenerative disorders, Biochimica et Biophysica Acta (BBA) - Molecular Basis of Disease 1842 (2014) 2427–2438.

[167] S. Johann, C. Beyer, Neuroprotection by gonadal steroid hormones in acute brain damage requires cooperation with astroglia and microglia, The Journal of Steroid Biochemistry and Molecular Biology 137 (2013) 71–81.

[168] Y. Zhu, M. Wu, C.-y. Wu, G.-q. Xia, Role of progesterone in TLR4-MyD88-dependent signaling pathway in pre-eclampsia, J. Huazhong Univ. Sci. Technol. [Med. Sci.] 33 (2013) 730–734.

[169] B.N. Martin, C. Wang, J. Willette-Brown, T. Herjan, M.F. Gulen, H. Zhou, K. Bulek, L. Franchi, T. Sato, E.S. Alnemri, G. Narla, X.-P. Zhong, J. Thomas, D. Klinman, K.A. Fitzgerald, M. Karin, G. Nuñez, G. Dubyak, Y. Hu, X. Li,

IKKα negatively regulates ASC-dependent inflammasome activation, Nat Comms 5 (2014) 4977.

[170] J.M. Abais, M. Xia, Y. Zhang, K.M. Boini, P.-L. Li, Redox Regulation of NLRP3 Inflammasomes: ROS as Trigger or Effector?, Antioxidants & redox signaling (2014).

[171] C. Munding, M. Keller, G. Niklaus, S. Papin, J. Tschopp, S. Werner, H.-D. Beer, The estrogen-responsive B box protein: a novel enhancer of interleukin-1beta secretion, Cell death and differentiation 13 (2006) 1938–1949.

[172] Y. Nishi, M. Satoh, H. Nagasu, H. Kadoya, C. Ihoriya, K. Kidokoro, T. Sasaki, N. Kashihara, Selective estrogen receptor modulation attenuates proteinuria-induced renal tubular damage by modulating mitochondrial oxidative status, Kidney international 83 (2013) 662–673.

[173] R. Dai, R.A. Phillips, Y. Zhang, D. Khan, O. Crasta, S.A. Ahmed, Suppression of LPS-induced Interferon-gamma and nitric oxide in splenic lymphocytes by select estrogen-regulated microRNAs: a novel mechanism of immune modulation, Blood 112 (2008) 4591–4597.

[174] R.J. González-Duarte, V. Cázares-Ordoñez, E. Ávila-Chávez, The microRNA biogenesis machinery: regulation by steroid hormones and alterations in cancer, Revista de investigación clínica; organo del Hospital de Enfermedades de la Nutrición 66 (2014) 460–464.

[175] P. Bhat-Nakshatri, G. Wang, N.R. Collins, M.J. Thomson, T.R. Geistlinger, J.S. Carroll, M. Brown, S. Hammond, E.F. Srour, Y. Liu, H. Nakshatri, Estradiol-regulated microRNAs control estradiol response in breast cancer cells, Nucleic acids research 37 (2009) 4850–4861.

[176] W.B. Nothnick, C. Healy, X. Hong, Steroidal regulation of uterine miRNAs is associated with modulation of the miRNA biogenesis components Exportin-5 and Dicer1, Endocrine 37 (2010) 265–273.

[177] C. Kilkenny, W. Browne, I.C. Cuthill, M. Emerson, D.G. Altman, Animal research: reporting in vivo experiments: the ARRIVE guidelines, British journal of pharmacology 160 (2010) 1577–1579.

[178] J.C. McGrath, G.B. Drummond, E.M. McLachlan, C. Kilkenny, C.L. Wainwright, Guidelines for reporting experiments involving animals: the ARRIVE guidelines, British journal of pharmacology 160 (2010) 1573–1576.

[179] E.Z. Longa, P.R. Weinstein, S. Carlson, R. Cummins, Reversible middle cerebral artery occlusion without craniectomy in rats, Stroke 20 (1989) 84–91.

[180] A. Zendedel, P. Habib, J. Dang, L. Lammerding, S. Hoffmann, C. Beyer, A. Slowik, Omega-3 polyunsaturated fatty acids ameliorate neuroinflammation and mitigate ischemic stroke damage through interactions with astrocytes and microglia, Journal of Neuroimmunology 278 (2015) 200–211.

[181] D. Reglodi, A. Somogyvari-Vigh, S. Vigh, T. Kozicz, A. Arimura, Delayed Systemic Administration of PACAP38 Is Neuroprotective in Transient Middle Cerebral Artery Occlusion in the Rat, Stroke 31 (2000) 1411–1417.

[182] M. Kipp, S. Karakaya, S. Johann, E. Kampmann, J. Mey, C. Beyer, Oestrogen and progesterone reduce lipopolysaccharide-induced expression of tumour necrosis factor-alpha and interleukin-18 in midbrain astrocytes, Journal of neuroendocrinology 19 (2007) 819–822.

[183] J. Pawlak, V. Brito, E. Küppers, C. Beyer, Regulation of glutamate transporter GLAST and GLT-1 expression in astrocytes by estrogen, Brain research. Molecular brain research 138 (2005) 1–7.

[184] E. Blasi, R. Barluzzi, V. Bocchini, R. Mazzolla, F. Bistoni, Immortalization of murine microglial cells by a v-raf / v-myc carrying retrovirus, Journal of Neuroimmunology 27 (1990) 229–237.

[185] P. Habib, D. Dreymueller, A. Ludwig, C. Beyer, J. Dang, Sex steroid hormone-mediated functional regulation of microglia-like BV-2 cells during hypoxia, The Journal of Steroid Biochemistry and Molecular Biology 138 (2013) 195–205.

[186] P. Habib, J. Dang, A. Slowik, M. Victor, C. Beyer, Hypoxia-induced gene expression of aquaporin-4, cyclooxygenase-2 and hypoxia-inducible factor 1α in rat cortical astroglia is inhibited by 17β-estradiol and progesterone, Neuroendocrinology 99 (2014) 156–167.

[187] P. Habib, A. Slowik, A. Zendedel, S. Johann, J. Dang, C. Beyer, Regulation of hypoxia-induced inflammatory responses and M1-M2 phenotype switch of primary rat microglia by sex steroids, Journal of molecular neuroscience MN 52 (2014) 277–285.

[188] L. Lammerding, A. Slowik, S. Johann, C. Beyer, A. Zendedel, Post-Stroke Inflammasome Expression and Regulation in the Peri-Infarct Area by Gonadal

Steroids after Transient Focal Ischemia in the Rat Brain, Neuroendocrinology (2015).

[189] D.W. Howells, M.J. Porritt, S.S.J. Rewell, V. O'Collins, E.S. Sena, van der Worp, H Bart, R.J. Traystman, M.R. Macleod, Different strokes for different folks: the rich diversity of animal models of focal cerebral ischemia, Journal of cerebral blood flow and metabolism official journal of the International Society of Cerebral Blood Flow and Metabolism 30 (2010) 1412–1431.

[190] F. Fluri, M. Schuhmann, C. Kleinschnitz, Animal models of ischemic stroke and their application in clinical research, DDDT (2015) 3445.

[191] K. Tureyen, R. Vemuganti, K.A. Sailor, R.J. Dempsey, Ideal suture diameter is critical for consistent middle cerebral artery occlusion in mice, Neurosurgery 56 (2005) 196-200; discussion 196-200.

[192] J.O. Strom, E. Ingberg, A. Theodorsson, E. Theodorsson, Method parameters' impact on mortality and variability in rat stroke experiments: a meta-analysis, BMC neuroscience 14 (2013) 41.

[193] S. Suzuki, C.M. Brown, P.M. Wise, Neuroprotective effects of estrogens following ischemic stroke, Frontiers in neuroendocrinology 30 (2009) 201–211.

[194] T. Inagaki, Am Etgen, Neuroprotective action of acute estrogens: animal models of brain ischemia and clinical implications, Steroids 78 (2013) 597–606.

[195] C.L. Gibson, S.P. Murphy, Progesterone Enhances Functional Recovery after Middle Cerebral Artery Occlusion in Male Mice, J Cereb Blood Flow Metab 24 (2004) 805–813.

[196] M. Ploughman, V. Windle, C.L. MacLellan, N. White, J.J. Dore, D. Corbett, Brain-derived neurotrophic factor contributes to recovery of skilled reaching after focal ischemia in rats, Stroke; a journal of cerebral circulation 40 (2009) 1490–1495.

[197] T. Ivanova, E. Kuppers, J. Engele, C. Beyer, Estrogen stimulates brain-derived neurotrophic factor expression in embryonic mouse midbrain neurons through a membrane-mediated and calcium-dependent mechanism, Journal of neuroscience research 66 (2001) 221–230.

[198] M.P. Mattson, S.L. Chan, Calcium orchestrates apoptosis, Nature cell biology 5 (2003) 1041–1043.

[199] E. Lee, M. Sidoryk-Wegrzynowicz, Z. Yin, A. Webb, D.-S. Son, M. Aschner, Transforming growth factor-alpha mediates estrogen-induced upregulation of glutamate transporter GLT-1 in rat primary astrocytes, Glia 60 (2012) 1024–1036.

[200] E.-S.Y. Lee, M. Sidoryk, H. Jiang, Z. Yin, M. Aschner, Estrogen and tamoxifen reverse manganese-induced glutamate transporter impairment in astrocytes, Journal of neurochemistry 110 (2009) 530–544.

[201] J.I. Luoma, B.G. Kelley, P.G. Mermelstein, Progesterone inhibition of voltage-gated calcium channels is a potential neuroprotective mechanism against excitotoxicity, Steroids 76 (2011) 845–855.

[202] T. Ishrat, I. Sayeed, F. Atif, F. Hua, D.G. Stein, Progesterone is neuroprotective against ischemic brain injury through its effects on the phosphoinositide 3-kinase/protein kinase B signaling pathway, Neuroscience 210 (2012) 442–450.

[203] S. Dziennis, T. Jia, O.K. Ronnekleiv, P.D. Hurn, N.J. Alkayed, Role of signal transducer and activator of transcription-3 in estradiol-mediated neuroprotection, The Journal of neuroscience the official journal of the Society for Neuroscience 27 (2007) 7268–7274.

[204] M.L. Circu, T.Y. Aw, Reactive oxygen species, cellular redox systems, and apoptosis, Free radical biology & medicine 48 (2010) 749–762.

[205] A.J. Bruce-Keller, J.L. Keeling, J.N. Keller, F.F. Huang, S. Camondola, M.P. Mattson, Antiinflammatory effects of estrogen on microglial activation, Endocrinology 141 (2000) 3646–3656.

[206] A.E. Baker, V.M. Brautigam, J.J. Watters, Estrogen modulates microglial inflammatory mediator production via interactions with estrogen receptor beta, Endocrinology 145 (2004) 5021–5032.

[207] F.O. Dimayuga, J.L. Reed, G.A. Carnero, C. Wang, E.R. Dimayuga, V.M. Dimayuga, A. Perger, M.E. Wilson, J.N. Keller, A.J. Bruce-Keller, Estrogen and brain inflammation: effects on microglial expression of MHC, costimulatory molecules and cytokines, Journal of Neuroimmunology 161 (2005) 123–136.

[208] E. Vegeto, V. Benedusi, A. Maggi, Estrogen anti-inflammatory activity in brain: a therapeutic opportunity for menopause and neurodegenerative diseases, Frontiers in neuroendocrinology 29 (2008) 507–519.

[209] S. Mariathasan, K. Newton, D.M. Monack, D. Vucic, D.M. French, W.P. Lee, M. Roose-Girma, S. Erickson, V.M. Dixit, Differential activation of the inflammasome by caspase-1 adaptors ASC and Ipaf, Nature 430 (2004) 213–218.

[210] I. Jorgensen, E.A. Miao, Pyroptotic cell death defends against intracellular pathogens, Immunological reviews 265 (2015) 130–142.

[211] S. Braeuninger, C. Kleinschnitz, G. Stoll, Interleukin-18 does not influence infarct volume or functional outcome in the early stage after transient focal brain ischemia in mice, Experimental & translational stroke medicine 2 (2010) 1.

[212] R.D. Wheeler, H. Boutin, O. Touzani, G.N. Luheshi, K. Takeda, N.J. Rothwell, No role for interleukin-18 in acute murine stroke-induced brain injury, Journal of cerebral blood flow and metabolism official journal of the International Society of Cerebral Blood Flow and Metabolism 23 (2003) 531–535.

[213] M. Hedtjarn, A.L. Leverin, K. Eriksson, K. Blomgren, C. Mallard, H. Hagberg, Interleukin-18 involvement in hypoxic-ischemic brain injury, The Journal of neuroscience the official journal of the Society for Neuroscience 22 (2002) 5910–5919.

[214] O. Fukui, Y. Kinugasa, A. Fukuda, H. Fukuda, E. Tskitishvili, S. Hayashi, M. Song, T. Kanagawa, T. Hosono, K. Shimoya, Y. Murata, Post-ischemic hypothermia reduced IL-18 expression and suppressed microglial activation in the immature brain, Brain research 1121 (2006) 35–45.

[215] L. Yang, Z. Zhang, D. Sun, Z. Xu, X. Zhang, L. Li, The serum interleukin-18 is a potential marker for development of post-stroke depression, Neurological Research 32 (2010) 340–346.

[216] T. Hlaing, R.F. Guo, K.A. Dilley, J.M. Loussia, T.A. Morrish, M.M. Shi, C. Vincenz, P.A. Ward, Molecular cloning and characterization of DEFCAP-L and -S, two isoforms of a novel member of the mammalian Ced-4 family of apoptosis proteins, The Journal of biological chemistry 276 (2001) 9230–9238.

[217] Z.L. Chu, F. Pio, Z. Xie, K. Welsh, M. Krajewska, S. Krajewski, A. Godzik, J.C. Reed, A novel enhancer of the Apaf1 apoptosome involved in cytochrome c-dependent caspase activation and apoptosis, The Journal of biological chemistry 276 (2001) 9239–9245.

[218] J.A. Kummer, R. Broekhuizen, H. Everett, L. Agostini, L. Kuijk, F. Martinon, R. van Bruggen, J. Tschopp, Inflammasome components NALP 1 and 3

show distinct but separate expression profiles in human tissues suggesting a site-specific role in the inflammatory response, The journal of histochemistry and cytochemistry official journal of the Histochemistry Society 55 (2007) 443–452.

[219] L. Xie, G.R. Choudhury, A. Winters, S.H. Yang, K. Jin, Cerebral regulatory T cells restrain microglia/macrophage-mediated inflammatory responses via IL-10, European journal of immunology 45 (2015) 180–191.

[220] D. Gill, R. Veltkamp, Dynamics of T cell responses after stroke, Current opinion in pharmacology 26 (2016) 26–32.

[221] D.Y.-W. Fann, T. Santro, S. Manzanero, A. Widiapradja, Y.-L. Cheng, S.-Y. Lee, P. Chunduri, D.-G. Jo, A.M. Stranahan, M.P. Mattson, T.V. Arumugam, Intermittent fasting attenuates inflammasome activity in ischemic stroke, Experimental neurology 257 (2014) 114–119.

[222] Z. Yang, L. Zhong, R. Xian, B. Yuan, MicroRNA-223 regulates inflammation and brain injury via feedback to NLRP3 inflammasome after intracerebral hemorrhage, Molecular immunology 65 (2015) 267–276.

[223] Y. Wang, Y. Zhang, J. Huang, X. Chen, X. Gu, Y. Wang, L. Zeng, G.-Y. Yang, Increase of circulating miR-223 and insulin-like growth factor-1 is associated with the pathogenesis of acute ischemic stroke in patients, BMC neurology 14 (2014) 77.

[224] M. Haneklaus, M. Gerlic, M. Kurowska-Stolarska, A.A. Rainey, D. Pich, I.B. McInnes, W. Hammerschmidt, La O'Neill, S.L. Masters, Cutting edge: miR-223 and EBV miR-BART15 regulate the NLRP3 inflammasome and IL-1beta production, Journal of immunology (Baltimore, Md. 1950) 189 (2012) 3795–3799.

[225] J.G. Walsh, S.E. Logue, A.U. Luthi, S.J. Martin, Caspase-1 promiscuity is counterbalanced by rapid inactivation of processed enzyme, The Journal of biological chemistry 286 (2011) 32513–32524.

[226] M.D. Wewers, IL-1β: An endosomal exit, PNAS 101 (2004) 10241–10242.

[227] R.M. Friedlander, Apoptosis and caspases in neurodegenerative diseases, The New England journal of medicine 348 (2003) 1365–1375.

[228] E.A. Miao, J.V. Rajan, A. Aderem, Caspase-1-induced pyroptotic cell death, Immunological reviews 243 (2011) 206–214.

[229] G. Sollberger, G.E. Strittmatter, M. Garstkiewicz, J. Sand, H.-D. Beer, Caspase-1: The inflammasome and beyond, Innate Immunity 20 (2014) 115–125.

[230] L. Gurcel, L. Abrami, S. Girardin, J. Tschopp, F.G. van der Goot, Caspase-1 activation of lipid metabolic pathways in response to bacterial pore-forming toxins promotes cell survival, Cell 126 (2006) 1135–1145.

[231] M. Saleh, Caspase-1 builds a new barrier to infection, Cell 126 (2006) 1028–1030.

[232] C. Taghibiglou, H.G. Martin, T.W. Lai, T. Cho, S. Prasad, L. Kojic, J. Lu, Y. Liu, Lo E, S. Zhang, J.Z. Wu, Y.P. Li, Y.H. Wen, J.H. Imm, M.S. Cynader, Y.T. Wang, Role of NMDA receptor-dependent activation of SREBP1 in excitotoxic and ischemic neuronal injuries, Nature medicine 15 (2009) 1399–1406.

[233] D. Amantea, R. Russo, M. Certo, L. Rombolà, A. Adornetto, L. Morrone, M. Corasaniti, G. Bagetta, Caspase-1-independent Maturation of IL-1β in Ischemic Brain Injury: Is there a Role for Gelatinases?, MRMC 16 (2016) 729–737.

[234] S.J. Won, D.Y. Kim, B.J. Gwag, Cellular and molecular pathways of ischemic neuronal death, Journal of biochemistry and molecular biology 35 (2002) 67–86.

[235] Johnson, J.C. O'Connor, M.E. Hartman, R.I. Tapping, G.G. Freund, Acute hypoxia activates the neuroimmune system, which diabetes exacerbates, The Journal of neuroscience the official journal of the Society for Neuroscience 27 (2007) 1161–1166.

[236] van de Veerdonk, Frank L, M.G. Netea, C.A. Dinarello, L.A.B. Joosten, Inflammasome activation and IL-1beta and IL-18 processing during infection, Trends in immunology 32 (2011) 110–116.

[237] M.J. Fenton, Review: transcriptional and post-transcriptional regulation of interleukin 1 gene expression, International journal of immunopharmacology 14 (1992) 401–411.

[238] M.L. Polan, J. Loukides, P. Nelson, S. Carding, M. Diamond, A. Walsh, K. Bottomly, Progesterone and estradiol modulate interleukin-1 beta messenger ribonucleic acid levels in cultured human peripheral monocytes, The Journal of clinical endocrinology and metabolism 69 (1989) 1200–1206.

[239] P.B. Kavathas, C.M. Boeras, M.J. Mulla, V.M. Abrahams, Nod1, but not the ASC inflammasome, contributes to induction of IL-1β secretion in human trophoblasts after sensing of Chlamydia trachomatis, Mucosal immunology 6 (2013) 235–243.

[240] V. Sagulenko, S.J. Thygesen, D.P. Sester, A. Idris, J.A. Cridland, P.R. Vajjhala, T.L. Roberts, K. Schroder, J.E. Vince, J.M. Hill, J. Silke, K.J. Stacey, AIM2 and NLRP3 inflammasomes activate both apoptotic and pyroptotic death pathways via ASC, Cell death and differentiation 20 (2013) 1149–1160.

[241] E.H. Kim, J.H. Won, I. Hwang, J.W. Yu, Cobalt Chloride-induced Hypoxia Ameliorates NLRP3-Mediated Caspase-1 Activation in Mixed Glial Cultures, Immune network 13 (2013) 141–147.

[242] J.-I. Abe, C. Morrell, Pyroptosis as a Regulated Form of Necrosis PI+/Annexin V−/High Caspase 1/Low Caspase 9 Activity in Cells = Pyroptosis?, Circ Res 118 (2016) 1457–1460.

[243] F. Li, T. Omae, M. Fisher, Spontaneous hyperthermia and its mechanism in the intraluminal suture middle cerebral artery occlusion model of rats, Stroke; a journal of cerebral circulation 30 (1999) 2464-70; discussion 2470-1.

[244] P.A. Barber, L. Hoyte, F. Colbourne, Am Buchan, Temperature-regulated model of focal ischemia in the mouse: a study with histopathological and behavioral outcomes, Stroke; a journal of cerebral circulation 35 (2004) 1720–1725.

[245] J.H. Garcia, S. Wagner, K.F. Liu, X.J. Hu, Neurological deficit and extent of neuronal necrosis attributable to middle cerebral artery occlusion in rats. Statistical validation, Stroke; a journal of cerebral circulation 26 (1995) 627.

6. Appendix

6.1. Behavioral testing

To evaluate neurological deficits after post-ischemic tMCAO, I assessed a motor and sensory behavioral test with minor modifications as described by Garcia *et al.* [245]. The six tests were performed by two blinded readers 15 min prior to sacrificing the animals for tissue preparation at the indicated time points (6, 12, 24 or 72 h after tMCAO). Individual scores of all tests were summed and overall a minimum of 3 and a maximum of 18 points were achievable. Spontaneous activity was tested in an unfamiliar environment. Therefore, the rat was placed into a cage with a size: of 35 x 55 cm and it was observed for 3 min. For forepaw outstretching, the rat was elevated at the tail and the ability for out stretching the forepaw was evaluated. Next, the climbing ability was tested by placing the rat on the call of a wire cage. Normally, they use all four limbs to climb the wall. Then, the body proprioception was tested by touching the side with a blunt stick on each side to induce a reaction. The assessment of spontaneous walking ability was finally followed by testing the sensory function. Here, the vibrissae were brushed and the reaction to the stimulus was evaluated. The test protocol is summarized in Table 6.

Table 6: Detailed description of behavioral scoring

SA: spontaneous activity; FO: forepaw outstretching; CA: climbing ability; BP: body proprioception; SW: spontaneous walking; SF: sensory function

test	score	description
SA	0	rat not moving
	1	severely affected, bare movement
	2	slightly affected, rat moving around in the cage but not approaching the walls and hesitating to move further
	3	rat moving around, exploring the environment, approaching at least 3 walls of the cage
FO	3	symmetrical outstretch of both forelimbs
	2	ability to move right forelimb, less outstretching on the right than on the left side
	1	slight movement of the right forelimb
	0	no moving of the right forelimb
CA	3	easy climbing and tight wire gripping
	2	right side impaired or gripping the wire on the tight side less tight failing to climb or circling instead of climbing
	1	
BP	3	rat turning the head and reacts equally to the stimulus on both sides
	2	slower reaction to the stimulus on the right side
	1	no reaction to the stimulus on the right side
SW	3	straight ahead walking
	2	right circling
	1	tendency to walk toward the right side
	0	no movement
SF	3	head turns to the stimulus side
	2	slow reaction to the stimulus on the right side
	1	no reaction to the stimulus on the right side

6.2. Buffer solutions

Table 7: List of used buffers

(All chemicals were purchased from Carl Roth, Germany)

name	ingrediants
transfer buffer 1 (100 mL)	0.58 g Tris base (Carl Roth, Germany) 0.29 g glycine (Carl Roth, Germany) + 90 mL purified water + 10 mL methanol + 0.1 – 0.2 µL 10 % (w/v) SDS solution
transfer buffer 2 (100 mL)	0.303 g Tris base 1.441 g glycine + 90 mL purified water + 10 mL methanol + 0.1 – 0.2 µL 10 % (w/v) SDS solution
preparation buffer (200 mL)	188.2 mL 0.9 % NaCl solution (BBraun, Germany) 60 mg KCl (Carl Roth, Germany) 0.476 g HEPES (Carl Roth, Germany) 0.45 g glucose (Carl Roth, Germany) 0.2 g BSA (Carl Roth, Germany) check pH 7.4